A STUDY ON MIX DESIGN AND MECHANICAL PROPERTIES OF REACTIVE POWDER CONCRETE (RPC) UTILIZING FINE QUARTZ SAND

BY

AHMED ZUBAIR

A Thesis Presented to the

DEANSHIP OF GRADUATE STUDIES

KING FAHD UNIVERSITY OF PETROLEUM & MINERALS

DHAHRAN, SAUDI ARABIA

In Partial Fulfillment of the

Requirements for the Degree of

MASTER OF SCIENCE

In

CIVIL ENGINEERING

MAY 2012

KING FAHD UNIVERSITY OF PETROLEUM AND MINERALS

DHAHRAN 31261, SAUDI ARABIA

DEANSHIP OF GRADUATE STUDIES

This thesis, written by **AHMED ZUBAIR** under the direction of his thesis advisor and approved by his thesis committee, has been presented to and accepted by the Dean of Graduate Studies, in partial fulfillment of the requirements for the degree of **MASTER OF SCIENCE IN CIVIL ENGINEERING**.

Thesis Committee

Dr. Shamshad Ahmad (Advisor)

Prof. Abul Kalam Azad (Co-advisor)

Prof. Mohammed Maslehuddin (Member)

Dr. Salah U. Al-Dulaijan (Member)

Dr. Hamoud Al-Dehwa (Member)

21 JUL 2012

Dr. Nedal T. Ratrout
Departmental Chairman

Dr. Salam A. Zummo
Dean of Graduate Studies

23/7/12

Date

IN THE NAME OF ALLAH, THE MOST GRACIOUS, THE MOST MERCIFUL

Dedicated

to

My Beloved Parents

ACKNOWLEDGEMENTS

All praise is due only to ALLAH subhana wa ta' aala, the sustainer of the worlds, the most merciful for granting me patience, health and knowledge to complete this work.

I would like to thank King Fahd University of Petroleum and Minerals for providing me the opportunity and financial assistance for pursuing MS program.

I acknowledge my sincere appreciation and thanks to Dr. Shamshad Ahmad for his supervision and guidance throughout this research. I am very much grateful to my co-advisor Prof. Abul Kalam Azad for his untiring efforts and valuable time spent during all the stages of this work. I would like to acknowledge my sincere appreciation to Prof. Mohammed Maslehuddin for his constant encouragement and support. I am grateful to my committee, Dr. Salah U. Al-Dulaijan and Dr. Hamoud Al-Dehwah for their guidance and cooperation. I am also obligated to the Department Chairman, Dr. Nedal T. Ratrout, and other faculty members for their support.

I acknowledge the efforts and guidance of Mr. Mukarram Khan, Mr. Syed Imran Ali, and Mr. Omer Ahmed during the execution of my experimental work and thank them whole heartedly. I would also like to thank Mr. Mohammed Ibrahim, Mr. Mohammed Shameem, for their support during this work.

I would like to thank my seniors Mr. Najam, Mr. Khaleel, Mr. Malik, Mr. Danish, and my friends Abdurrahman, Ajmal, Khaja, Moiz, Tauseef for always being there for me.

Lastly, special thanks are due to my parents for their sacrifices, efforts, prayers and encouragement during all the stages of my life.

TABLE OF CONTENTS

LIST OF FIGURES

LIST OF TABLES

THESIS ABSTRACT (ENGLISH)

Name: **AHMED ZUBAIR**

Title: **A STUDY ON MIX DESIGN AND MECHANICAL PROPERTIES OF REACTIVE POWDER CONCRETE (RPC) UTILIZING LOCAL FINE QUARTZ SAND**

Degree: **MASTER OF SCIENCE**

Major Field: **CIVIL ENGINEERING**

Deficiency of good quality coarse aggregates in many parts of the world is a major concern in producing high performance concrete. There has been a growing interest in developing a new concrete possessing superior properties, namely Reactive Powder Concrete (RPC).

RPC is characterized as a material with high cementitious material content and low water/binder ratio and other additives, such as silica fume, plasticizer, fibers and quartz powder. The coarse aggregate is entirely replaced by the fine quartz sand. RPC has significantly higher rate of strength development with excellent mechanical and durability properties. It exhibits high ductility, greatly improved by the incorporation of steel fibers. It has exceptionally high energy absorption capacity and resistance to fragmentation, making it ideal for structural members that are needed to perform under explosives, blast loads, impact or shock loads along with enhanced fire resistance. While noticeable research has been conducted on RPC, there is a need to investigate the possibility of utilizing fine quartz sand instead of quartz powder because obtaining quartz powder required for RPC is a difficult and expensive process.

This study was conducted to investigate the possibility of producing RPC utilizing the local sand and to study its mechanical properties.

The results of the study indicated that the local fine quartz sand can be utilized for the production of RPC. The developed RPC exhibited excellent mechanical properties and durability characteristics.

MASTER OF SCIENCE DEGREE

KING FAHD UNIVERSITY OF PETROLEUM AND MINERALS

Dhahran, Saudi Arabia

ملخص الرسالة

الإسم : احمد زبير

عنوان الرسالة : دراسة الخلطة الخرسانية والخصائص الميكانيكية للخلطات الخرسانية المصنوعة باستخدام مسحوق الخرسانة وباستخدام حبيبات الكوارتز من الرمل الناعمة المحلية

التخصص : الهندسةالمدنية

الدرجة العلمية : ماجستير بالعلوم الهندسية

تاريخ التخرج : ايار 2012م

ان نقص كفاءة ونوعية الركام الخشن في أجزاء كثيرة من العالم هو مصدر قلق كبير في انتاج خرسانة عالية الجودة و الاداء, وبالتالي كان هناك وجود اهتمام متزايد في تطويرخرسانة جديدة تمتلك خصائص متفوقة، وهي رد فعل مسحوق الخرسانة .

وتتميز مسحوق الخرسانة كمادة ذات نسبة عالية من مواد لاصقة وانخفاض النسبة بين المياه والمواد المضافة الأخرى، مثل دخان السليكا، والألياف، والملدنات ومسحوق الكوارتز. يتم استبدال تماما الركام الخشن في حبيبات رمل الكوارتز الناعمة . مسحوق الخرسانة لديه قدرة أعلى بكثير من تطوير قوة ومتانة خصائص ميكانيكية ممتازة. فإنه يسلك ليونة عالية، وتحسنت بدرجة كبيرة من خلال دمج من الألياف الفولاذية. وبشكل استثنائي لديه القدرة على امتصاص الطاقة العالية والمقاومة للتجزئة، مما يجعلها مثالية للهيكلية التي يحتاجها لأداء أعضاء تحت المتفجرات، والأحمال الانفجار، أو تأثير صدمة الأحمال جنبا.

وباالتالي كان هناك حاجة هناك حاجة للتحقيق في إمكانية الاستفادة من الرمل الكوارتز بدلا من الحصول على مسحوق الكوارتز لأن الحصول على مسحوق الكوارتز للعملية صعبة ومكلفة.

وقد أجريت هذه الدراسة للتحقيق في إمكانية إنتاج و الاستفادة من الرمال المحلية ودراسة الخواص الميكانيكية.

نتائج الدراسة خصائص ممتازة للحبيبات الرمل الكوارتز المحلية و التي يمكن استخدامها لانتاج خرسانة ذات خصائص ميكانيكية و متانة وديمومة.

ماجستير بالعلوم الهندسية
جامعة الملك فهد للبترول والمعادن
الظهران- المملكة العربية السعودية

CHAPTER 1

INTRODUCTION

1.1 BACKGROUND

Because of the lack of good quality coarse aggregates in many parts of the world, it has been a challenging task to produce a very high performance concrete. Recently, advances in concrete technology have been reported in literature leading to the development of the reactive powder concrete (RPC). Many a times a combination of very low water to cementitious materials ratio, high cementitious materials content, silica fume or fly ash, steel or polymer fibers, filler materials and high dosage of superplasticizer are utilized to produce the RPC. These developments could be utilized to produce RPC utilizing local sand. Such an effort is highly desirable since the local coarse aggregates are weak and hence not suitable for the production of high performance concrete.

The harsh environmental conditions prevailing in the coastal areas of the Arabian Gulf cause reinforcement corrosion that poses a serious threat to the durability of concrete structures. This causes safety problems and loss of resources. Furthermore, the local concrete also suffers from the use of marginal aggregates, leading to low strength and less durable concrete. Thus, there is a need to develop RPC utilizing local fine aggregate.

Since the quality of coarse aggregates significantly affects the properties of the resulting concrete, the possibility of minimizing its use should be explored.

Developing a RPC, which is dense and impermeable, may impact durability in the following ways:

High impermeability will reduce the penetration of corrosive specimens through concrete, thus delaying the initiation and propagation of reinforcement corrosion, and

Since the compressive strength of RPC is high, its bond and tensile strength are also expected to be increased. High tensile strength will resist the concrete cracking and high bond strength will resist the loss of load-bearing capacity of the member even at increased rate of reinforcement corrosion.

Therefore, there is a need for developing RPC using the locally available materials, particularly the very good quality quartz sand. It is expected that the developed RPC would be durable and hence significantly increase the service-life of concrete structures subjected to harsh environmental conditions. This will save a lot of national resources and would be helpful in ensuring sustainable development. Furthermore, the abundantly available fine sand in the eastern province will be a good source for RPC.

1.2 NEED FOR THIS RESEARCH

Though some information is available on the development of RPC in the other parts of the world, there is lack of data on the RPC prepared utilizing the local fine aggregates, which is characterized as very fine with a low fineness modulus. Also, very limited information is available on the durability of RPC, particularly under the local aggressive environmental conditions. As stated earlier, the environmental conditions in many parts

of the Kingdom of Saudi Arabia are very conducive for reinforcement corrosion; therefore, for any new concrete the durability study is very much needed prior to its acceptance.

1.3 OBJECTIVES

The general objective of this study was to develop RPC mixtures utilizing local fine aggregate.

The specific objectives were the following:

i. To develop RPC mixtures using local sand,

ii. To assess the mechanical properties and shrinkage characteristics of the developed RPC mixtures,

iii. To develop regression models relating some of the mechanical properties with mixture variables, and

iv. Identifying venues of applications of the developed RPC mixtures.

It is expected that the developed RPC mixtures would result in considerable cost savings since the local sand will be utilized as against quartz powder that is used in the other parts of the world.

1.4 THESIS ORGANIZATION

This thesis is organized in a total of 5 chapters. The content of each of these chapters is explained below.

Chapter 1: This chapter consists of the background of the thesis work, and a brief description for the need for this research is explained. Then the thesis objectives are stated.

Chapter 2: In this chapter, a detailed literature review is presented. A brief description of UHPC is given. Development of RPC is mentioned and the ingredients used therein are elaborated. Techniques adopted for optimizing the constituents of the RPC are discussed. Mix design usually followed and the mechanical properties thus, obtained are summarized. Lastly, recent applications of RPC are discussed.

Chapter 3: Chapter three presents in detail the ingredient used and there mix proportions. Mixing procedure adopted and preparation and casting of the samples is deeply discussed. Lastly, the tests employed for RPC, the equipment and procedure for carrying out these tests is discussed.

Chapter 4: In this chapter, trial mixtures used for optimizing the various ingredients of the RPC are discussed. Followed by the in depth analysis and discussion of the results obtained.

Chapter 5: This chapter has been dedicated to the conclusions and recommendations based on the discussion from the previous chapters.

CHAPTER 2

LITERATURE REVEIW

2.1 ULTRA HIGH PERFORMANCE CONCRETE

The ultra-high performance concrete (UHPC) also called reactive powder concrete (RPC)UHPC is relatively new generation of concrete optimized at the nano and micro-scale to provide superior mechanical and durability properties compared to conventional and high performance concretes. The Improvements in UHPC are achieved through: limiting the water-to-cementitious materials ratio (i.e., w/c < 0.20), optimizing particle packing, eliminating coarse aggregate, using specialized materials, and implementing high temperature and high pressure curing regimes. In addition, and randomly dispersed and short fibers are typically added to enhance the material's tensile and flexural strength, ductility, and toughness [1].

The constituents of RPC include: Portland cement, silica fume, quartz powder (also referred as quartz flour), sand, superplasticizer, water, and fibers. Each of the components in UHPC aids in optimizing the material properties, thus contributing to its extraordinary strength.

As shown in Figure 2.1, the compressive strength of RPC or UHPC may be as high as 200 MPa while a normal high performance concrete has a compressive strength of around 80 MPa.

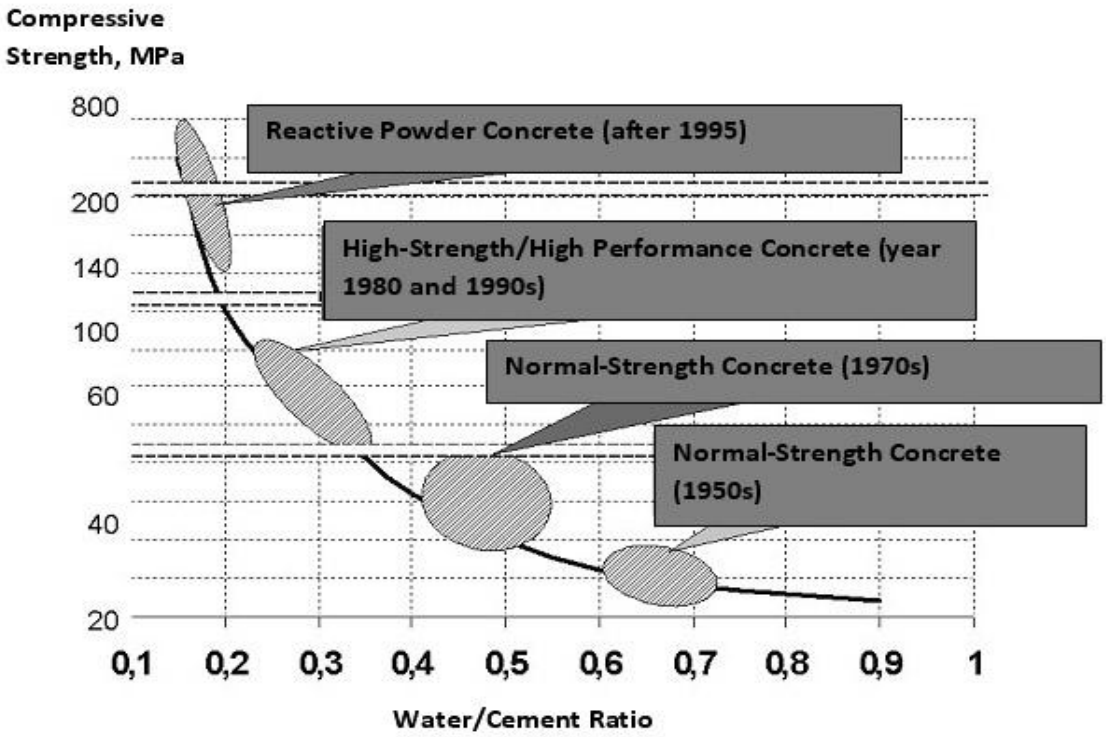

Figure 2.1: Strength comparison of various types of concrete.

Silica fume is one of the main constituents of RPC. According to Vander Voort et al. [2], silica fume in RPC has the three main functions:

- Filling the voids in the next larger granular class, namely cement,
- Enhancing lubrication of the mix due to the perfect sphericity of the basic particles;
- Production of secondary hydrates by the pozzolanic reaction with the products from primary hydration of cement [3].

The other additional constituent of RPC is quartz powder. Quartz powder has an average diameter of 10–15 μm, approximately the same granular size as cement particles. Since quartz powder is a reactive material, it acts as an excellent paste-aggregate interface filler. For cases where heat-treatment is employed, quartz powder demonstrates even higher reactivity. Other advantages of it include extreme hardness and availability. Sand constitutes the largest portion of RPC with about 41 percent by weight. To obtain a highly homogeneous matrix as well as minimum void, RPC contains finely graded sand between 150 μm to 600 μm, as shown in Figure 2.2.

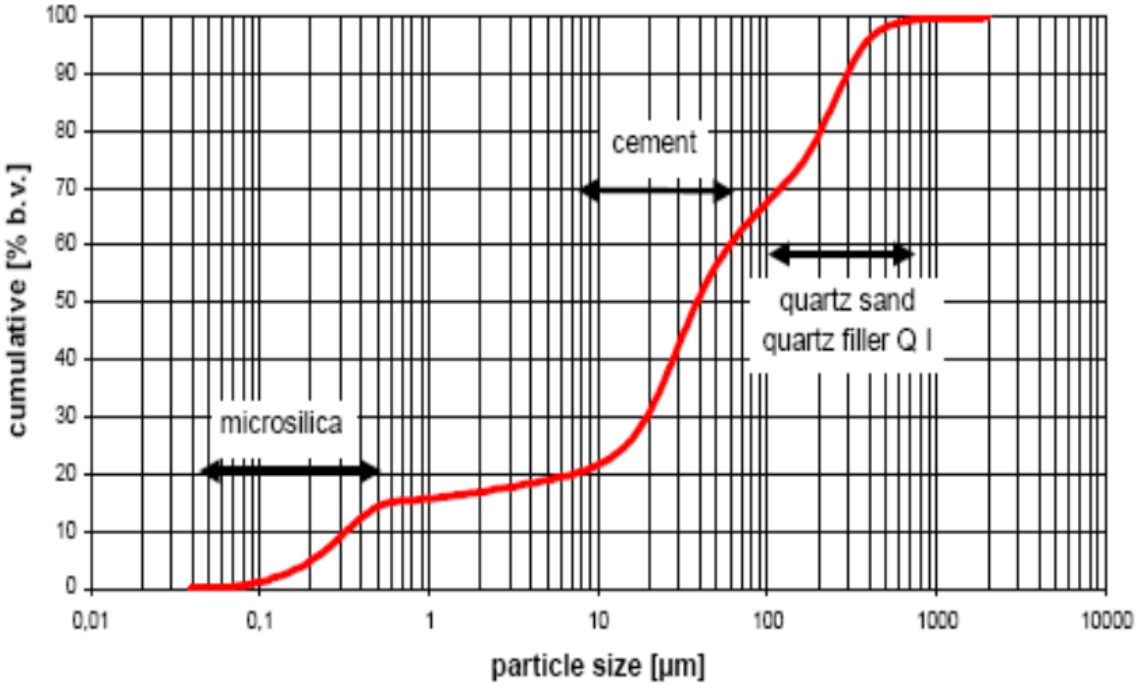

Figure 2.2: Particle Size distribution of silica fume, cement and quartz sand.

To create a gradation of particle sizes that result in a tightly packed matrix of materials the fine aggregates are carefully selected in order to minimize voids. This has the effect of creating a very durable material with low porosity and permeability. The dense microstructure also eliminates shrinkage and limits creep when heat treated during curing. Since RPC uses a small w/cement ratio, superplasticizer is needed to increase its

workability. Today's high performance superplasticizers having either a polycarboxylate (PC), NapthaleneSulfonate (NS), or Melamine Sulfonate (MS) base allow the dense, highly homogeneous mixture to be poured with the concerns of segregation being lessened The addition of a superplasticizer helps to increase the workability.

RPC without fibers is very strong but very brittle, consequently fibers are included to increase the tensile capacity and improve its ductility. Studies using different fiber materials, contents, sizes, and shapes have been conducted by various researchers [4].

Dimensionally, the largest constituent in the mix are the steel fibers. Given the relative sizes of the sand and the fibers, the steel fibers are able to reinforce the concrete matrix on a micro level [5]. The addition of steel fibers helps in preventing the propagation of micro-cracks and macro-cracks and thereby limits crack width and permeability. This is the largest particle in the mix and is added at 6.2 percent by weight to the mix. Because of its size relative to the other constituents, it reinforces the concrete on the micro level and eliminates the need for secondary reinforcement in prestressed bridge girders [6].

2.2 DEVELOPMENT OF RPC

RPC with a compressive strength of more than 150 MPa and other superior material properties is a new generation cementitious material that originated through intensive research work mostly conducted in France and Canada since 1994 [7]. The basic principle on which RPC is based is to achieve a cement matrix as dense as possible (by reducing micro cracks and capillary pores in the cement matrix) and a dense transition zone between matrix and the aggregates.

Following measures are suggested to produce RPC:

- Enhancing the homogeneity by elimination of coarse aggregates. It is well known that the transition zone between the coarse aggregate and paste matrix is often the source of micro cracks in concrete, due to their different mechanical and physical properties. It is suggested that the maximum aggregate size in RPC should be less than 600 μm [3].

- Improving the properties of cement matrix by the addition of supplementary cementing materials, such as silica fume. The modifying effects of silica fume in concrete are attributed to its pozzolanic reaction with $Ca(OH)_2$ and filler effect in voids among cement or other component particles. In typical Portland cement based concrete, 18% silica fume, by weight of the cementitious materials, is enough for total consumption of $Ca(OH)_2$ released from cement hydration [8]. However, considering the filler effect the optimal share of the silica fume increases to about 30% of cement [3]. Therefore, the silica fume content in RPC is normally in the range of 25-30% of the cementitious material.

- Improving the properties of cement matrix by reducing water to cementitious materials ratio.

- Enhancing the packing density of powder mixture. A mixture with a wide size distribution has a low void among the particles. This means powder mixture should be composed of a number of classes of granular powder.

- Enhancing the microstructure by post-set heat-treatment. This increases the reactivity of the cementing materials and constituents to a dense microstructure.

While RPC shows substantially increased compressive strength and decreased porosity, it tends to be brittle. Short high carbon steel or polymer fibers of various dimensions and mechanical properties are commonly used in RPC at various volume fractions to improve its tensile and flexural strength, impact resistance or toughness, decrease cracking, and alter the mode of failure by increasing post cracking ductility [9].

2.3 INGREDIENTS OF RPC

Fine quartz sand (150 to 600 μm) is used as aggregate because coarse aggregate is eliminated from RPC. An ordinary Portland cement (Type I) with low C_3A content is used as binder. Silica fume (0.1 to 1.0 μm) is generally used as supplementary cementing material. Quartz powder (smaller than 10 μm) is used as micro-filler. Super-plasticizer is used to achieve the desirable fluidity [3, 7].

Richard and Cheyrezy [3], have recommended the following criteria regarding the selection of ingredients of RPC:

Sand

Sand selection parameters to be defined are:

- Mineral composition;
- Mean particle size;
- Granular range;
- Particle shape; and
- Mixture ratio by weight.

As far as mineral composition is concerned, quartz offers the following advantages:

- Very hard material;

- Excellent paste/aggregate interfaces; and
- Ready availability.

Sand with a mean particle size of about 250 μm is selected.

The particle size range is defined indirectly by the desirable maximum and minimum particle sizes. Maximum particle size is limited to 600 μm, and for the minimum value, particle sizes below 150 μm are avoided, in order to prevent interference with the largest cement particles (80-100 μm).

Fine sand is obtained by screening crushed sand, where the grains are highly angular or natural quarry sand, where the grains are more spherical. Both types of sand can be used for the RPC. However the water demand is slightly less for natural sand, which is therefore preferable.

Cement

From the point of view of chemical composition, cements with low C_3A content (for reducing the water demand) give better results. As for particle size, it is observed that over-ground cements with a high fineness are not satisfactory, due to their high water demand. The best cement in terms of rheological characteristics and mechanical performance is high silica-modulus cement. However, this type of cement has the disadvantage of a very slow setting rate, preventing its use for certain applications. Conventional quick-setting high performance cement offers very similar mechanical performance, despite a higher water demand.

Superplasticizer

The most efficient superplasticizers are polyacrylate-based dispersing agents, but which also exhibit a retarding characteristic which can present a problem for practical

applications. The conventional superplasticizers selected for their compatibility with the cement give slightly poorer results. For the low w/c ratios used for RPCs, the optimum superplasticizer ratio is high (solid content of approximately 1.6% of cement content).

Silica fume

Silica fume used in RPCs has three main functions, as follows:

- Filling the voids between the next larger class particles (cement);
- Enhancement of rheological characteristics by the lubrication effect resulting from the perfect sphericity of the basic particles; and
- Production of secondary hydrates by pozzolanic reaction with the lime resulting from the primary hydration.

The following parameters are used for silica fume characterization:

- Degree of particle aggregation;
- Nature and quantity of impurities;
- Basic particle size.

The main quality of a silica fume is the absence of aggregates. This leads to the use of non-compacted silica fumes. Slurry cannot be used, as the quantity of water contained in the slurry exceeds the total quantity of water required for the mixture. The most injurious impurities are carbon and alkalis.

Particle size is a secondary factor. The best results are obtained with silica fume procured from the zirconia industry, being free from impurities and totally disaggregated. However the Blaine fineness is lower than that for conventional fumes (14 m^2/g compared with 18 m^2/g). On the other hand, an impurity-free fume with a high Blaine fineness value (22 m^2/g), produced mediocre results, due to the aggregation of the finest particles.

Typically, the silica fume/cement ratio used for RPC is 0.25. This ratio corresponds to optimum filling performance and it is close to the dosage required for complete consumption of the lime resulting from total hydration of cement. However, cement hydration is incomplete in an RPC, and the available quantity of silica fume is more than that required by the pozzolanic reaction.

Utilization of fly ash (FA) and ground granulated blast furnace slag (GGBFS) as an alternative to silica fume in RPC has been reported in the literature [10, 11]. Test results obtained by Yazici et al. [11], indicate that RPC containing high volume binary (SF–FA or SF–GGBFS) or ternary (SF–FA–GGBFS) blends have satisfactory mechanical performance. In other words, utilization of FA and/or GGBFS in RPC production is very effective. Cement and silica fume content can be decreased by FA and/or GGBFS replacement. Mixtures having 1.30 M CaO/SiO_2 ratio performed generally better than mixtures containing constant and high amount of SF. In other words, FA and GGBFS can be used as an alternative silica source in RPC. Moreover, the reduction in SF content reduced the superplasticizer demand considerably. Therefore, besides the reduced heat of hydration and shrinkage, these mixtures have also important environmental benefits.

Quartz powder

Crushed crystalline quartz powder is an essential ingredient for heat-treated RPC. Maximum reactivity during heat-treatment is obtained for a mean particle size of between 5 and 25 μm. The mean particle size of the crushed quartz used for an RPC is l0 μm, and is therefore in the same granular class as the cement.

The ratio by weight adopted corresponds to the stoichiometric optimum for conversion of amorphous hydrates into tobermorite characterized by a C/S molar ratio of 5/6 = 0.83.

This is achieved with a silica/cement ratio of 0.62. This ratio is obtained by adding silica fume and crushed quartz as a complement.

2.4 OPTIMIZATION OF RPC MIXTURES

RPC mixtures are obtained by optimizing several technologies: minimizing the amount of water added, using superplasticizers and a wide particle size distribution, and packing the particles to improve fluidity with minimized water additions and to optimize load-carrying capacity. Methodologies for optimizing the RPC mixtures are reported in the literature [12, 13].

Larrard and Sedran [12] have recommended the following approach for optimizing the RPC mixtures using a packing model (solid suspension model):

First of all, a reference viscosity should be chosen, depending on the production method. Higher the viscosity, lower the minimum water content. However, if the mix is too sticky, the entrapped air volume will increase. Therefore, a critical viscosity should be determined for obtaining a minimal content of voids.

Secondly, the minimal matrix porosity should be looked for. This criterion leads to the determination of the silica fume/cement ratio. However, any increment of aggregate volume increases the viscosity, entailing an increase of the matrix porosity in order to keep the viscosity constant. Thus, a first attempt should be made to test different mixes having a low porosity to determine the respective influence of each parameter. For minimizing matrix porosity, it is possible to act on the size of aggregate. From this point of view, the lowest maximum size of aggregate (sand) is desirable. On the other hand, as a dense packing of the matrix is aimed at, the sand size should be high enough as

compared to the maximum size of cement grains, in order to reduce the wall effect. Therefore, a mono-size sand appears to be the best solution. This is why an ultra-reactive powder concrete will be generally an ultra-high-performance mortar.

Sobolev [13] has presented the following approach for optimizing RPC using the rheological and strength models:

First, the optimal SF content and SP dosage are selected according to the strength model of modified mortars: for optimal performance SF content is specified within 10–15% and SP dosage is set to 10% of SF. Second, the aggregates are optimized to fit a specific grading curve. Then w/c ratio is selected using the strength model.

2.5 MIX DESIGN

The parameters considered in the mix design of RPC are mainly, water to binder ratio, cement content, micro silica to cement ratio, total cementitious material content, total fine aggregate content, fiber content and water to binder ratio. The ranges for these parameters have been obtained from literature survey [3, 5, 10-27] are as follows:

Water to total binder ratio (w/b):- 0.15-0.24

Cement content: - 800-1100 kg/m^3

Silica fume content: - 150-300 kg/m^3

Silica fume to cement ratio (SF/C): -0.15-0.35

Cement and Micro silica content: - 950-1400 kg/m^3

Quartz and Sand: - 1000-1400 kg/m^3

Fiber Content: - 190-250 kg/m^3

Fiber to total binder ratio (f/b): - 0.15-0.30

2.6 MECHANICAL PROPERTIES

The mechanical properties relevant to this work and which were proposed to be investigated are compressive strength, modulus of elasticity, flexural tensile strength, fracture toughness and drying shrinkage. From the literature survey [3, 5, 10-27], the ranges of mechanical properties of RPC are summarized below:

Compressive Strength at 28 days: - 130-260 MPa

Modulus of Elasticity: - 40-70 GPa

Flexural Tensile Strength: - 30-60 MPa

Direct Tensile Strength: - 6-8 MPa

Fracture Energy: - 20-40 kJ/m^2

Drying Shrinkage at 90 days: - 700 x 10^{-6} - 900 x 10^{-6} mm/mm

One of the most significant properties of RPC is its high compressive strength. The increase in compressive strength, over normal concrete or high performance concrete, can be attributed to the particle packing and the selection of specific constituents, and thermal curing of RPC.

Several researchers have attempted to characterize the flexural strength of RPC with single or two-point bending tests on small prisms. The increase in the flexural behavior of RPC is attributed to the particle packing and the addition of fibers which hold the cement matrix together after cracking has occurred. RPC with steel fibers exhibits ductility due to the fact that the small scale fibers reinforce the matrix causing smaller, less damaging cracks to form [28].

The drying shrinkage refers to the volume reduction in the cement matrix resulting from an overall loss of water to the environment through evaporation. Investigation for the drying shrinkage of RPC led to the discovery that the drying shrinkage is most intense during the first 21 days, reaching a magnitude of 40 x 10^{-6} at day 21 and 80 x 10^{-6} by day 90.

Fracture energy represents the total amount of work that must be done on a concrete beam to achieve complete failure. The large amount of energy required to pull out or fracture the steel fibers in the matrix gives UHPC much greater fracture energy than normal concrete.

However, the rate of development of fracture energy is slower than the rates of development of the elastic modulus, compressive strength, and tensile strength. This slow development is most likely due to the fact that fracture energy depends largely on bond strength, which is affected by the tensile strengths and elastic modulus of the RPC mix [2].

Normal concrete and HPC exhibit virtually no post-cracking flexural strength, but the fracture energy of RPC is relatively much higher because of the presence of fibers. The fracture energy of RPC was estimated by Gilliland [29] to be 250 times that of typical HPC [29].

2.7 APPLICATIONS

Different applications of RPC include: heavily (conventionally) reinforced precast elements for bridge decks; in situ applications for the rehabilitation of deteriorated concrete bridges and industrial floors [30]. With or without additional “passive”

reinforcement it is used for precast elements and other applications like offshore bucked foundations. In addition, coarse grained RPC with artificial or natural high strength aggregates were developed for highly loaded columns and for extremely high-rise buildings [22].

Breakthroughs in application are the very first prestressed hybrid pedestrian bridge at Sherbrooke in Canada in 1997, the replacement of steel parts of the cooling tower at Cattenom and two 20.50 and 22.50 m long road bridges used by cars and trucks at Bourg-lès-Valence in France built in 2001 [16]. For these projects the RPC was reinforced with about 2.5 to 3% of steel fibers (by volume) of different shape. Other footbridges with decks and/or other load bearing components made of fine grained, fiber reinforced RPC exist in Seoul and in Japan [14]. A spectacular example of architectural design, taking advantage of the special benefits of RPC, is the toll-gate of the Millau Viaduct in France. Figure 2.3 through 2.5 shows some structures built using RPC.

Figure 2.3: Sherbrooke Bridge, Canada 1997.

Figure 2.4: Seonyu foot-bridge, Korea, 2003, Arch span 120 m deck, thickness 3 cm.

Figure 2.5: Toll-gate of the Millau Viaduct in France.

So far, the previous research shows the performance of RPC developed using fine sand and crushed quartz powder, with particle size ranging from 45μm -600μm. But in this present study, an attempt is made to produce RPC using local fine quartz sand meeting the particle size range criteria and at the same time being rich in silica.

CHAPTER 3

METHODOLOGY OF RESEARCH

3.1 MATERIALS

3.1.1 Cement

Ordinary Portland cement conforming to ASTM C 150 Type I with a specific gravity of 3.15 was used in all the concrete mixtures. Sufficient quantity of cement was procured and stockpiled safely to prevent its hardening. The chemical composition of the cement was carried out in the Central Analytical Laboratories of the Research Institute, KFUPM as shown in Table 3-1.

Table 3-1: Chemical Composition of Cement.

Constituent	Weight %
CaO	64.35
SiO_2	22.0
Al_2O_3	5.64
Fe_2O_3	3.80
K_2O	0.36
MgO	2.11
Na_2O	0.19
Equivalent alkalis ($Na_2O + 0.658K_2O$)	0.33
SO_3	2.10
Loss on ignition	0.7
C_3S	55
C_2S	19
C_3A	10
C_4AF	7

3.1.2 Silica fume

The chemical composition of the silica fume is used as shown in Table 3-2. ASTM method C114 was used to determine SiO_2 gravimetrically using Pt crucibles. Separate sample were weighed to determine oxides of Al, Ca, Na, K, Mg and sulfur and treated by EPA method 3050B. The digested extract was diluted to 100 ml and elements were determined by ICP-OES. Later the concentrations in ppm were converted to their oxides by calculation.

Table 3-2 : Chemical Composition of silica fume.

Parameters	%
Si O_2 –ASTM, C – 114	86.75
Ca/CaO	0.29/0.41
Al/Al_2O_3	0.22/0.41
Fe/Fe_2O_3	1.48/2.12
Mg/MgO	0.11/0.18
K/K2O	0.56/0.67
Na/Na_2O	0.13/0.17
Sulfur/SO3	0.31/0.77
Na_2O+(0.658K_2O)-%	0.62%
Loss on Ignition %, 950 ^oC – ASTM-C 114	3.35
Moisture % - 105 ^oC	0.716

3.1.3 Fine Aggregates

Local fine quartz sand with water absorption of 0.5% and specific gravity of 2.53 was used as the fine aggregate. The grading for this sand is given in Table 3-3.

Table 3-3: Fine aggregate grading.

Sieve Opening, mm	Cumulative % Retained
4.75	0
2.4	0
1.2	0
0.6	3.8
0.3	38.6
0.15	78.1
0.075	99.0

3.1.4 Superplasticizer

A liquid superplasticizer (commercial name: Glenium 51) was used to obtain the desired flow. Glenium 51 is a polycarboxylic ether (PCE) based superplasticizer which does not contain chlorides and complies with AS 1478.1 2000 Type HWR and ASTM C494 Types A and F The specific gravity of Glenium 51 is 1.095 kg/L with 65% water content by weight. Varying dosage of this superplasticizer was used to obtain a flow of 200 ± 2 mm for all the mixes. Figure 3.1 shows Glenium 51 in a measuring cylinder.

Figure 3.1: Superplasticizer Glenium 51.

3.1.5 Steel Fibers

Micro copper coated Steel fibers of 0.22 mm diameter and 13 mm long with an aspect ratio l/d of 59 were utilized. These are, made up of high strength steel greater than 2850 MPa and complies with ASTM A820-90 [31]. These were imported from *HEBEI YU SEN*, Metal Wire Mesh Co. Ltd. China. Figure 3.2 shows the steel fibers.

Figure 3.2: Micro copper coated steel fibers.

3.2 MIXTURE PROPORTIONS

To achieve the objectives of the study, three mix variables were considered with their three levels so as to investigate a total of 27 RPC mixtures as per 3^3 factorial experiment design, as detailed below:

w/b ratio:	0.15, 0.175, 0.20	(3 variables)
Cement content (kg/m^3):	1000, 1100, 1200	(3 variables)
Silica fume content (% of cement):	15%, 20%, 25%	(3 variables)
Steel fiber (kg/m^3):	157	(1 variable)

Total mixtures (3×3×3×1) = 27

Absolute volume method was used to design the mixtures. The weights of constituents determined for one cubic meter of each of the RPC mixtures are presented in Table 3-4.

Table 3-4: Weights of Ingredients in the Mixtures Investigated.

Mix	w/b	Cement (kg/m^3)	Silica fume (%)	Silica fume (kg/m^3)	Water (kg/m^3)	Fiber (kg/m^3)	SP (%)	SP (kg/m^3)	Sand (kg/m^3)
M1	0.15	1000	15	150	172.5	157	3.55	40.83	976.81
M2	0.15	1000	20	200	180	157	3.55	42.6	897.51
M3	0.15	1000	25	250	187.5	157	3.55	44.38	818.21
M4	0.15	1100	15	165	189.75	157	3.55	44.91	826.55
M5	0.15	1100	20	220	198	157	3.55	46.86	739.32
M6	0.15	1100	25	275	206.25	157	3.55	48.81	652.09
M7	0.15	1200	15	180	207	157	3.55	48.99	676.29
M8	0.15	1200	20	240	216	157	3.55	51.12	581.13
M9	0.15	1200	25	300	225	157	3.55	53.25	485.97
M10	0.175	1000	15	150	201.25	157	2	23	945.25
M11	0.175	1000	20	200	210	157	2	24	864.58
M12	0.175	1000	25	250	218.75	157	2	25	783.91
M13	0.175	1100	15	165	221.375	157	1.5	18.98	806.45
M14	0.175	1100	20	220	231	157	1.5	19.8	718.35
M15	0.175	1100	25	275	240.625	157	1.5	20.63	630.25
M16	0.175	1200	15	180	241.5	157	1.5	20.7	654.37
M17	0.175	1200	20	240	252	157	1.5	21.6	558.26
M18	0.175	1200	25	300	262.5	157	1.5	22.5	462.15
M19	0.20	1000	15	150	230	157	1.5	17.25	885.8
M20	0.20	1000	20	200	240	157	1.5	18	802.55
M21	0.20	1000	25	250	250	157	1.5	18.75	719.29
M22	0.20	1100	15	165	253	157	1	12.65	741.06
M23	0.20	1100	20	220	264	157	1	13.2	650.11
M24	0.20	1100	25	275	275	157	1	13.75	559.17
M25	0.20	1200	15	180	276	157	1	13.8	583.03
M26	0.20	1200	20	240	288	157	1	14.4	483.81
M27	0.20	1200	25	300	300	157	1	15	384.60

A total number of 660 specimens were prepared for conducting tests to determine compressive strength, modulus of elasticity, modulus of rupture, shrinkage and fracture toughness.

3.3 MIXING PROCEDURE

The conventional mixing method is based on BS 1881: part 125 (BSI, 1986). However, since RPC is composed of very fine materials, the conventional mixing method is not appropriate. The following sequence in mixing of RPC was followed based on the previous studies [20, 21, 23], and as well as from the experience gained after several trials. The mixing procedure adopted is as follows:

(a) Dry mixing the powders (including cement, sand and silica fume) for about three minutes with a low speed of about 140 revolutions/minutes.

(b) Addition of half volume of water containing half amount of superplasticizer.

(c) Mixing for about three min with a high speed of about 285 revolutions/minutes.

(d) Addition of the remaining water and superplasticizer.

(e) Mixing for about ten min with a high speed of about 285 revolutions/minutes.

(f) Finally, adding steel fibers in small amounts over the course of the next two minutes into the mixture.

(g) After the fibers have been added, continue running mixer for further three minutes to ensure that the fibers are well dispersed.

The entire mixing process takes about 20-25 minutes and is specific to the constituents of the mix and the mixer, shown in Figure 3.3, was used. Mixing of the RPC requires special attention to have uniform consistency. After preparation, the RPC was poured into the molds and consolidated using a vibrating table.

Figure 3.3: Planetary Mixer (MIKRONS) used for mixing the constituents of RPC.

As soon as mixing was completed, RPC mix was tested for consistency. ASTM C1437 [32], standard test method for measuring flow of hydraulic cement was used for this purpose in this test. The mini slump cone is filled with RPC mix and then it is removed slowly to allow the RPC to flow evenly on the table and then the flow table is dropped 25 times and its average diameter is recorded. The average flow diameter of RPC mix ranged from 180 to 220 mm.

3.4 PREPARATION AND CURING OF SPECIMENS

Specimens of RPC were prepared and cured to carry out various tests planned in this research study. Batching of each mix was proportioned by weight. After mixing, the flow was measured and RPC was poured in the moulds. The moulds were then vibrated until complete consolidation was achieved. After casting, the specimens were covered with plastic sheet for 24 hours and placed in the laboratory environment (22 ± 3 ^{0}C) to minimize loss of mix water. After 24 hours, the specimens were demolded and placed in a curing tank till the time of test. Table 3-5 shows the type and number of specimens for each of the RPC mixture. Figure 3.4 shows the prepared RPC specimens.

Table 3-5: Type and Number of Specimens Prepared and Tested.

Test	Specimen Type	Dimensions (mm)	Test Standard	Number of Specimens from each mixture
Compressive strength	Cube	50 x 50 x 50	ASTM C 109	15
Modulus of elasticity	Cylinder	75 x 150	ASTM C 469	3
Flexural tensile strength (MOR)	Prism	40 x 40 x 160	ASTM C 78 & ASTM C 1609	3
Drying shrinkage	Prism	25 x 25 x 275 prism	ASTM C 356	3
Fracture toughness	Prism	40 x 40 x 160	RILEM Committee on Fracture Mechanics[33]	1
Total number of specimens				27 × (15+3+3+3)+ 12×1 = 660

Figure 3.4: A set of RPC specimens prepared from each RPC mixture.

3.5 TESTING OF SPECIMENS

3.5.1 Compressive Strength

The compressive strength was determined on 50 mm cube specimens according to ASTM C 109 [34]. The specimens were tested using a digital compression testing machine (MATEST) after 3, 7, 14, 28 and 90 days of water curing. Three specimens were tested at each age and the average values are reported. Figure 3.5 shows the 3000 KN capacity compression testing machine (MATEST) utilized to test the RPC specimens in compression.

Figure 3.5: Compression testing machine used to determine the compressive strength of RPC cubical specimens.

3.5.2 Modulus of Elasticity

As specified in ASTM C 469 standard test method for static modulus of elasticity and Poisson's ratio of concrete in compression, the elastic portion of the compressive stress-strain curve up to 40 percent of the ultimate compressive strength (0.40 $f`_c$) was used to determine the modulus of elasticity. Three 75 mm diameter and 150 mm height cylindrical specimens were utilized to determine the modulus of elasticity. The test setup included a specially designed axial deformation gauge shown in Figure 3.6. The two parallel rings are both rigidly attached to the cylinder with a 3 in. gage length between the attachment points.

Figure 3.6: RPC cylindrical specimen installed with the dial gauge.

The lower ring holds two LVDTs whose ends bear on the upper ring. Thus, the axial deformation of the cylinder can be accurately measured from initiation of loading through failure. The load and the output from the three LVDTs were digitally recorded throughout the test using a data logger. The setup is shown in the Figure 3.7. The testing of each cylinder was completed in a single constant load application from start to failure. In this test program, proper seating of the cylinder could be assured by monitoring the load-deformation response during the test. The modulus of elasticity was calculated based on the average LVDT-based deformation measurements and the load reading. Figure 3.8 shows the cylindrical RPC specimens after their testing.

Figure 3.7: Setup for testing for the modulus of elasticity of RPC.

Figure 3.8: Deformed cylindrical RPC specimens after testing.

3.5.3 Flexural Tensile Strength

The standard four-point flexural test to determine the modulus of rupture (MOR) according to ASTM C 78 is the most common method for obtaining flexural tensile strength of normal as well as high-performance concretes. The test setup is shown in Figure 3.9.

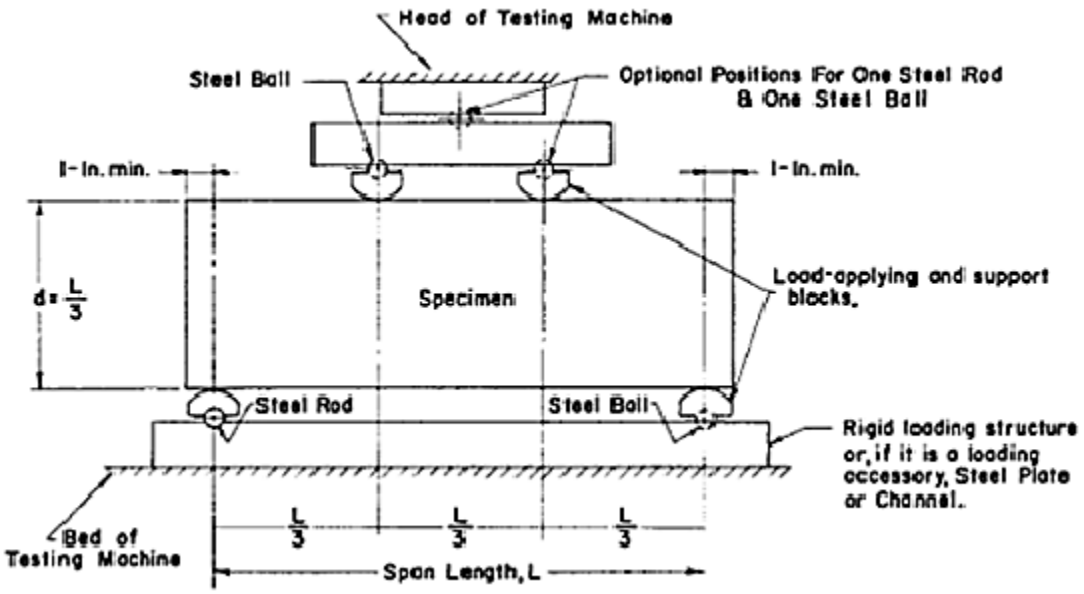

Figure 3.9: Schematic of loading and measuring system for the four-point bending test.

The flexural toughness can be determined as equal to the area under the load-deflection curve obtained from the four-point load test. However, the method for the determination of residual flexural strength, which is crucial to ultra-high performance concrete, is not covered by ASTM C78. For more than a decade, the ASTM C1018 standard has been used for flexural toughness of fiber reinforced concrete. However, this method evaluates the flexural toughness in terms of dimensionless parameters, such as toughness index and residual strength factor. In the year 2005, the ASTM C 1018 standard was replaced with a new standard, ASTM C1609, for determination of MOR at peak flexural strength,

flexural toughness, and residual flexural strength. The ASTM C1609 (titled “Standard Test Method for Flexural Performance of Fiber-Reinforced Concrete using Beam with Third-Point Loading”) is now being commonly used to determine the flexural properties of ultra-high performance concrete such as RPC. This test involves the four-point flexural loading of small-scale concrete prisms measuring 40×40×160 mm (Figure 3.10). During the test, the load and the mid-span deflection of the prism are monitored. These data are then used to determine the MOR and flexural toughness. The residual flexural strength is also determined using the same load-deflection curve. This method uses similar test specimens and testing procedure as that of ASTM C 1609 method.

Figure 3.10: Setup for conducting four-point bending test for MOR.

Steel fibers play a major role in enhancing the flexural capacity of RPC. Additions of these fibers increases the peak value of MOR and are responsible for increasing the area under load vs. deflection curve and increasing the flexural toughness of the specimen by the bridging action, as shown in Figure 3.11, thus signifying enhanced ductility.

Figure 3.11: Specimen after failing under four point bending test depicting the bridging effect of the steel fibers.

Calculations of MOR and Flexural Toughness according to ASTM C 1609:

Eighty one prisms were tested, three prisms for each mix of RPC after 28 days of water curing. Testing of prisms was conducted on a 600 KN INSTRON machine with a loading rate of 0.5 mm/min and the deflection was measured using one LVDT at mid span of the prisms. The load-deflection data was recorded by using a data logger. The data from the data logger was transferred to a computer to plot the load-deflection curve. From each set of the load-deflection curves, the following parameters were recorded for each specimen of RPC.

- First-Peak Strength
- Peak strength or MOR
- *P*100,0.5, *F*100,0.5, *P*100,2, and *F*100,2
- Flexural toughness, *T*100,2

Where, *P*100, 0.5, *F*100, 0.5 are the residual load and strength at deflection of 0.5 mm in the load deflection curve, respectively, and *P*100, 2, and *F*100, 2 are the residual load and strength at deflection of 2 mm in the load deflection curve, respectively. *T*100,2 is the flexural toughness which is equal to the area under load deflection curve up to 2 mm according to ASTM C 1609 (Figure 3.12).

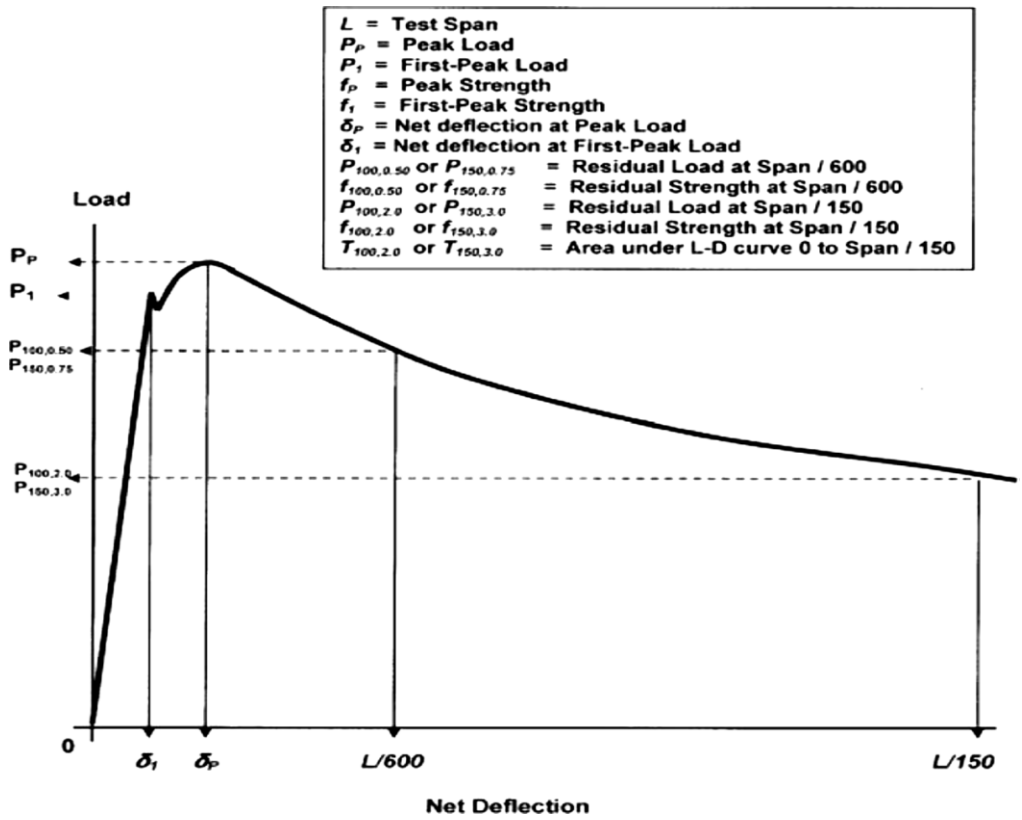

Figure 3.12: Definition of toughness index according to ASTM C 1609.

3.5.4 Fracture Toughness

RPC is reported to have excellent fracture properties besides its very high strength and elasticity. The fibers added to RPC make it able to resist the fracture by improving its ductility. The ductile behavior of RPC was tested through cyclic loading and unloading. The data generated through this test was utilized to study the fracture properties of RPC in terms of various parameters, such as: critical stress intensity factor (K_{ic}), critical crack tip opening displacement (*CTODc*), and fracture energy. In the present study, fracture properties of RPC were determined using fracture toughness test developed by Jenq and Shah (1985). For this testing, prism specimens, having dimensions of 40×40×160 mm with a notch created at center point, were used. The fracture toughness tests were conducted after 28 days of normal water curing.

Fracture toughness test developed by [33] uses a single-edge notched beam (SEN) specimen (dimensions 100×100×400 mm) to determine the fracture properties of the concrete. Two-Parameter Fracture Model (TPFM) is used to determine fracture properties. For TPFM: a span-to-depth ratio (*S*/*d*) of 3; initial notch depth (*a*0) as one-third of the total depth of the beam (~30 mm), and the notch width of 4 mm are used. Three-point bending with the load (*P*) and crack mouth opening displacement (CMOD) are measured for single edge notched beam specimen as shown in Figure 3.13. TPFM is used to determine the critical stress intensity factor (K_{ic}) and critical crack tip opening displacement (*CTODc*) of a monolithic beam based on an effective elastic crack approach. The nonlinear fracture behavior was accounted for by using linear elastic fracture mechanics equations to calculate the effective elastic crack length based on the measured loading and unloading compliance of the beam. Geometric factors were included in the calculations to account for the geometry and size of the beams. The test was conducted on INSTRON machine of 600 KN capacity (Figure 3.14).

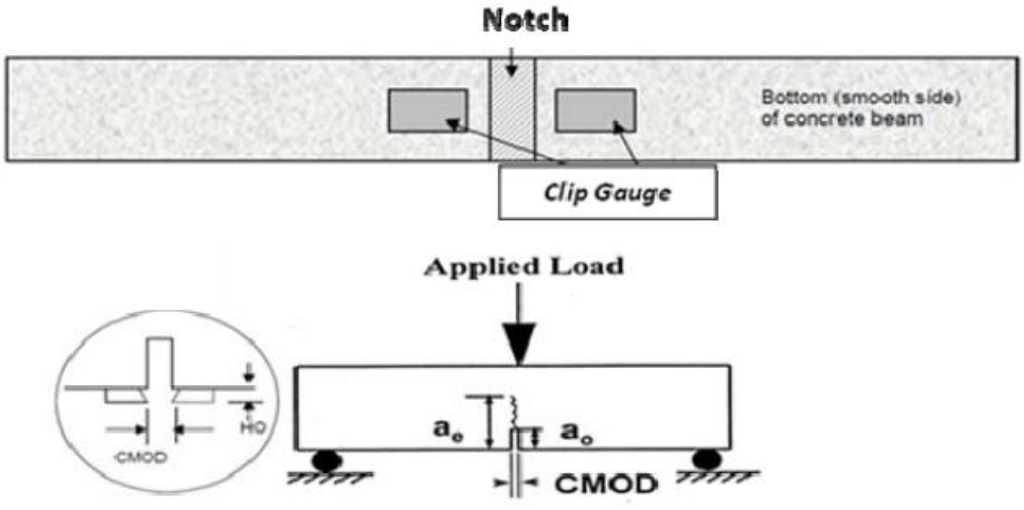

Figure 3.13: Details of attaching clip gauge to RPC prism which measures crack mouth opening displacement (CMOD).

Figure 3.14: Complete test setup for measuring fracture toughness of RPC prisms.

Fracture Parameters

The two fracture parameters determined using the TPFM are the *Kic* and *CTODc*. These are computed by first obtaining the critical effective crack length (a_c). By equating, the concrete's modulus of elasticity from the loading and unloading curves ($E = E_i = E_u$) as shown in equations below, the critical effective crack length (a_c) could be determined as follows:

$$E_i = \frac{6Sa_0g_2(\alpha_0)}{c_i d^2 b} \quad \text{.....Equation (3.1)}$$

$$E_u = \frac{6Sa_cg_2(\alpha_c)}{c_u d^2 b} \quad \text{.....Equation (3.2)}$$

With,

$$\alpha_0 = \frac{(a_0+H_0)}{(D+H_0)} \quad \text{.....Equation (3.3)}$$

$$\alpha_c = \frac{(a_c+H_0)}{(D+H_0)} \quad \text{.....Equation (3.4)}$$

where *S* is the span, *d* is the depth, *b* is the width, a_0 is the initial notch depth of the beam, α_0 is the initial notch/depth ratio, αc is the critical notch/depth ratio, H_0 is the thickness of

the clip gauge holder (Figure 3.13), and $g_2(\alpha)$ is the opening displacement geometric factor for the Three-Point Bending (TPB) specimen given by:

$$g_2(\alpha) = 0.76 - 2.28\alpha + 3.87\alpha^2 - 2.04\alpha^3 + \frac{0.66}{(1-\alpha)^2} \text{.....Equation (3.5)}$$

Once a_c is computed, we can calculate K_{ic} by:

$$K_{ic} = 3(P_c + \frac{W_0 S}{2L}) \frac{S\sqrt{\pi a_c} g_1(a_c/d)}{2d^2 b} \text{.....Equation (3.6)}$$

where, (P_c) is the peak load, W_o is the weight of the specimen, L is the length of the specimen and (g_1) is the stress intensity factor geometric function for the beam specimen defined as follows:

$$g_1(\alpha_c) = \frac{1.99-(\alpha_c)(1-\alpha_c)[2.15-3.93\alpha_c+2.70\alpha_c^2}{\sqrt{\pi}[1+2\alpha_c][1-\alpha_c]^{2/3}} \text{.....Equation (3.7)}$$

The loading compliance (C_i) is calculated as the inverse of the slope from 10% of the peak load until 50% of the peak load. This is estimated to be in the linear elastic range ignoring any initial seating load discontinuities in the curve. The unloading compliance (*Cu*) is the inverse of slope of the unloading curve. *Cu* should be calculated between 10% and 80% of the peak load on the unloading curve. The criteria for the determination of *Ci* and *Cu*, as given by Bordelon (2007), are shown in Figure 3.15. Figure 3.16 and Figure 3.17 show the close-up view of the fracture toughness test and the bridging effect of fibers during fracture testing, respectively.

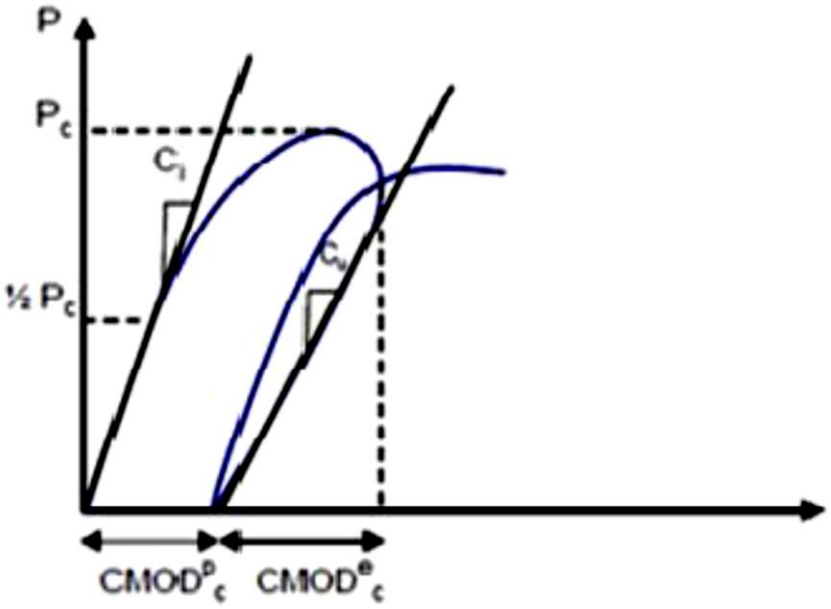

Figure 3.15: Loading and unloading compliance C_i and C_u.

Figure 3.16: Close up view of fracture toughness test.

Figure 3.17: Bridging effect of fibers.

Fracture Energy

Fracture energy represents the total amount of work that must be done on a concrete beam to achieve complete failure. The large amount of energy required to pull out or fracture the steel fibers in the matrix gives UHPC much greater fracture energy than normal concrete. According to [35], the fracture energy in UHPC subjected to standard heat treatment ranges from 20,000 N/m to 47,300 N/m. There is little information in the literature focused on the fracture energy of RPC. In this study, the specimens were tested to determine the critical energy release rate and the total fracture energy.

Critical Energy Release Rate (Gf)

By using a thin TPB (Three-Point Bending) beam, plane stress was assumed and the critical energy release rate (*Gf*), or also known as the initial fracture energy, was related to K_{ic} and the modulus of elasticity, *E*, by equation

$$G_f = \frac{K^2_{ic}}{E}$$

3.5.5 Drying Shrinkage

Shrinkage is the reduction in the volume of concrete caused mainly by the loss of water due to evaporation from a freshly hardened concrete exposed to air. Shrinkage may result in cracking of restrained concrete members. A total of three prisms of RPC specimens of 25 x 25 x 275 mm were prepared for determining the drying shrinkage according to ASTM C 356. Three specimens were tested and their average values are reported. A setup consisting of a stand fitted with a LVDT connected to a data logger was used, as shown in Figure 3.18. Shrinkage measurements were taken after every 7 days.

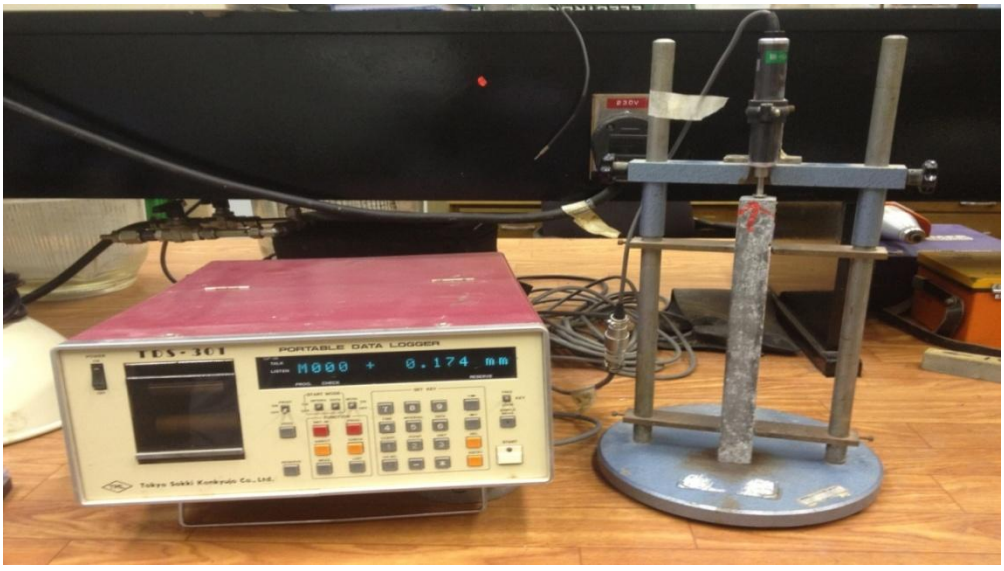

Figure 3.18: Setup for measuring drying shrinkage.

CHAPTER 4

RESULTS AND DISCUSSION

The experimental program was discussed in Chapter 3. In this chapter, the results of the experimental work for RPC and discussion are given, thereon.

4.1 TRIAL MIXTURES

Several trial mixtures were prepared to optimize various constituents of the RPC. Firstly, the grading of sand was optimized to obtain the maximum particle packing leading to higher density and strength. To satisfy the flow criteria the dosage of a plasticizer was optimized to meet the required flow. The Optimization of other constituents like water-binder ratio and cement and silica fume content can be determined from the tests conducted in detail.

4.1.1 Optimization of Sand Grading

Sand constitutes about 50% of all the constituents in RPC. To achieve the desired properties of the RPC, it is desirable to optimize the grading of the sand. This will help us in achieving denser microstructure with closely packed particles, thereby enhancing its performance.

For this purpose, specimens for compression testing were prepared using the following mix design with only one variable, i.e. the sand grading.

w/b = 0.20

Cement = 1000 kg/m^3

Silica fume = 150 kg/m^3

Water = 230 kg/m^3

Sand = 977 kg/m^3

The various sand grades used were:

- Natural (ungraded)
- Passing 600 µm-Retained 150 µ
- Passing 600 µm
- Passing 300 µm
- Passing 150 µm
- Mixed - 1/3rd passing 600 µm, 1/3rd passing 300 µm, 1/3rd passing 150 µm

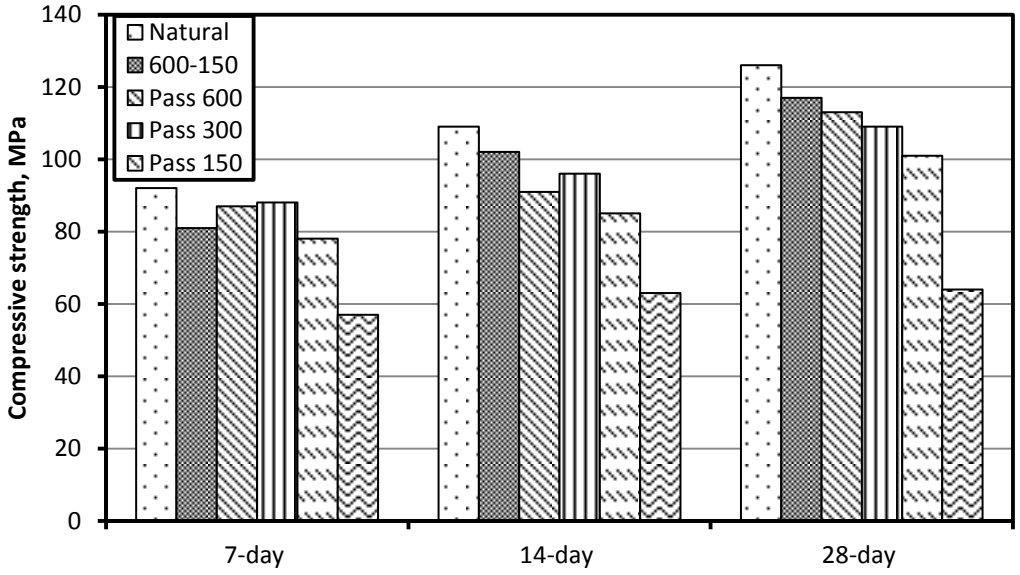

Figure 4.1: Compressive strength of RPC specimens prepared with different sand grading.

The results obtained from compression testing on the mixtures prepared using various sand grades are presented in Table 4-1.

Table 4-1: Compressive strength of RPC specimens prepared with different sand grading.

Mix #	Sand grade	SP (%)	Flow (cm)	Density (kg/m^3)	7-Day f_c` (MPa)	14-day f_c` (MPa)	28-day f_c` (MPa)
1	Natural	1.5	20	2282	92	109	126
2	600-150	1.7	18	2239	81	102	117
3	Pass 600	1.8	16	2265	87	91	113
4	Pass 300	2.0	21.5	2260	88	96	109
5	Pass 150	2.1	17.5	2280	78	85	101
6	Mixed	1.9	19.5	2004	57	63	64

7, 14, and 28-day compressive strengths for all six trial mixtures are shown in Figure 3.1. From the plot shown in Figure 4.1, it is clearly evident that the natural sand grading is giving the best results. Hence, natural sand grading was used for the preparation of RPC mixtures for detailed study.

4.1.2 Optimization of Superplasticizer

The optimization of superplasticizer dosage is very crucial for RPC, as it provides RPC mixtures the required flow for very low water to binder ratio. Flowability is essential for pouring RPC mixture into the molds and for the adequate consolidation. Several trials were carried out to optimize the super plasticizer dosage for each of the 27 RPC mixtures to meet the targeted flow of 200±20mm in each case. Results showing the optimum super plasticizer dosages and corresponding flow for all 27 mixtures are presented in Table 4-2.

Table 4-2: Optimum dosages of superplasticizer for all 27 RPC mixtures to meet flow criteria of 200±20mm.

Mix #	w/b	Cement (kg/m^3)	Silica fume (%)	Silica fume (kg/m^3)	Water (kg/m^3)	Optimum SP dosage (%)	Flow (cm)
M1	0.15	1000	15	150	172.50	3.60	18.0
M2	0.15	1000	20	200	180.00	3.60	18.0
M3	0.15	1000	25	250	187.50	3.60	18.0
M4	0.15	1100	15	165	189.75	3.60	20.0
M5	0.15	1100	20	220	198.00	3.60	21.0
M6	0.15	1100	25	275	206.25	3.60	19.0
M7	0.15	1200	15	180	207.00	3.60	20.0
M8	0.15	1200	20	240	216.00	3.60	20.5
M9	0.15	1200	25	300	225.00	3.60	20.5
M10	0.175	1000	15	150	201.25	2.00	22.0
M11	0.175	1000	20	200	210.00	2.00	20.0
M12	0.175	1000	25	250	218.75	2.00	22.0
M13	0.175	1100	15	165	221.38	1.50	18.5
M14	0.175	1100	20	220	231.00	1.50	20.5
M15	0.175	1100	25	275	240.63	1.50	19.0
M16	0.175	1200	15	180	241.50	1.50	22.5
M17	0.175	1200	20	240	252.00	1.50	20.0
M18	0.175	1200	25	300	262.50	1.50	20.0
M19	0.20	1000	15	150	230.00	1.50	22.0
M20	0.20	1000	20	200	240.00	1.50	21.5
M21	0.20	1000	25	250	250.00	1.50	22.0
M22	0.20	1100	15	165	253.00	1.00	19.0
M23	0.20	1100	20	220	264.00	1.00	18.8
M24	0.20	1100	25	275	275.00	1.00	19.0
M25	0.20	1200	15	180	276.00	1.00	21.0
M26	0.20	1200	20	240	288.00	1.00	20.0
M27	0.20	1200	25	300	300.00	1.00	19.0

From Table 4.2, it is evident that the optimum superplasticizer dosage was 3.6% by the cementitious material for all mixtures with a w/b ratio of 0.15. For mixtures with w/b ratio of 0.175 optimum super plasticizer dosage was in the range of 1.5% to 2% of the cementitious material. The optimum dosage of superplasticizer was in the range of 1% to 1.5% in the RPC mixtures with a w/b ratio of 0.20. As expected, it is evident that the requirement of superplasticizer increases with a decrease in the w/b ratio.

4.2 COMPRESSIVE STRENGTH

Table 4-3 lists the compressive strength development of RPC specimens prepared with varying mixture design variables.

Table 4-3: Compressive strength development at different ages.

Mix #	Average compressive strength, (MPa)				
	3 days	7 days	14 days	28 days	90 days
1	92.0	104.0	118.0	132.0	140.0
2	94.0	106.0	122.7	135.6	145.4
3	107.0	120.7	129.4	136.9	150.7
4	100.8	108.6	119.1	132.0	136.7
5	103.7	113.2	125.2	136.3	147.0
6	110.0	119.1	131.0	138.9	154.4
7	99.9	107.2	119.4	132.8	136.4
8	104.1	110.6	123.0	135.0	140.0
9	108.0	115.0	126.0	137.0	143.8
10	98.7	111.6	125.4	129.4	142.0
11	101.3	119.6	129.3	133.3	146.3
12	104.0	121.0	133.0	135.0	149.0
13	108.2	117.2	119.3	128.4	140.0
14	108.6	119.8	123.4	130.0	147.1
15	110.0	121.0	127.0	133.0	148.5
16	90.1	107.0	112.4	130.0	133.0
17	91.6	112.1	120.2	134.0	136.7
18	98.4	113.2	121.9	136.0	154.5
19	91.0	105.6	115.7	121.5	130.3
20	99.9	108.0	119.5	126.2	140.1
21	100.5	109.8	122.0	128.0	143.8
22	83.8	102.0	114.5	123.3	130.9
23	98.8	104.5	115.5	125.7	133.3
24	101.0	107.0	117.0	128.3	136.6
25	90.3	102.5	111.1	128.0	138.3
26	99.7	108.6	115.7	132.2	142.8
27	102.0	110.2	117.1	135.0	144.0

4.2.1 Compressive strength variation with curing duration

All the specimens had been water cured for 3, 7, 14, 28 and 90 days. The results show higher compressive strength, much greater than that reported for high strength concrete. The highest compressive strength at 3 days, 7 days, 14 days, 28 days and 90 days was 110, 121, 133, 138.9 and 154.5 MPa, respectively.

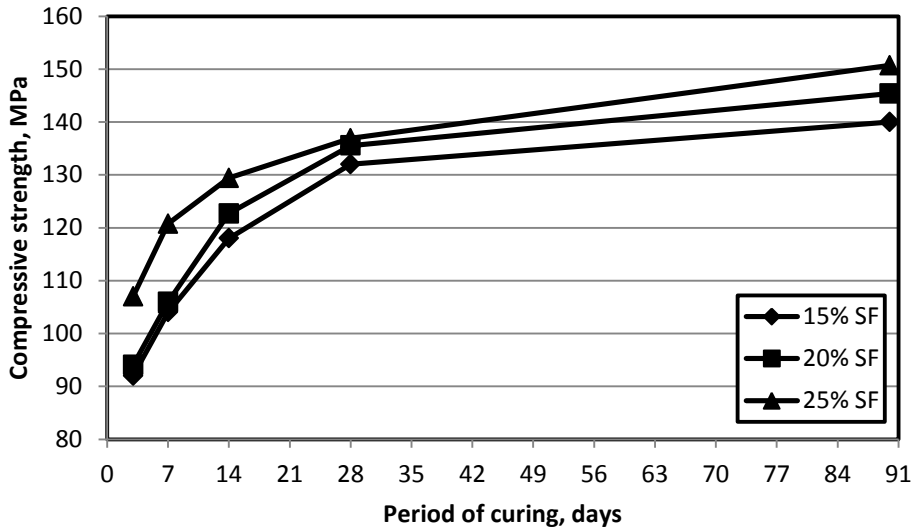

Figure 4.2: Compressive strength development for w/b o f 0.15; CC of 1000 kg/m3

The compressive strength development in the RPC specimens prepared with a w/b of 0.15, cement content of 1000 kg/m^3 and silica fume content varying from 15 to 25%, as replacement of sand, is depicted in Figure 4.2. The compressive strength increased with age in all the RPC specimens. The compressive strength development of 20 and 25% silica fume RPC was almost similar for up to 28 days. However, a significant improvement in strength was noted after 90 days of curing. Highest compressive strength was noted in the 25% RPC specimens followed by 20 and 15% SF RPC specimens. After

90 days of curing, the compressive strength of 15%, 20 % and 25% silica fume RPC specimens was 140, 145.4, 150.7 MPa, respectively.

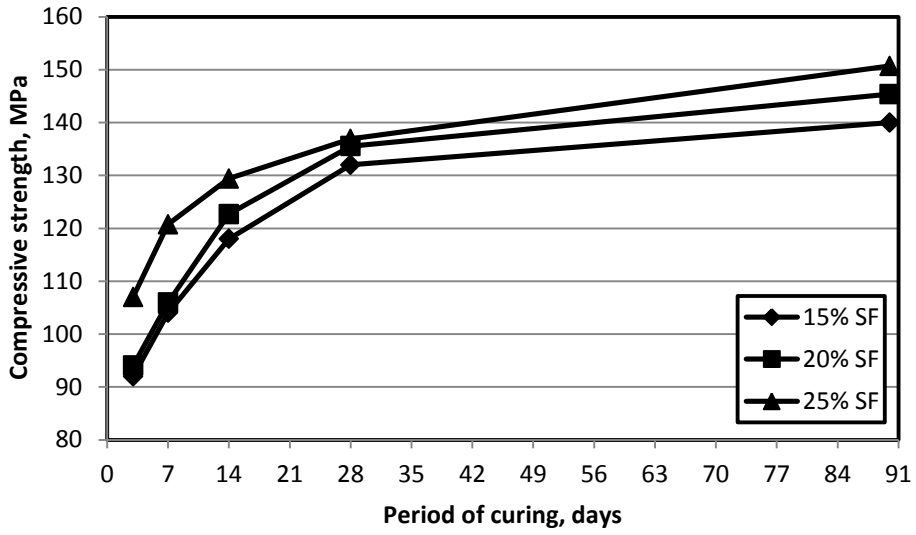

Figure 4.2: Compressive strength development for w/b o f 0.15; CC of 1000 kg/m^3.

The compressive strength development in the RPC specimens prepared with w/b of 0.15, cement content of 1100 kg/m^3 and silica fume content varying from 15 to 25%, as replacement of sand, is depicted in Figure 4.3. Again the compressive strength increased with increase in silica fume content. After 90 days of curing, the compressive strength of 15%, 20% and 25% silica fume RPC specimens was 136.7, 147, 154.4 MPa, respectively.

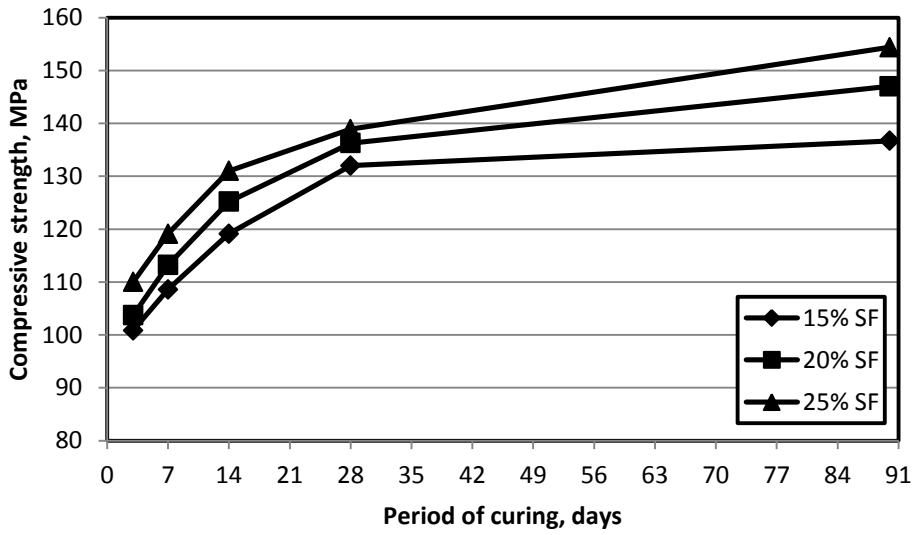

Figure 4.3: Compressive strength development for w/b of 0.15; CC of 1100 kg/m^3.

The compressive strength development in the RPC specimens prepared with w/b of 0.15, cement content of 1200 kg/m^3 and silica fume content varying from 15 to 25%, as replacement of sand, is depicted in Figure 4.4. The compressive strength increased with age in all the concrete specimens. The compressive strength in all specimens was almost the same. After 90 days of curing, the compressive strength of 15%, 20 % and 25% silica fume RPC specimens was 136.4, 140, 143.8 MPa, respectively.

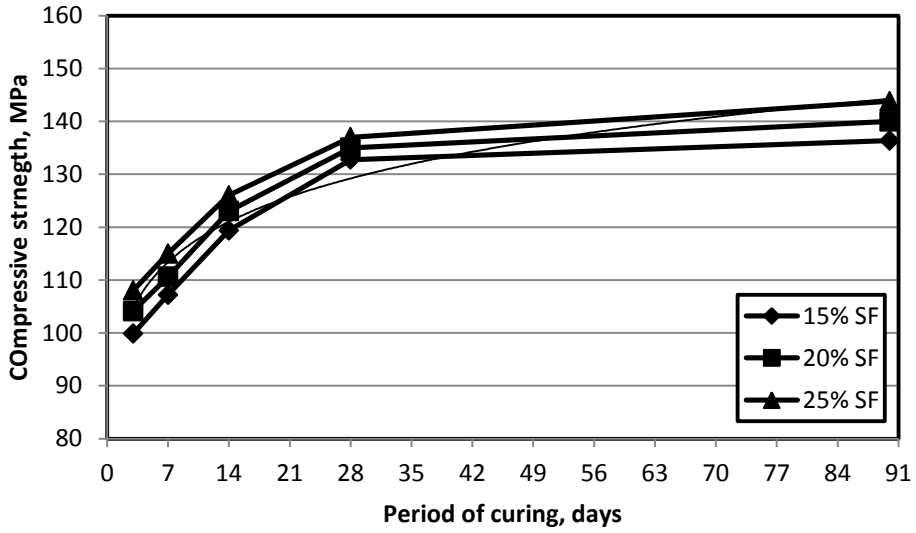

Figure 4.4: Compressive strength development for w/b of 0.15; CC of 1200 kg/m^3.

The compressive strength development in the RPC specimens prepared with w/b of 0.175, cement content of 1000 kg/m^3 and silica fume content varying from 15 to 25%, as replacement of sand, is depicted in Figure 4.5. The compressive strength increased with age in all the specimens and these were the same in all specimens. After 90 days of curing, the compressive strength of 15%, 20 % and 25% silica fume RPC specimens was 142.0, 146.3 and 149 MPa, respectively.

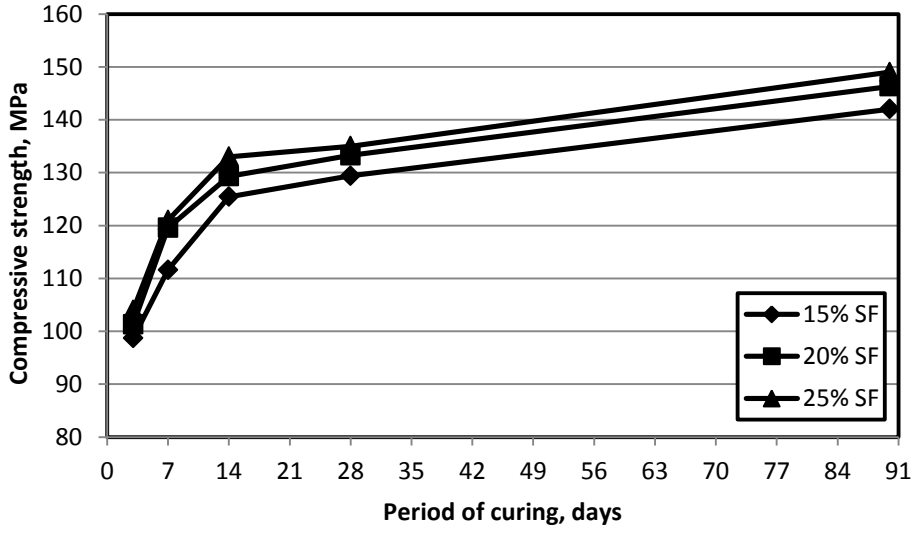

Figure 4.5: Compressive strength development for w/b of 0.175; CC of 1000 kg/m^3.

The compressive strength development in the RPC specimens prepared with w/b of 0.175, cement content of 1100 kg/m^3 and silica fume content varying from 15 to 25%, as replacement of sand, is depicted in Figure 4.6. The compressive strength increased with age in all the concrete specimens. The compressive strength development of 20 and 25% silica fume RPC was almost similar while strength of 15% silica fume was slightly less than the other two mixtures. After 90 days of curing, the compressive strength of 15%, 20 % and 25% silica fume RPC specimens was 140.0, 147.1 and 148.5 MPa, respectively.

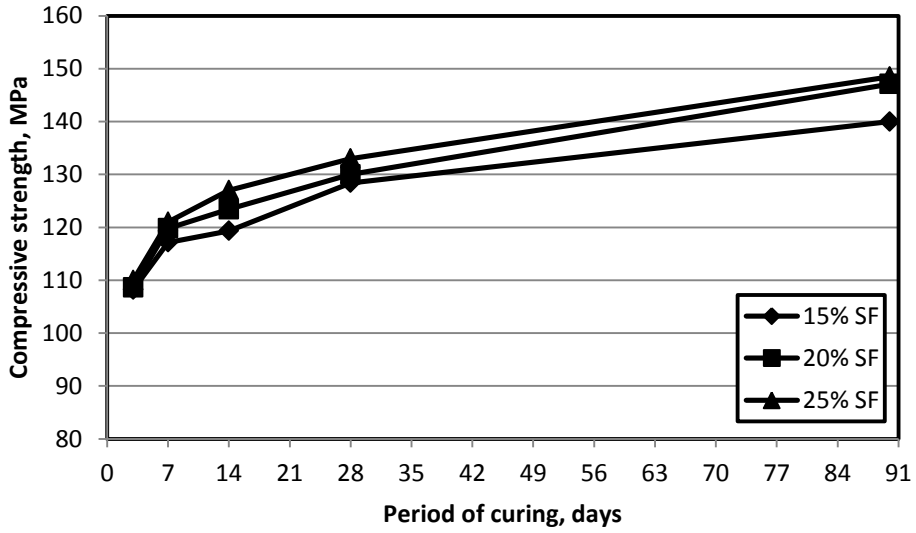

Figure 4.6: Compressive strength development for w/b of 0.175; CC of 1100 kg/m^3.

The compressive strength development in the RPC specimens prepared with w/b of 0.175, cement content of 1200 kg/m^3 and silica fume content varying from 15 to 25%, as replacement of sand, is depicted in Figure 4.7. The compressive strength increased with age in all the concrete specimens. The compressive strength of 20 and 25% silica fume RPC was almost similar up to 28 days while a significant increase was noted later in the specimens with 25% SF. RPC mixture containing 25 % silica fume exhibited higher ultimate compressive strength than the 15%, 20% silica fume RPC mixtures. After 90

days of curing, the compressive strength of 15%, 20 % and 25% silica fume RPC specimens was 133, 136.7 and 154.5 MPa, respectively.

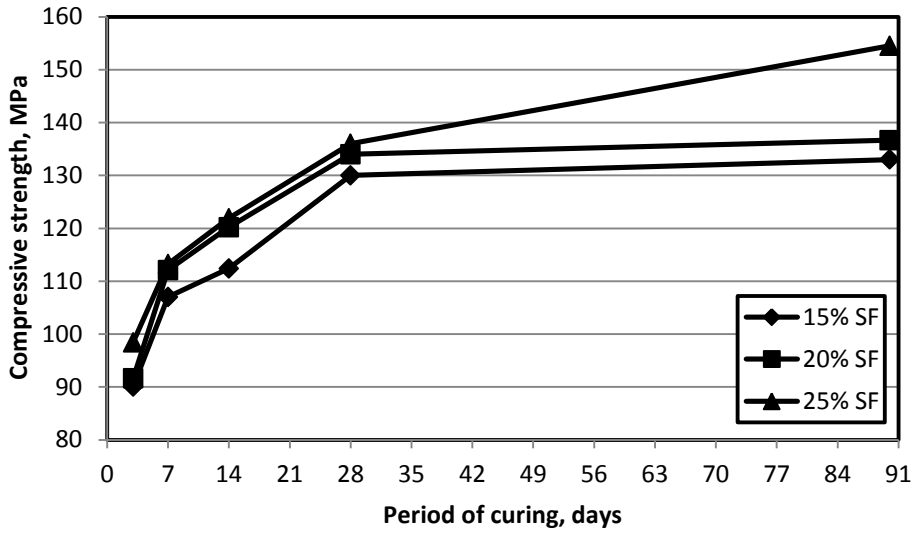

Figure 4.7: Compressive strength development for w/b of 0.175; CC of 1200 kg/m^3.

The compressive strength development in the RPC specimens prepared with w/b of 0.20, cement content of 1000 kg/m^3 and silica fume content varying from 15 to 25%, as replacement of sand, is depicted in Figure 4.8. The compressive strength increased with age in all the concrete specimens. The compressive strength development of all the specimens was almost similar up to 14 days. After that time, the compressive strength of 20 and 25% SF specimens was more than that of 15% SF specimens. After 90 days of curing, the compressive strength of 15%, 20% and 25% silica fume RPC specimens was 130.3, 140.1 and 143.8 MPa, respectively.

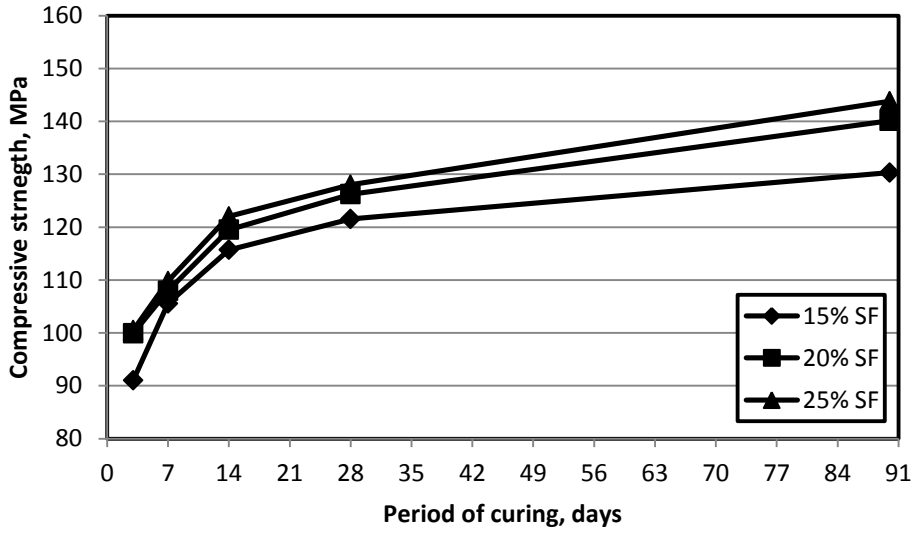

Figure 4.8: Compressive strength development for w/b of 0.20; CC of 1000 kg/m^3.

The compressive strength development in the RPC specimens prepared with w/b of 0.20, cement content of 1100 kg/m^3 and silica fume content varying from 15 to 25%, as replacement of sand, is depicted in Figure 4.9. The compressive strength increased with age in all the concrete specimens. The compressive strength was almost similar in all the specimens. After 90 days of curing, the compressive strength of 15%, 20 % and 25% silica fume RPC specimens was 130.9, 133.3 and 136.6 MPa, respectively.

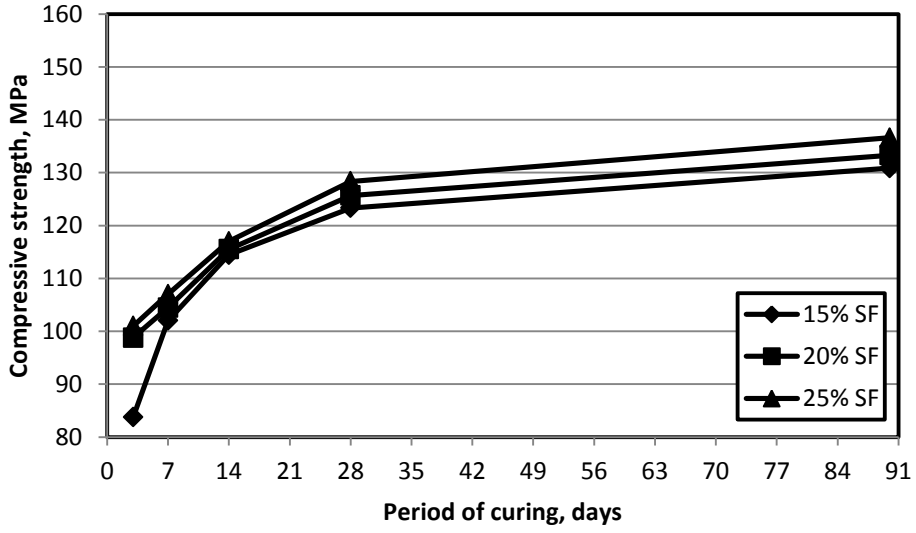

Figure 4.9: Compressive strength development for w/b of 0.20; CC of 1100 kg/m^3.

The compressive strength development in the RPC specimens prepared with w/b of 0.20, cement content of 1200 kg/m^3 and silica fume content varying from 15 to 25%, as replacement of sand, is depicted in Figure 4.10. The compressive strength increased with age in all the concrete specimens. The compressive strength development of 20 and 25% silica fume RPC was almost similar. After 90 days of curing, the compressive strength of 15%, 20 % and 25% silica fume RPC specimens was 138.3, 142.8 and 144 MPa, respectively.

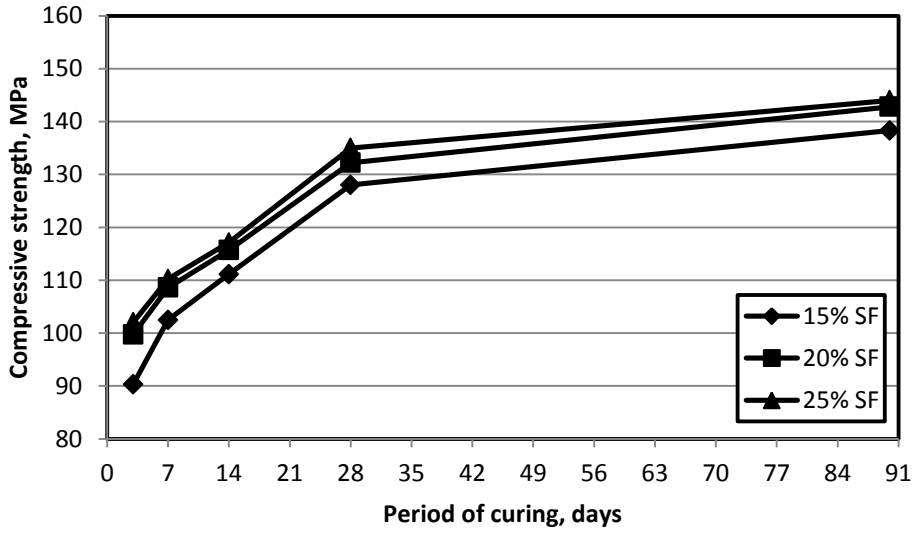

Figure 4.10: Compressive strength development for w/b of 0.20; CC of 1200 kg/m^3.

4.2.2 28-day compressive strength variation with mixture variables

The 28-day compressive strength in the RPC specimens prepared with w/b of 0.15, cement content of 1000 kg/m^3 and silica fume content varying from 15 to 25%, as replacement of sand, is depicted in Figure 4.11. The compressive strength of RPC specimens shows increment with increase in quantity of silica fume %. While, there is significant increase in the compressive strength of 20% silica fume RPC mixtures,

compared to 15% silica fume RPC mixture, such an increase was not noticed in the 25% SF specimens. The compressive strength of 15%, 20 % and 25% silica fume RPC specimens was 132, 135.6 and 136.9 MPa, respectively.

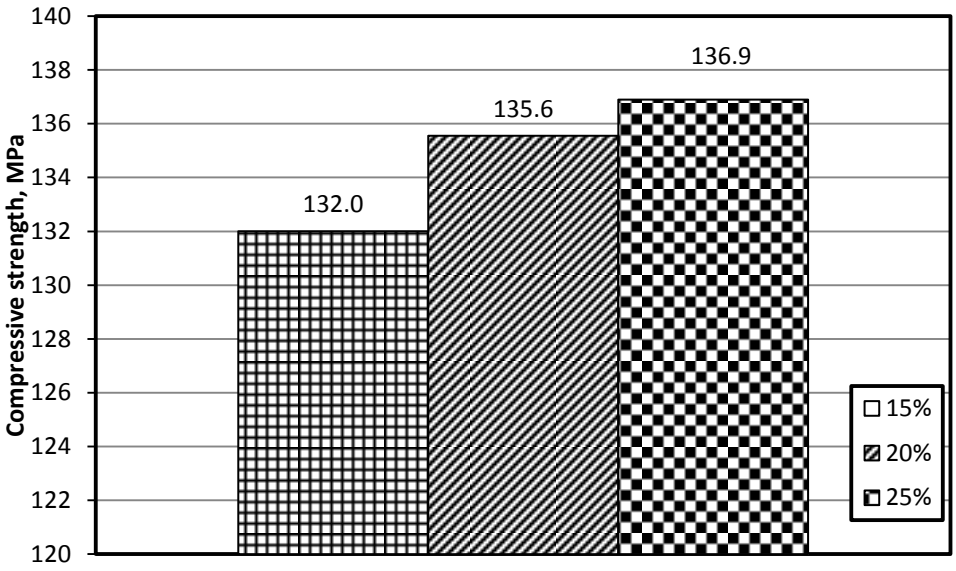

Figure 4.11: 28 day Compressive strength for w/b of 0.15; CC of 1000 kg/m^3.

The 28-day compressive strength in the RPC specimens with w/b of 0.15, cement content of 1100 kg/m^3 and silica fume content varying from 15 to 25%, as replacement of sand, is depicted in Figure 4.12. The compressive strength of RPC specimens increases with increase in quantity of silica fume %. However, there is significant increase in 20% and 25% silica fume RPC mixtures compared to 15% silica fume RPC specimens. The compressive strength of 15%, 20 % and 25% silica fume RPC specimens were 132, 136.3 and 138.9 MPa, respectively.

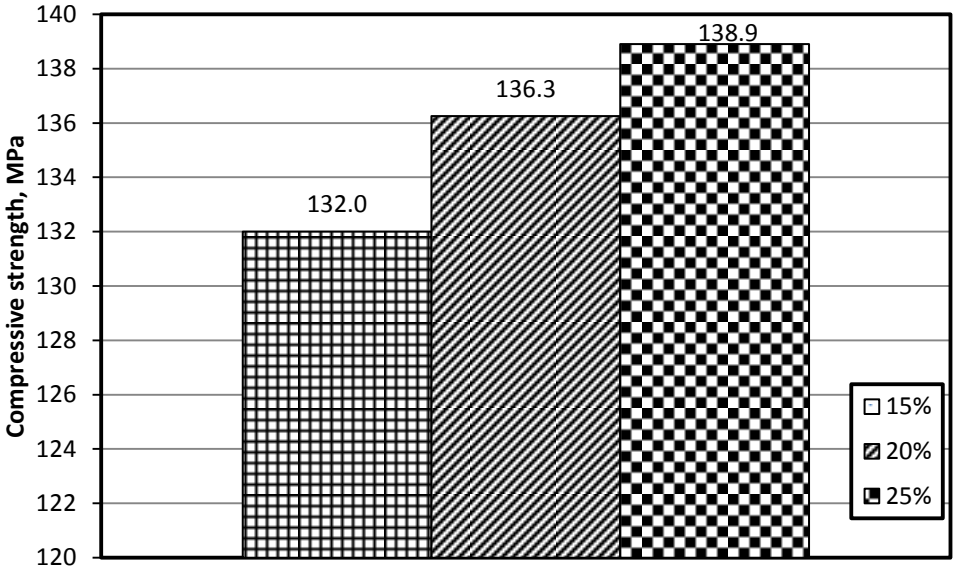

Figure 4.12: 28 day Compressive strength for w/b of 0.15; CC of 1100 kg/m^3.

The 28-day compressive strength in the RPC specimens prepared with w/b of 0.15, cement content of 1200 kg/m^3 and silica fume content varying from 15 to 25%, as replacement of sand, is depicted in Figure 4.13.The compressive strength of RPC specimens increases with increase in the quantity of silica fume; the increase being gradual with increasing silica fume content. The compressive strength of 15%, 20 % and 25% silica fume RPC specimens were 132.8, 135 and 137 MPa, respectively.

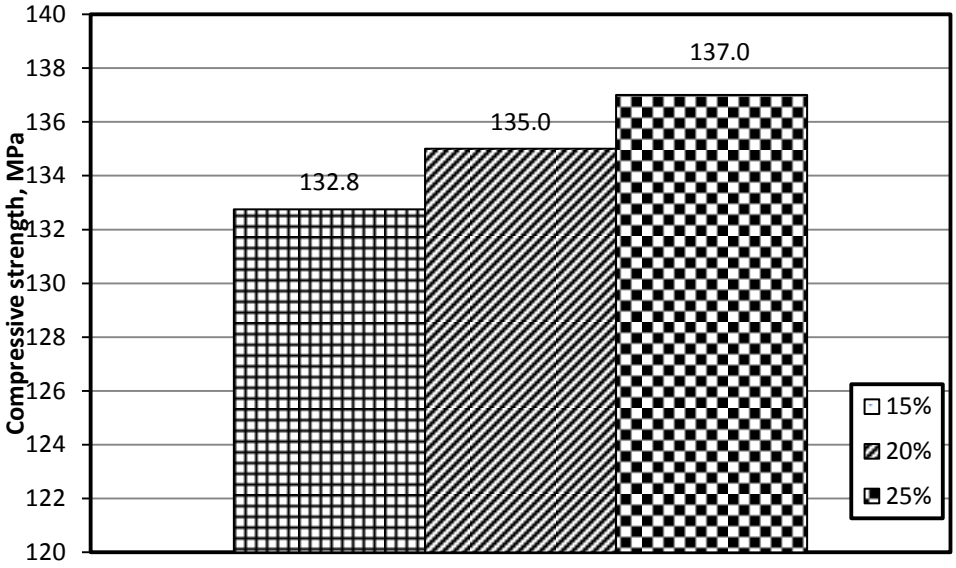

Figure 4.13: 28 day Compressive strength for w/b of 0.15; CC of 1200 kg/m^3.

The 28-day compressive strength in the RPC specimens with w/b of 0.175, cement content of 1000 kg/m^3 and silica fume content varying from 15 to 25%, as replacement of sand, is depicted in Figure 4.14. The compressive strength of RPC specimens increases with increase in the quantity of silica fume ass in the other batches the compressive strength. There is significant increase in 20% and 25% silica fume RPC mixtures when compared to 15% silica fume RPC specimens. The compressive strength of 15%, 20% and 25% silica fume RPC specimens was 129.4, 133.2 and 135 MPa, respectively.

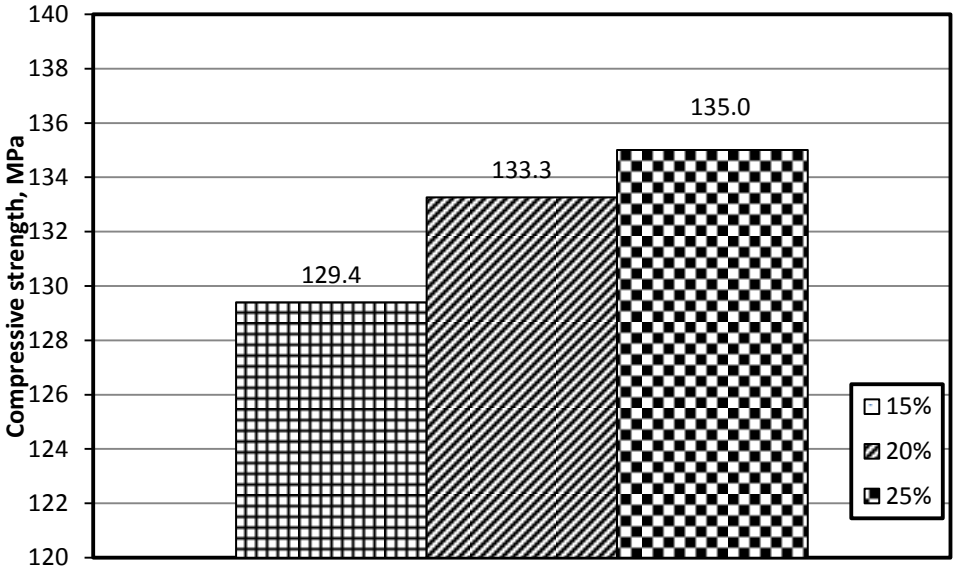

Figure 4.14: 28 day Compressive strength for w/b of 0.175; CC of 1000 kg/m^3.

The 28-day compressive strength in the RPC specimens with w/b of 0.175, cement content of 1100 kg/m^3 and silica fume content varying from 15 to 25%, as replacement of sand, is depicted in Figure 4.15. The compressive strength of RPC specimens increases with increase in silica fume quantity. The increase in 25% silica fume specimens was more than that of 20 % SF specimens. The compressive strength of 15%, 20 % and 25% silica fume RPC specimens was 128.4, 130 and 133 MPa, respectively.

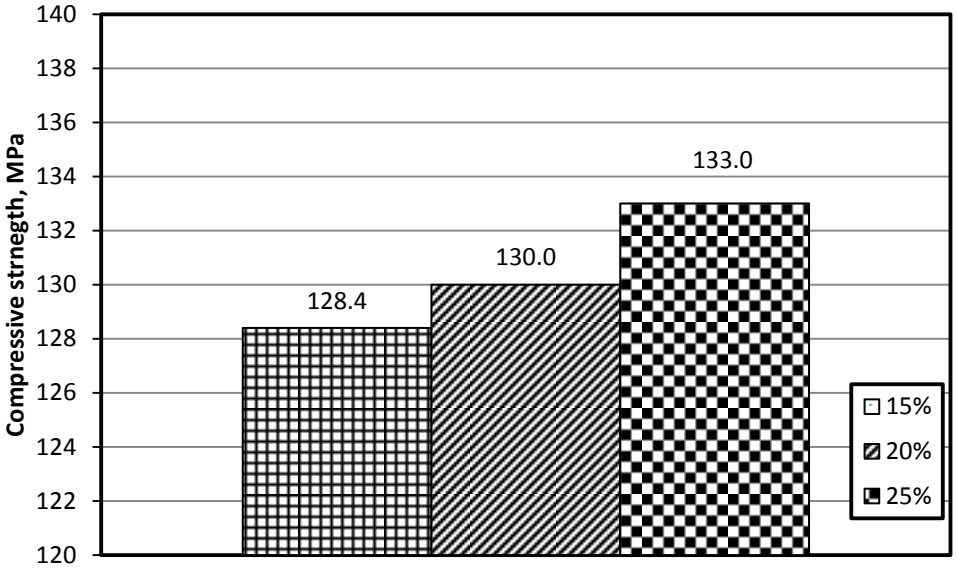

Figure 4.15: 28 day Compressive strength for w/b of 0.175; CC of 1100 kg/m^3.

The 28-day compressive strength in the RPC specimens with w/b of 0.175, cement content of 1200 kg/m^3 and silica fume content varying from 15 to 25%, as replacement of sand, is depicted in Figure 4.16. The compressive strength of RPC specimens increases with increase in silica fume quantity. There was significant increase in 20% silica fume RPC mixtures compared to 15% silica fume RPC specimens. After 90 days of curing, the compressive strength of 15%, 20 % and 25% silica fume RPC specimens was 130, 134 and 136 MPa, respectively.

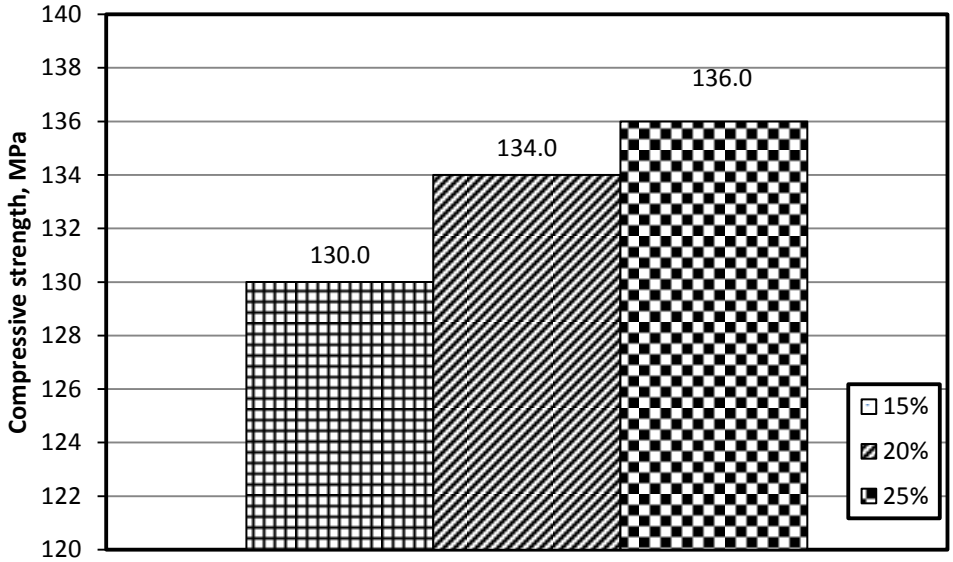

Figure 4.16: 28 day Compressive strength for w/b of 0.175; CC of 1200 kg/m^3.

The 28-day compressive strength in the RPC specimens prepared with w/b of 0.20, cement content of 1000 kg/m^3 and silica fume content varying from 15 to 25%, as replacement of sand, is depicted in Figure 4.17. A significant increase in strength was noted as the SF was increased from 15% to 25%. The compressive strength of 15%, 20 % and 25% silica fume RPC specimens were 121.5, 126.2, 128 MPa, respectively.

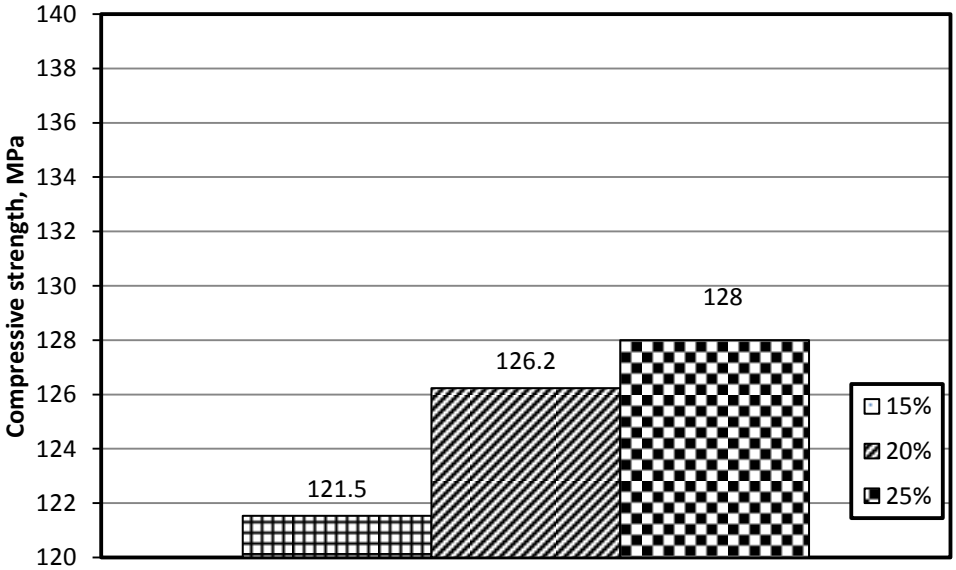

Figure 4.17: 28 day Compressive strength for w/b of 0.20; CC of 1000 kg/m^3.

The 28-day compressive strength in the RPC specimens with w/b of 0.20, cement content of 1100 kg/m^3 and silica fume content varying from 15 to 25%, as replacement of sand, is depicted in Figure 4.18. A gradual increase in the strength was noted with increasing silica fume content. The compressive strength of 15%, 20 % and 25% silica fume RPC specimens were 123.3, 125.6 and 128.3 MPa, respectively.

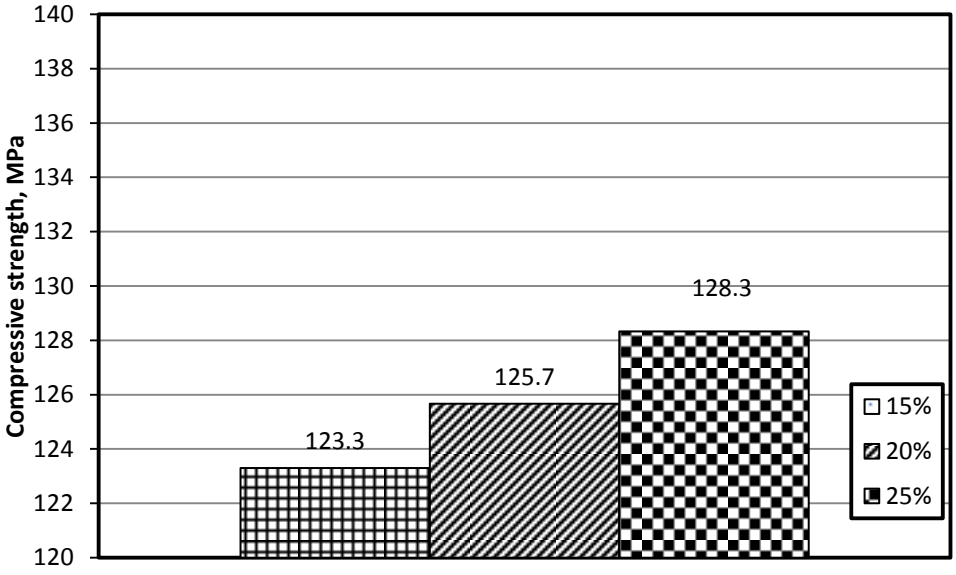

Figure 4.18: 28 day Compressive strength for w/b of 0.20; CC of 1100 kg/m^3.

The 28-day compressive strength in the RPC specimens with w/b of 0.20, cement content of 1200 kg/m^3 and silica fume content varying from 15 to 25%, as replacement of sand, is depicted in Figure 4.19. The compressive strength of RPC specimens increased with increase in silica fume quantity. However, there is significant increase in 20% and 25% silica fume RPC mixtures when compared to 15% silica fume RPC mixture. The compressive strength of 15%, 20 % and 25% silica fume RPC specimens was 128, 132.2 and 135 MPa, respectively.

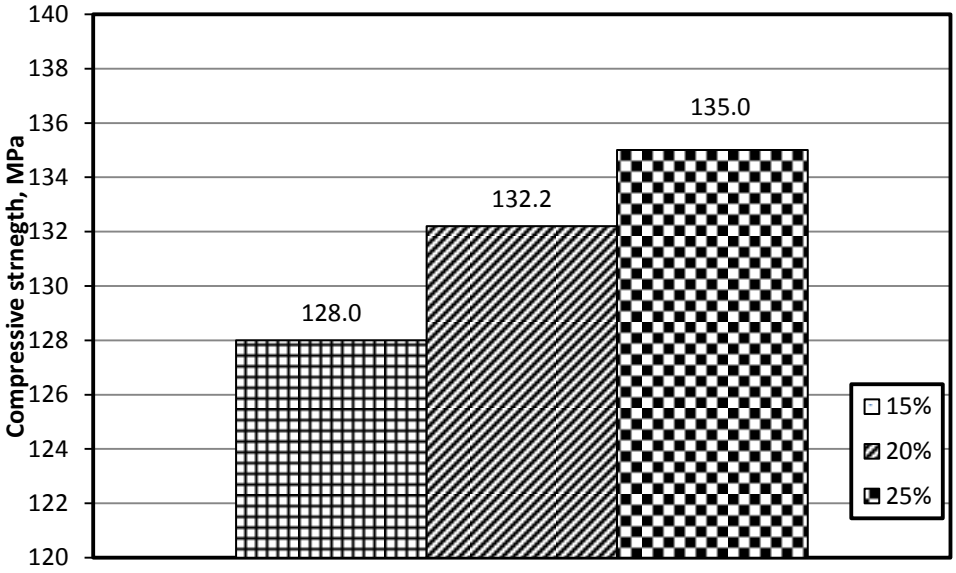

Figure 4.19: 28 day Compressive strength for w/b of 0.20; CC of 1200 kg/m^3.

The 28-day compressive strength in the RPC specimens prepared with cement content of 1000 kg/m^3, different w/b ratios, and silica fume content varying from 15 to 25%, as replacement of sand, is depicted in Figure 4.20. There was almost linear increase in the compressive strength of RPC with increasing silica fume content. As expected, the compressive strength increased with a decrease in the w/b ratio. However, there was nor much difference in the compressive strength of RPC with w/b ratio of 0.15 and 0.175. The compressive strength of RPC with w/b ratios of 0.15 was in the range of 132 to 137 MPa, while in the specimens with a w/b ratio of 0.175 it was in the range 130 to 136 MPa. The compressive strength of RPC specimens with a w/b ratio of 0.20 was in the range of 122 to 128 MPa. These results show the significance of w/b ratio on the compressive strength of RPC.

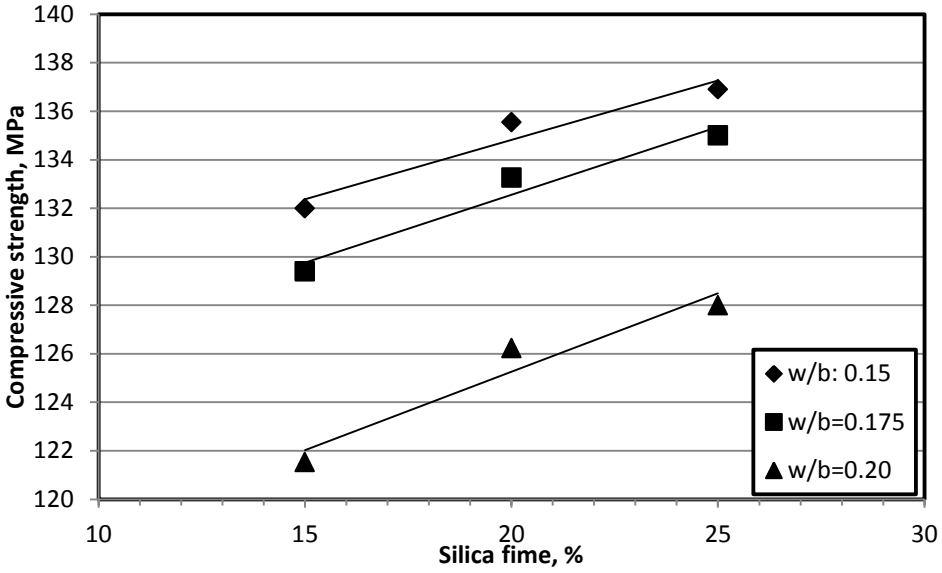

Figure 4.20: 28 day Compressive strength for CC: 1000 kg/m^3 for different w/b and silica fume.

The 28-day compressive strength in the RPC specimens with cement content of 1100 kg/m^3, different w/b ratios, and silica fume content varying from 15 to 25%, as replacement of sand, is depicted in Figure 4.21. The compressive strength of this batch of specimens also increased with increasing silica fume content. For specimens with similar silica fume content the compressive strength increased with decreasing w/b ratio. The compressive strength of specimens with a w/b ratio of 0.15 was in the range of 132 to 139 MPa, while it was in the range of 128 to 133 MPa in the specimens prepared with a w/b ratio of 0.175. The compressive strength of RPC specimens prepared with w/b ratio of 0.20 was in the range of 123 to 129 MPa.

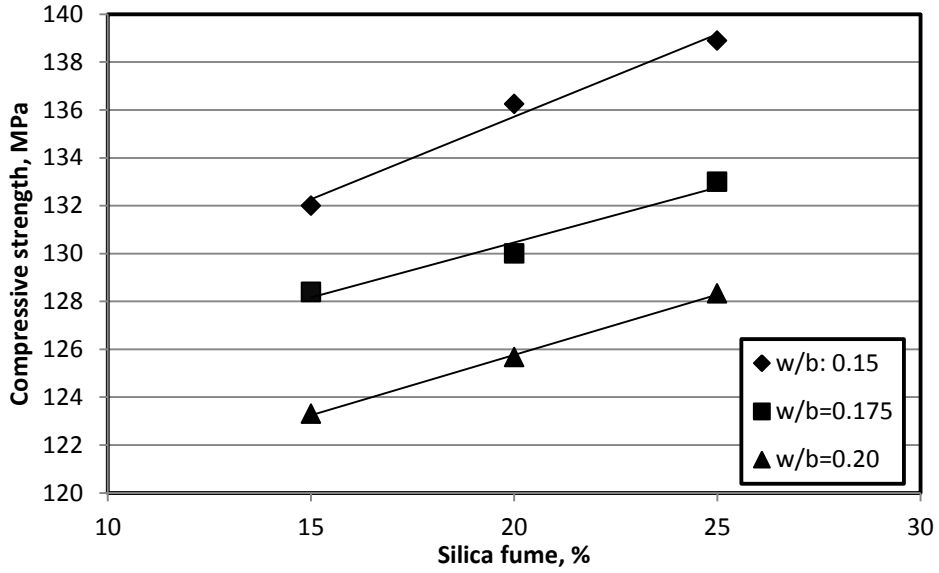

Figure 4.21: 28 day Compressive strength for CC: 1100 kg/m^3 for different w/b and silica fume.

The 28-day compressive strength of RPC specimens with cement content of 1000 kg/m^3, varying w/b ratios, and silica fume content varying from 15 to 25%, as replacement of sand, is depicted in Figure 4.22. The compressive strength increased with increase in silica fume content and decreasing w/b ratio. However, there was not difference in the compressive strength of specimens prepared with 25% silica fume.

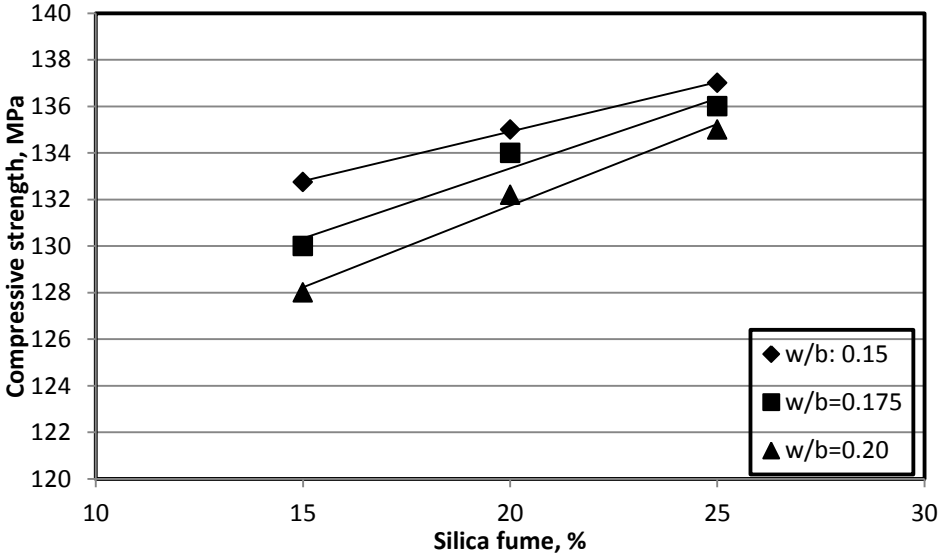

Figure 4.22: 28 day Compressive strength for CC: 1200 kg/m^3 for different w/b and silica fume %.

4.2.3 Combined Effect of Curing Duration and Mix Variables on Compressive strength

In order to show the combined effect of curing period and mixture variables on compressive strength, the values of compressive strength of all 27 mixtures at each curing period were plotted as shown in Figure 4.23. It can be observed from that the Figure 4.23 that there is increase in compressive strength with increase in the curing period. Also, the mix variables have significant effect on compressive strength at each curing period. The maximum effect of mix variables at a given curing period can be realized by the difference between minimum and maximum values of compressive strengths. The minimum and maximum values of compressive strengths for each curing period along with the percentage difference between minimum and maximum values are presented in Table 4-4.

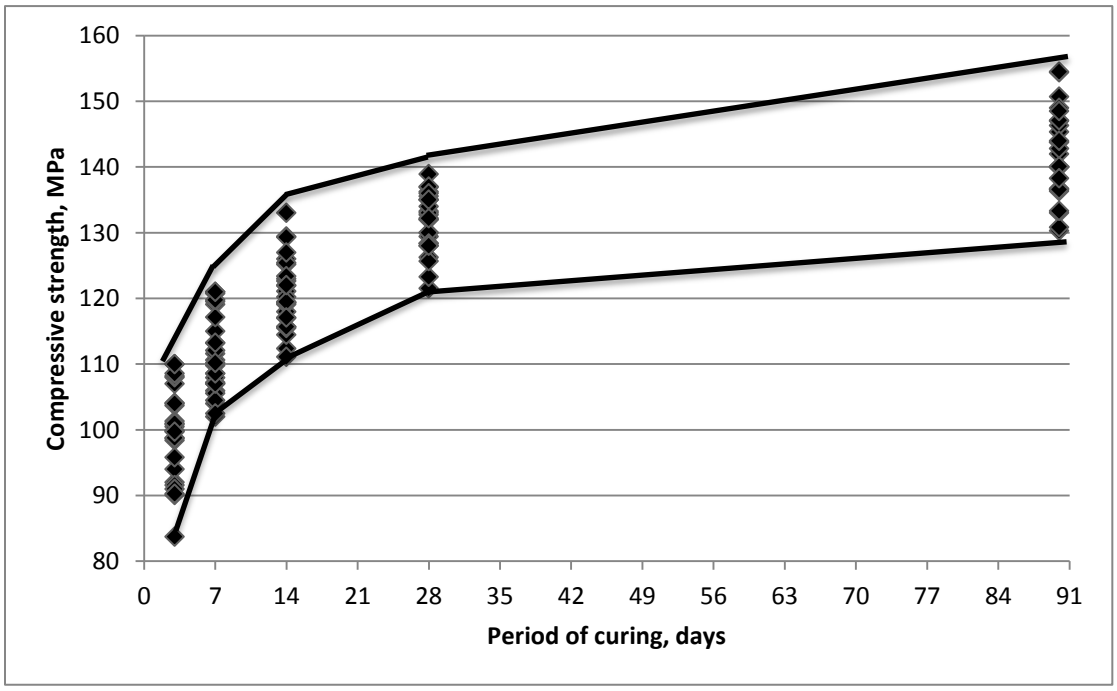

Figure 4.23: Compressive strength development for all the 27 RPC mixtures.

Table 4-4: Minimum and maximum compressive strength and mix details at various ages of curing.

Curing period (days)	Compressive strength (MPa)		Difference between Min. and Max. (%)
	Min.	Max.	
3	84	110	31
7	102	121	19
14	111	133	20
28	122	139	14
90	130	155	19

As observed from Table 4-4, the effect of the mix variables is highest at 3-days curing period and lowest for 28-days curing period because the difference in minimum and maximum values are 31% and 14%, respectively for 3-days and 28-days curing period. Effect of mix variables for 28-days curing period is almost half of that for 3-days cuing period. For other curing durations (7, 14, and 90 days) the difference in minimum and maximum values is almost same (around 20%).

4.3 MODULUS OF ELASTICITY

Table 4-5 lists the average values of secant modulus of RPC specimens after 28 days of water curing.

Table 4-5: Secant Modulus of Elasticity of RPC prepared with varying w/b ratios.

w/b	Mix #	Average Secant Modulus, (GPa)
0.15	M 1	51.0
	M 2	52.5
	M 3	53.0
	M 4	44.8
	M 5	46.5
	M 6	47.6
	M 7	45.7
	M 8	47.8
	M 9	48.4
0.175	M 10	48.3
	M 11	49.2
	M 12	50.0
	M 13	42.9
	M 14	44.4
	M 15	45.0
	M 16	41.2
	M 17	42.4
	M 18	45.7
0.20	M 19	40.3
	M 20	43.2
	M 21	44.5
	M 22	41.6
	M 23	42.0
	M 24	43.0
	M 25	40.0
	M 26	41.0
	M 27	42.5

The modulus of elasticity was in the range of 40 to 53 GPa.

Only one selected sample of the stress-strain response of the RPC samples tested at 28 days water curing is presented in Figure 4.24 and all the other test results for all specimens are shown in Appendix A.

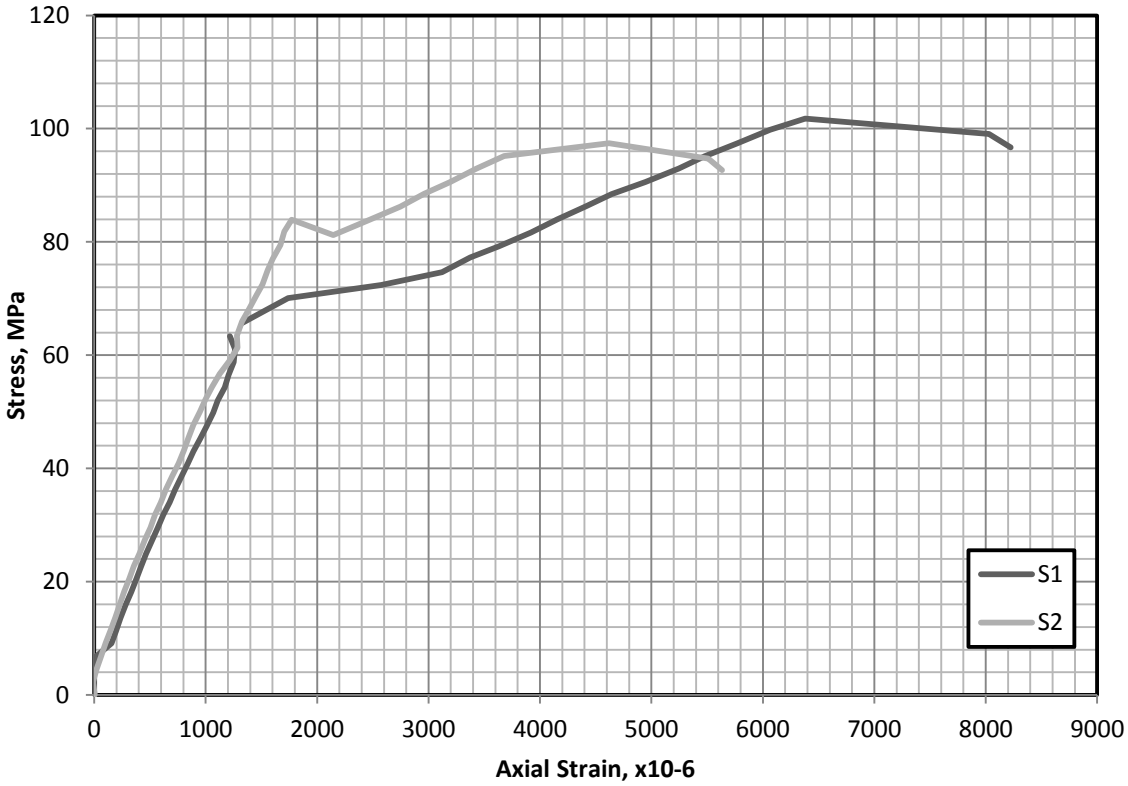

Figure 4.24: Selected stress-strain responses for 28 days water-cured RPC specimens.

The secant modulus of elasticity of RPC specimens with w/b of 0.15, cement content of 1000 kg/m^3 and silica fume content varying from 15 to 25%, as replacement of sand, is depicted in Figure 4.25. The secant modulus increased with the increase in silica fume. These values were 51, 52.5, 53 GPa, in the RPC specimens with 15, 20, 25 % silica fume.

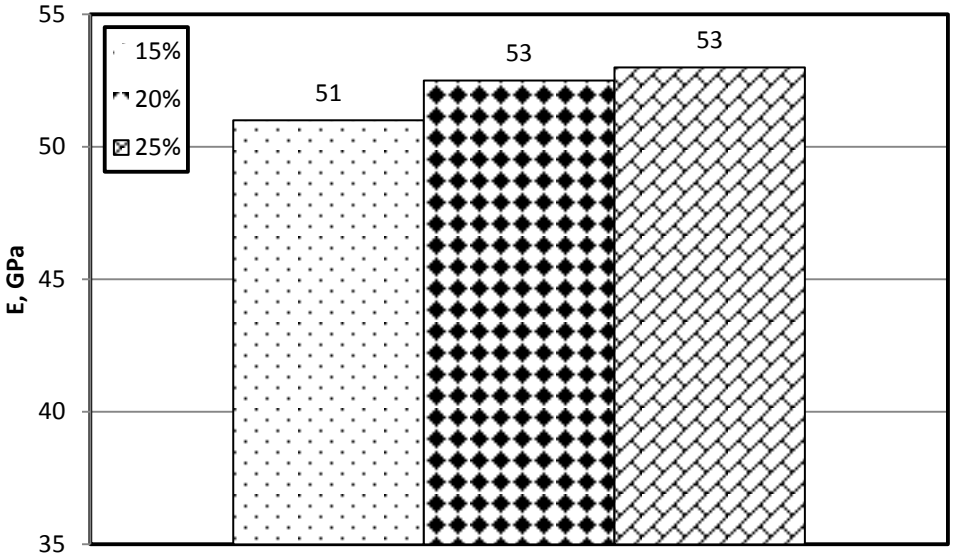

Figure 4.25: Secant Modulus for w/b of 0.15; CC of 1000 kg/m^3.

The secant modulus of elasticity of RPC specimens with w/b of 0.15, cement content of 1100 kg/m^3 and silica fume content varying from 15 to 25%, as replacement of sand, is depicted in Figure 4.26. The secant modulus of RPC specimens shows increment with increasing silica fume quantity. There is significant increase in 20% and 25% silica fume RPC mixtures when compared to 15% silica fume RPC mixture. The secant modulus of 15%, 20 % and 25% silica fume RPC specimens was 44.8, 46.5 and 47.6 GPa, respectively.

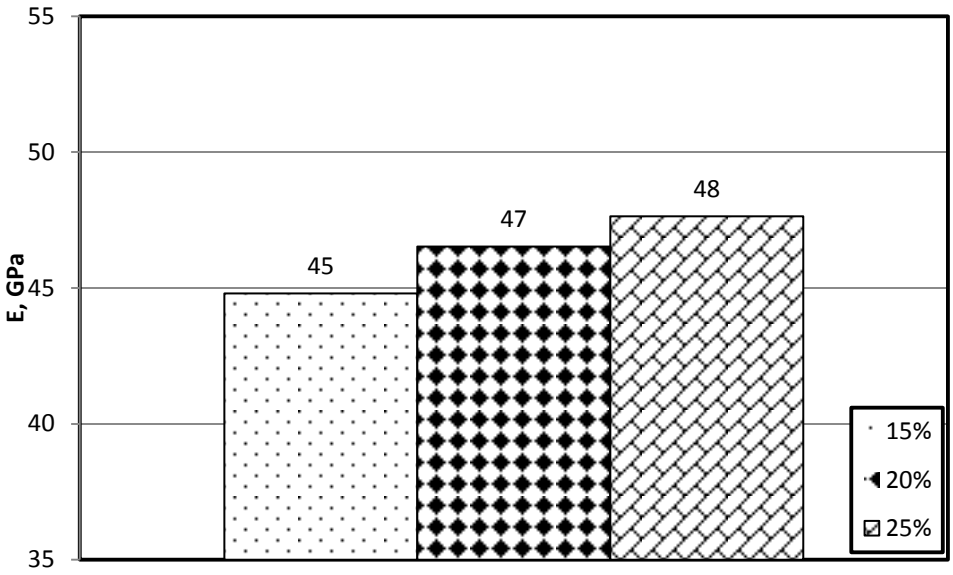

Figure 4.26: Secant Modulus for w/b of 0.15; CC of 1100 kg/m^3.

The secant modulus of elasticity of RPC specimens prepared with w/b of 0.15, cement content of 1200 kg/m^3 and silica fume content varying from 15 to 25%, as replacement of sand, is depicted in Figure 4.27. As in the other batch the secant modulus increased with increase in silica fume %. The secant modulus of 15%, 20 % and 25% silica fume RPC specimens was 45.7, 47.8 and 48.4 GPa, respectively.

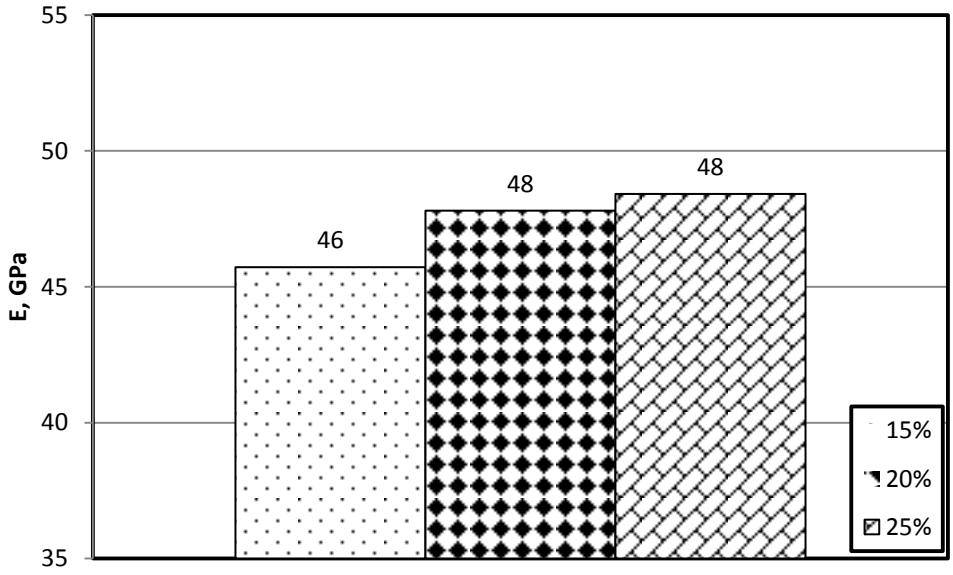

Figure 4.27: Secant Modulus for w/b of 0.15; CC of 1200 kg/m^3.

The secant modulus of elasticity in the RPC specimens with w/b of 0.175, cement content of 1000 kg/m^3 and silica fume content varying from 15 to 25%, as replacement of sand, is depicted in Figure 4.28. Though the secant modulus of RPC specimens increased with increase in silica fume quantity, the change in these values was marginal. The secant modulus of 15%, 20 % and 25% silica fume RPC specimens was 48.3, 49.2 and 50 GPa, respectively.

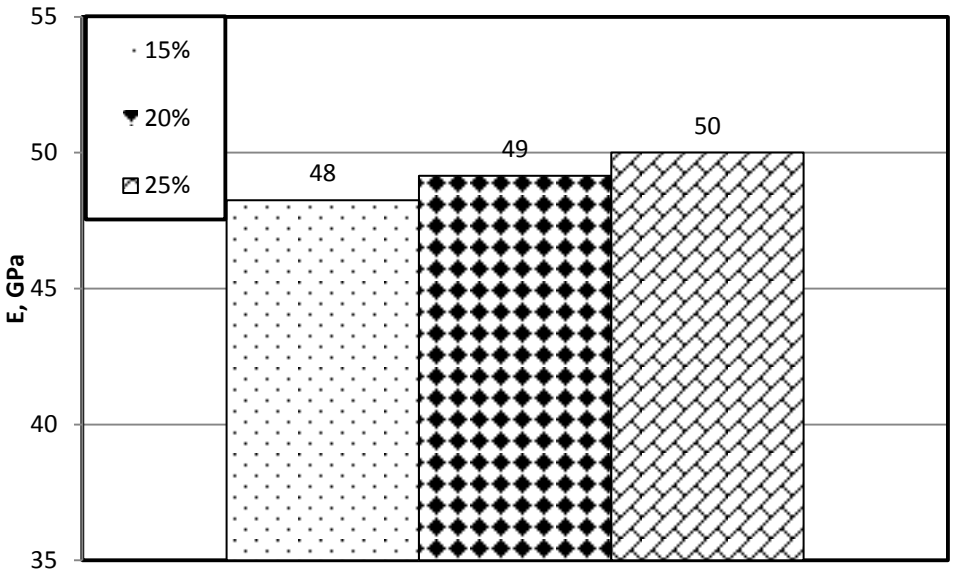

Figure 4.28: Secant Modulus for w/b of 0.175; CC of 1000 kg/m^3.

The secant modulus of elasticity in the RPC specimens prepared with w/b of 0.175, cement content of 1100 kg/m^3 and silica fume content varying from 15 to 25%, as replacement of sand, is depicted in Figure 4.29. The secant modulus of 25% SF RPC was more than that of 15 and 25 % SF specimens. The secant modulus of 15%, 20% and 25% silica fume RPC specimens was 42.9, 44.4 and 45 GPa, respectively.

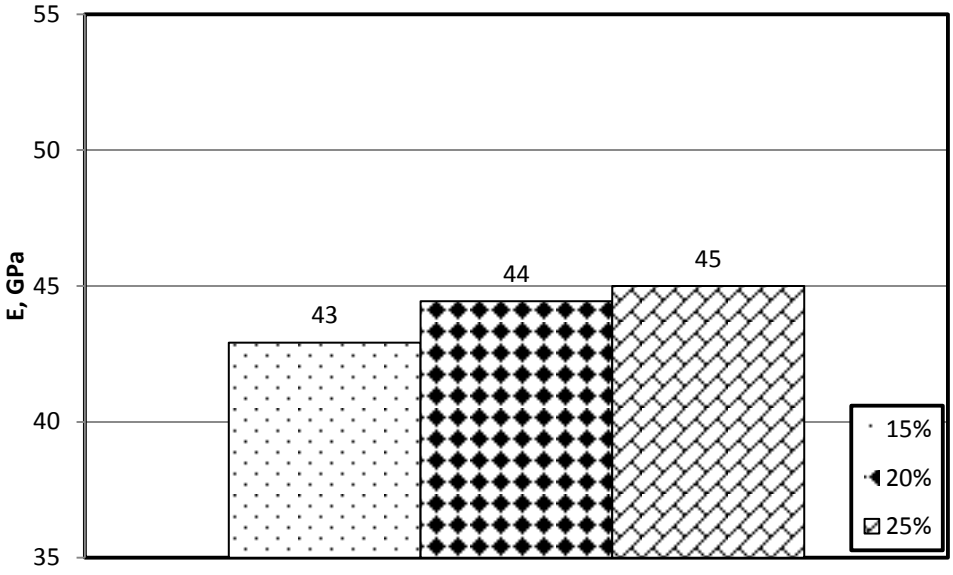

Figure 4.29: Secant Modulus for w/b of 0.175; CC of 1100 kg/m^3.

The secant modulus of elasticity in the RPC specimens prepared with w/b of 0.175, cement content of 1200 kg/m^3 and silica fume content varying from 15 to 25%, as replacement of sand, is depicted in Figure 4.30. While, the secant modulus of 15 and 20% silica fume was almost similar, there is significant increase in 25% silica fume RPC specimens. The secant modulus of 15%, 20% and 25% silica fume RPC specimens was 41.2, 42.4 and 45.7 GPa, respectively.

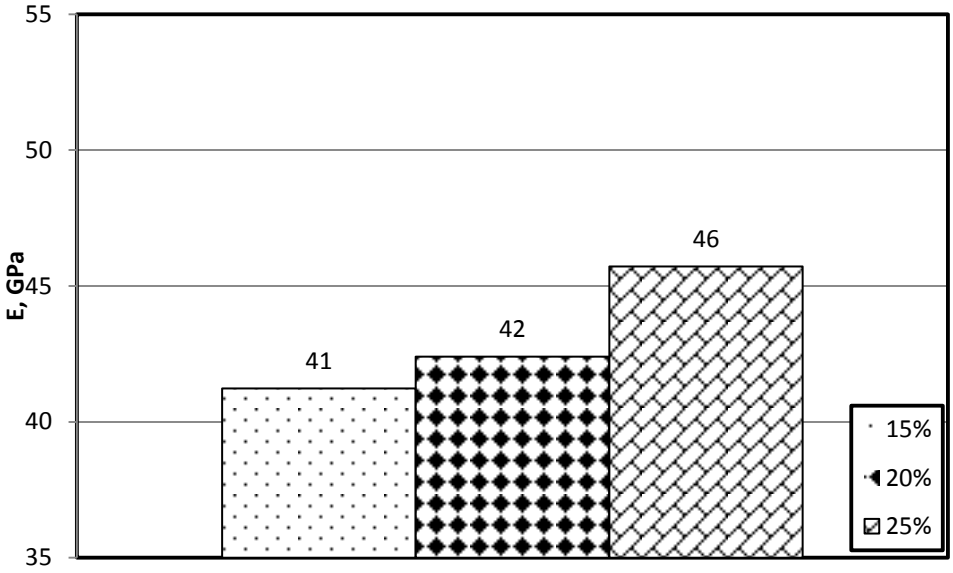

Figure 4.30: Secant Modulus for w/b of 0.175; CC of 1200 kg/m^3.

The secant modulus of elasticity in the RPC specimens prepared with w/b of 0.20, cement content of 1000 kg/m^3 and silica fume content varying from 15 to 25%, as replacement of sand, is depicted in Figure 4.31. The secant modulus of RPC specimens increased with increase in silica fume content. The secant modulus of 15%, 20 % and 25% silica fume RPC specimens was 40.3, 43.2 and 44.5 GPa, respectively.

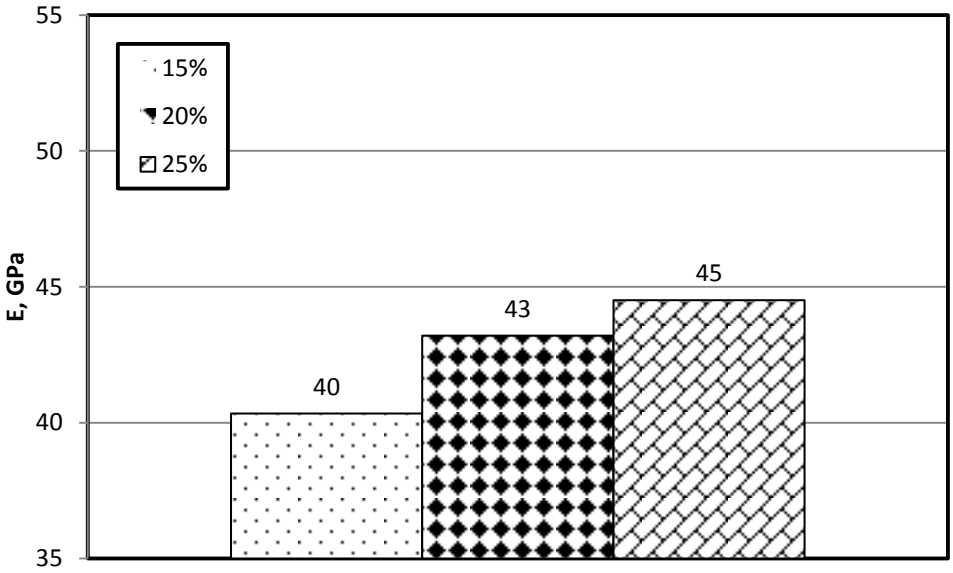

Figure 4.31: Secant Modulus for w/b of 0.20; CC of 1000 kg/m^3.

The secant modulus of elasticity in the RPC specimens prepared with w/b of 0.20, cement content of 1100 kg/m^3 and silica fume content varying from 15 to 25%, as replacement of sand, is depicted in Figure 4.32. The secant modulus increases with increase in silica fume content. The secant modulus of 15%, 20% and 25% silica fume RPC specimens was 41.6, 42 and 43 GPa, respectively.

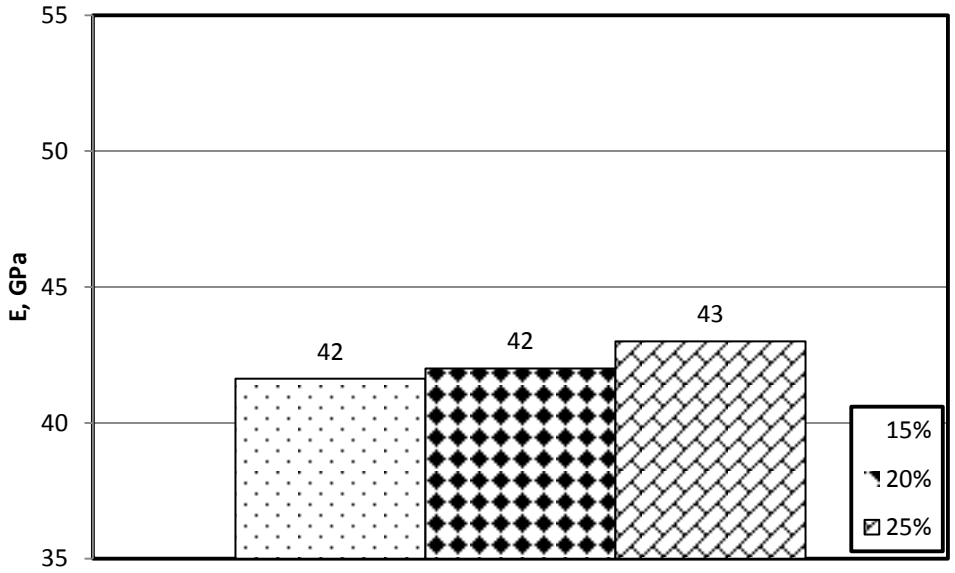

Figure 4.32: Secant Modulus for w/b of 0.20; CC of 1100 kg/m^3.

The secant modulus of elasticity in the RPC specimens prepared with w/b of 0.20, cement content of 1200 kg/m^3 and silica fume content varying from 15 to 25%, as replacement of sand, is depicted in Figure 4.33. The secant modulus increases with increase in silica fume. The secant modulus of 15%, 20 % and 25% silica fume RPC specimens was 40, 41 and 42.5 GPa, respectively.

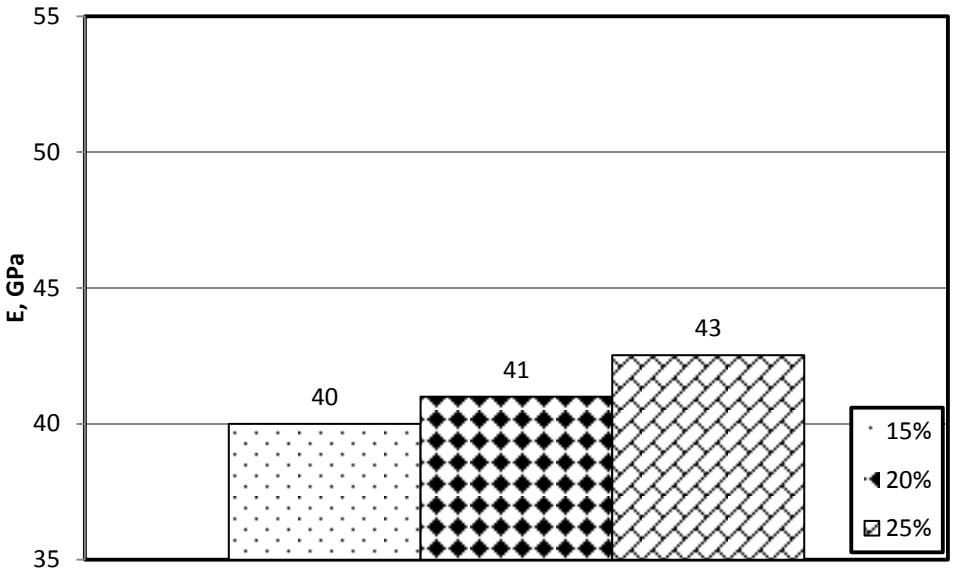

Figure 4.33: Secant Modulus for w/b of 0.20; CC of 1200 kg/m^3.

The secant modulus of the RPC specimens prepared with cement content of 1000 kg/m^3, varying w/b ratios, and silica fume content varying from 15 to 25%, as replacement of sand, is depicted in Figure 4.34. The secant modulus increases with increase in silica fume quantity. While there is marginal difference in the secant modulus of specimens prepared with w/b ratio of 0.15 and 0.175, there was significant change between those prepared with w/b ratio of 0.175 and 0.20. The modulus of elasticity of RPC specimens with w/b ratio of 0.15 was in the range of 51 to 53 GPa while the values in the specimens worth w/b ratio were in the range of 48.5 to 49.5 GPa. The modulus of elasticity of RPC specimens prepared with w/b ratio of 0.20 was in the range of 41 to 45 GPa.

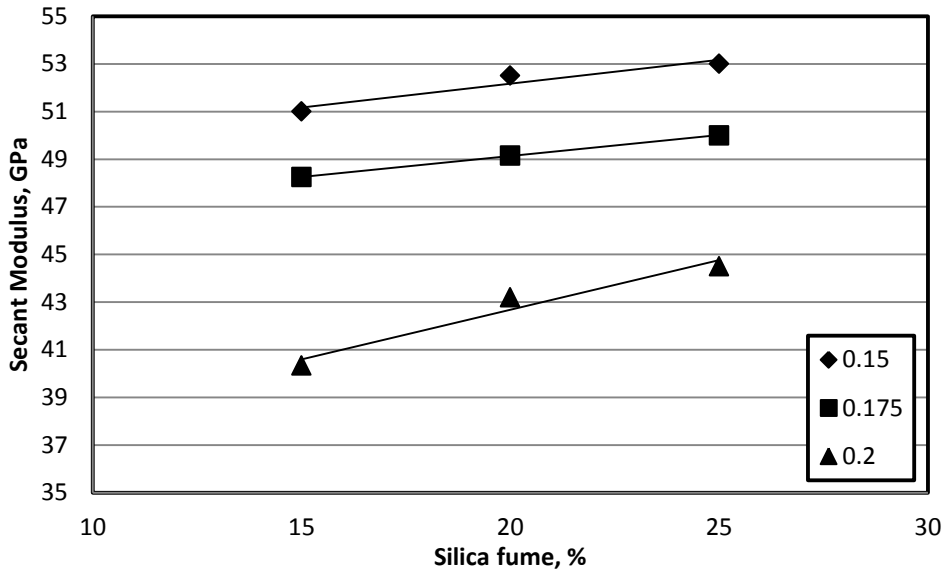

Figure 4.34: Secant modulus for CC: 1000 kg/m^3 for different w/b ratio and silica fume.

The secant modulus in the RPC specimens with cement content of1100 kg/m^3, different w/b ratios, and silica fume content varying from 15 to 25%, as replacement of sand, is depicted in Figure 4.35. While there is small marginal difference in the secant modulus of specimens prepared with w/b ratio of 0.15 and 0.175, there was significant change between those prepared with w/b ratio of 0.175 and 0.20. The modulus of elasticity of RPC specimens with w/b ratio of 0.15 was in the range of 51 to 53 GPa while the values in the specimens worth w/b ratio were in the range of 48.5 to 49.5 GPa. The modulus of elasticity of RPC specimens prepared with w/b ratio of 0.20 was in the range of 41 to 45 GPa.

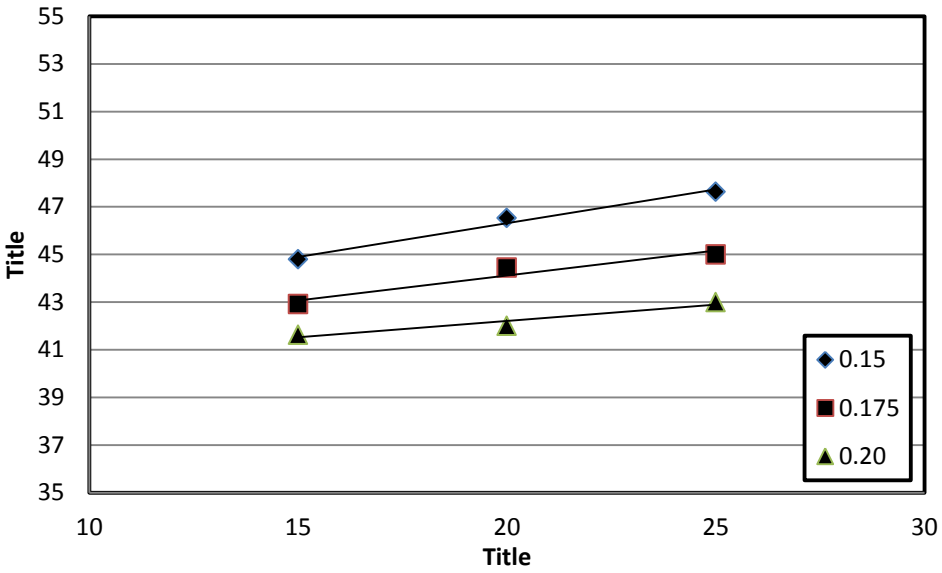

Figure 4.35: Secant modulus for CC: 1100 kg/m^3 for different w/b ratio and silica fume.

The secant modulus in the RPC specimens with cement content of 1100 kg/m^3, different w/b ratios, and silica fume content varying from 15 to 25%, as replacement of sand, is depicted in Figure 4.36. While there is small marginal difference in the secant modulus of specimens prepared with w/b ratio of 0.15 and 0.175, there was significant change between those prepared with w/b ratio of 0.175 and 0.20. The modulus of elasticity of RPC specimens with w/b ratio of 0.15 was in the range of 46 to 49 GPa while the values in the specimens with w/b ratio were in the range of 41 to 45 GPa. The modulus of elasticity of RPC specimens prepared with w/b ratio of 0.20 was in the range of 40 to 42 GPa.

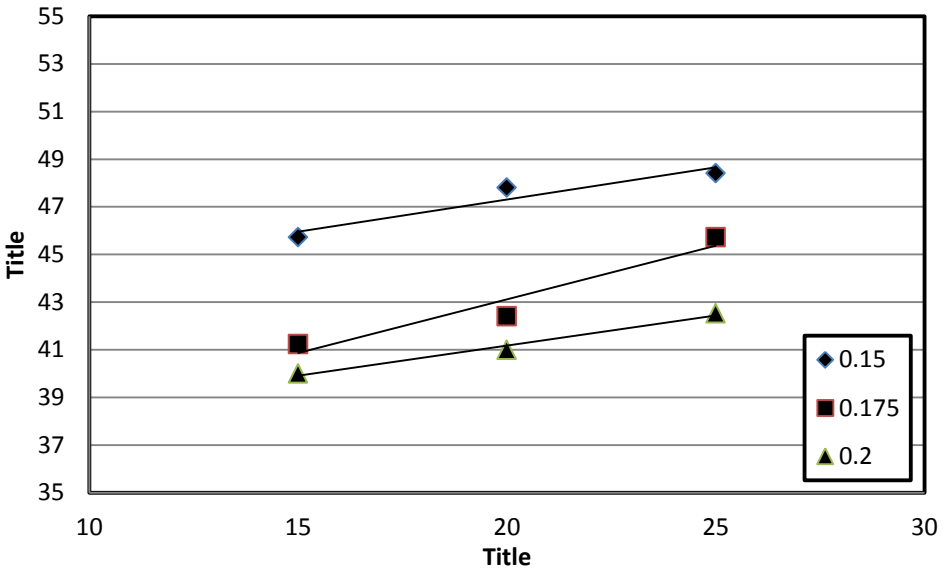

Figure 4.36: Secant modulus for CC: 1200 kg/m^3 for different w/b ratio and silica fume.

4.4 FLEXURAL TENSILE STRENGTH

Typical load-deflection plots of three replicate prisms of the same mixture, water-cured for 28 days, are shown in Figure 4.37. These plots were utilized to determine the modulus of rupture after 28 days water curing which are presented in Table 4-6.

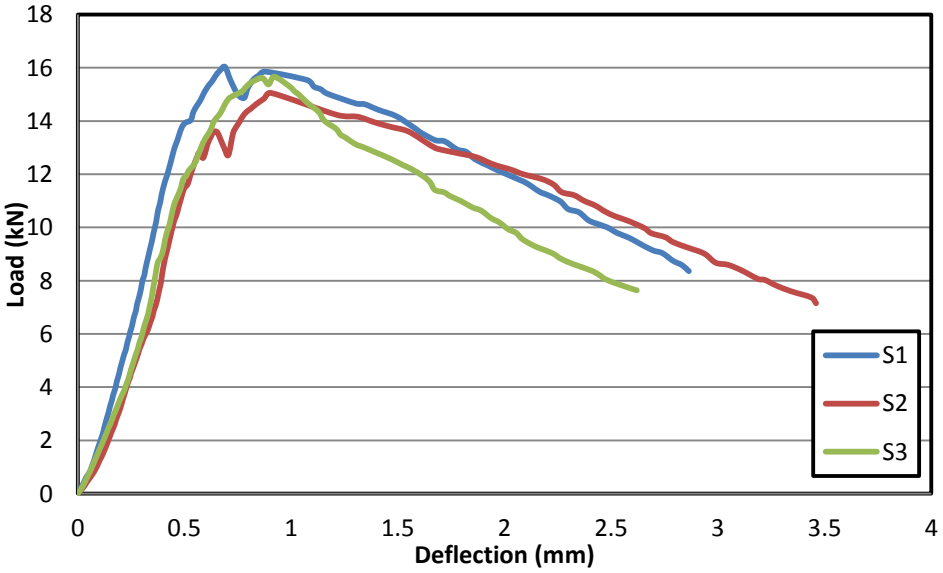

Figure 4.37: Load-deflection curves for three similar specimens tested after 28 days of water curing, belonging to a mixture with w/b of 0.15, cement content of 1200 kg/m^3 and 300 kg/m^3 silica fume.

Table 4-6: Modulus of Rupture for RPC mixtures for different w/b ratios.

w/b ratio	Mix	Average MOR (MPa)
0.15	M 1	33.0
	M 2	34.4
	M 3	36.6
	M 4	27.8
	M 5	29.8
	M 6	32.9
	M 7	26.0
	M 8	30.9
	M 9	34.8
0.175	M10	32.4
	M 11	34.0
	M 12	34.9
	M 13	24.5
	M 14	25.8
	M 15	28.0
	M 16	24.9
	M 17	26.5
	M 18	27.5
0.20	M 19	27.9
	M 20	30.7
	M 21	31.5
	M 22	23.0
	M 23	25.7
	M 24	27.1
	M 25	25.0
	M 26	26.0
	M 27	26.0

Tests have shown that after the cracking load, which is defined as the load corresponding to the development of first crack at the bottom (tension) face, the beams continue to carry more loads with an increase in the deflection until the maximum load (peak load) is reached. This increase in load is attributable to the presence of steel fibers, which become

fully mobilized as crack arrestor after first cracking. Following the attainment of peak load, softening mode of collapse takes place, exhibiting gradual decrease in load with increased deflection and crack-growth as shown in Figure 4.37.

The flexural behavior of fiber-reinforced RPC can be characterized by elastic deformation up to the first cracking load, followed by a further increase in deformation due to increase in the load (stiffening due to mobilization of fibers as crack arrestors) and subsequent prolonged softening after reaching the peak-load. The first cracking load corresponds approximately to the load at which specimens without fiber would fail in flexure i.e. to the tensile strength of plain RPC in flexure. Consistent with the definition of modulus of rupture, the tensile strength at the peak-load can be taken as modulus of rupture (MOR) for fiber-reinforced RPC. The Load-deflection plots Figure 4.37 show that for all practical purposes, a linear relationship between load and deflection can be assumed up to about 70% of the peak-load. The beam stiffness is essentially constant up to about this load level. The presence of longer softening zone in the post peak-load deformation indicates high ductility of fiber-reinforced RPC. As an indication of the appreciable softening, the deflection at about 60% of the post peak-load level becomes almost 3 times the value of deflection at the peak-load. The peak-load strength is calculated on the basis of elastic section modulus of the gross section of the prisms, and is taken as the value of MOR.

The MOR of RPC specimens prepared with w/b of 0.15, cement content of 1000 kg/m^3 and silica fume content varying from 15 to 25%, as replacement of sand, is depicted in Figure 4.38. The MOR increased with the increase in silica fume quantity. The MOR of

15%, 20 % and 25% silica fume RPC specimens was 33.0, 34.4 and36.6 MPa, respectively.

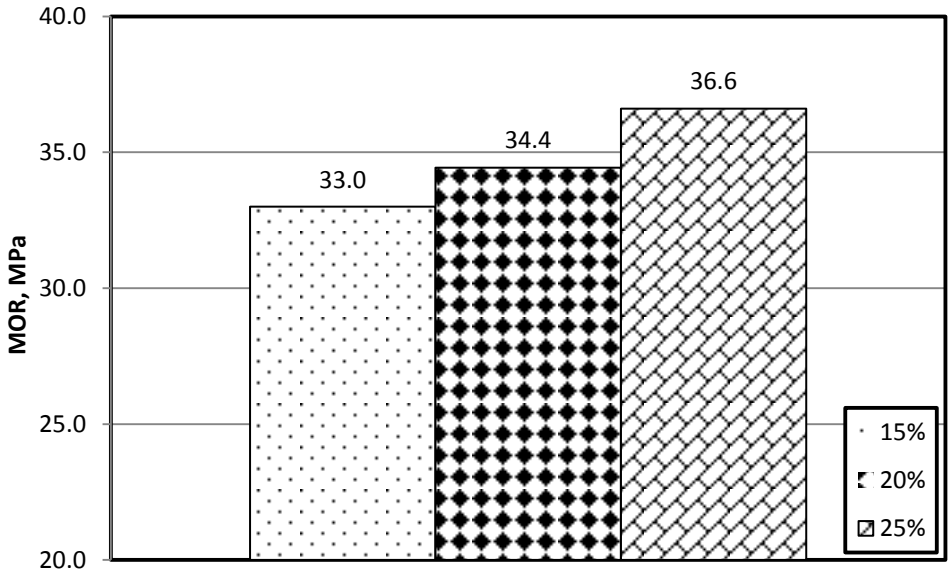

Figure 4.38: MOR of RPC specimens prepared with w/b of 0.15; CC of 1000 kg/m^3.

Figure 4.39 shows the MOR of the RPC specimens prepared with w/b of 0.15, cement content of 1100 kg/m^3 and silica fume content varying from 15 to 25%, as replacement of sand. The MOR increased with the quantity of silica fume. RPC mixture containing 25 % silica fume showed higher MOR than the 15%, 20% silica fume RPC mixtures. After 90 days of curing, the MOR of 15%, 20 % and 25% silica fume RPC specimens was 27.8, 29.8 and 32.9 MPa, respectively.

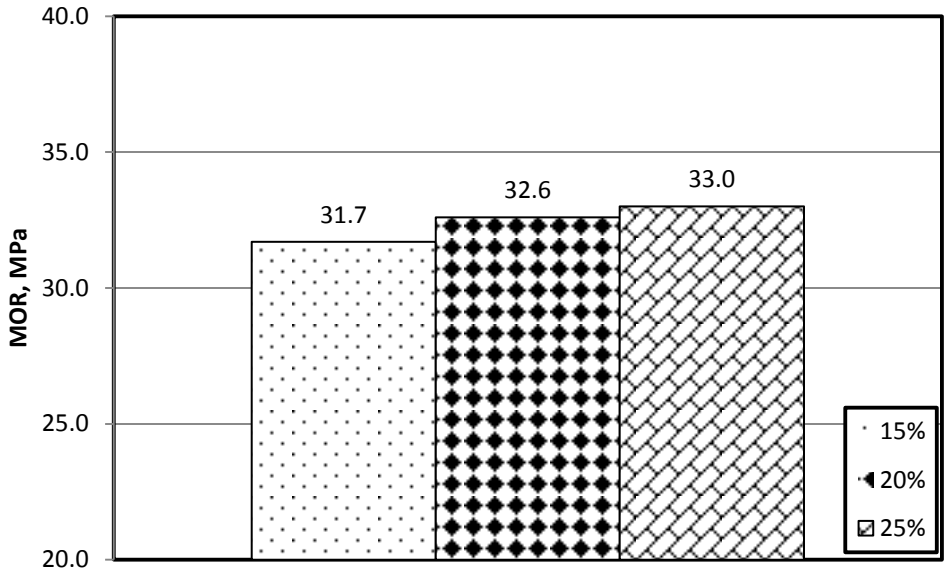

Figure 4.39: MOR of RPC specimens prepared with w/b of 0.15; CC of 1100 kg/m^3.

The MOR increased with the quantity of silica fume. The MOR of the RPC specimens with w/b of 0.15, cement content of 1200 kg/m^3 and silica fume content varying from 15 to 25%, as replacement of sand, is depicted in Figure 4.40. RPC specimens containing 25 % silica fume was higher than that of 15, 20% silica fume. The MOR of 15%, 20 % and 25% silica fume RPC specimens was 26, 30.9 and 34.8 MPa, respectively.

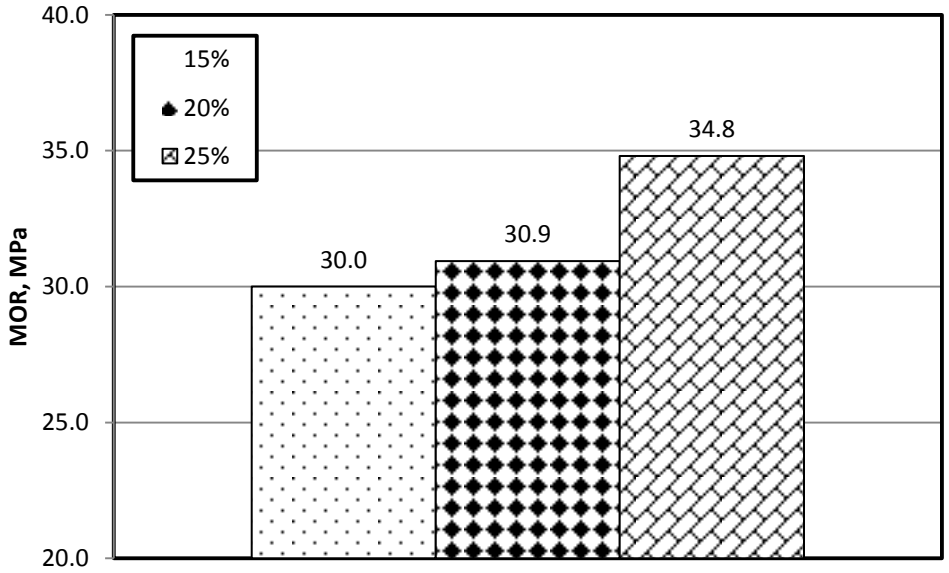

Figure 4.40: MOR of RPC specimens prepared with w/b of 0.15; CC of 1200 kg/m^3.

The MOR of the RPC specimens prepared with w/b of 0.175, cement content of 1000 kg/m^3 and silica fume content varying from 15 to 25%, as replacement of sand, is depicted in Figure 4.41.The MOR increased with the quantity of silica fume. The MOR of 15%, 20 % and 25% silica fume RPC specimens was 32.4, 34.0 and 34.9 MPa, respectively.

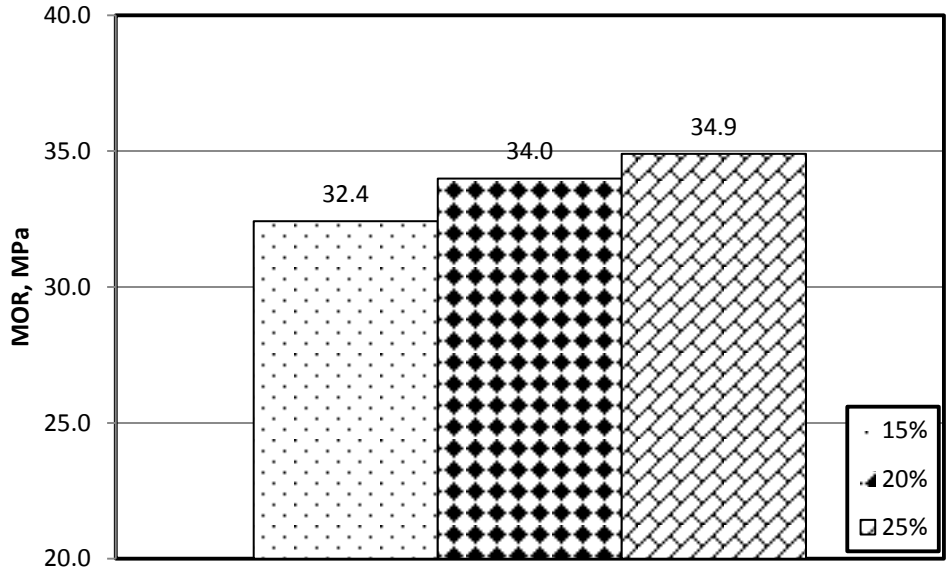

Figure 4.41: MOR of RPC specimens prepared with w/b of 0.175; CC of 1000 kg/m^3.

Figure 4.42 shows the MOR of the RPC specimens prepared with w/b of 0.175, cement content of 1100 kg/m^3 and silica fume content varying from 15 to 25%, as replacement of sand. RPC mixture containing 25 % silica fume showed higher MOR than the 15%, 20% silica fume RPC mixtures. The MOR of 15%, 20 % and 25% silica fume RPC specimens was 24.5, 25.8 and 28.0 MPa, respectively.

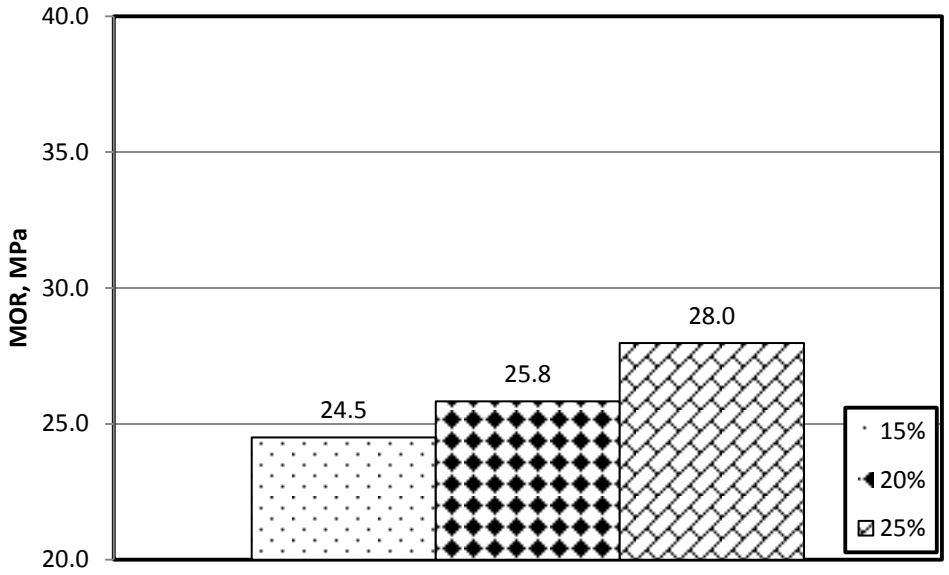

Figure 4.42: MOR of RPC specimens prepared with w/b of 0.175; CC of 1100 kg/m^3.

The MOR of the RPC specimens prepared with w/b of 0.175, cement content of 1200 kg/m^3 and silica fume content varying from 15 to 25%, as replacement of sand, is depicted in Figure 4.43. RPC mixture containing 25 % silica fume showed higher MOR than the 15%, 20% silica fume RPC mixtures. The MOR of 15%, 20 % and 25% silica fume RPC specimens was 24.9, 26.5 and 27.5 MPa, respectively.

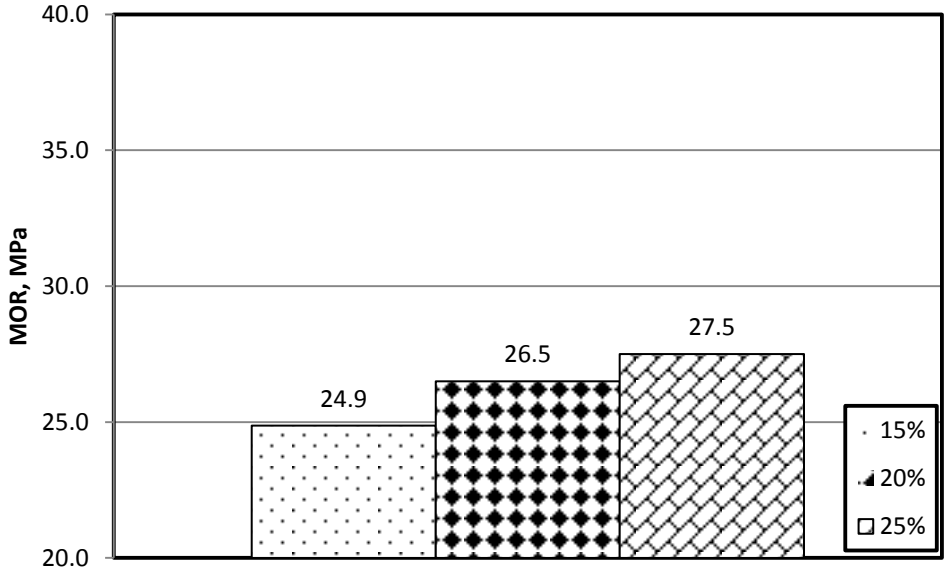

Figure 4.43: MOR of RPC specimens prepared with w/b of 0.175; CC of 1200 kg/m^3.

The MOR of the RPC specimens with w/b of 0.20, cement content of 1000 kg/m^3 and silica fume content varying from 15 to 25%, as replacement of sand, is depicted in Figure 4.44. The MOR increased with the quantity of silica fume. The MOR of 15%, 20 % and 25% silica fume RPC specimens was 27.9, 30.7 and 31.5 MPa, respectively.

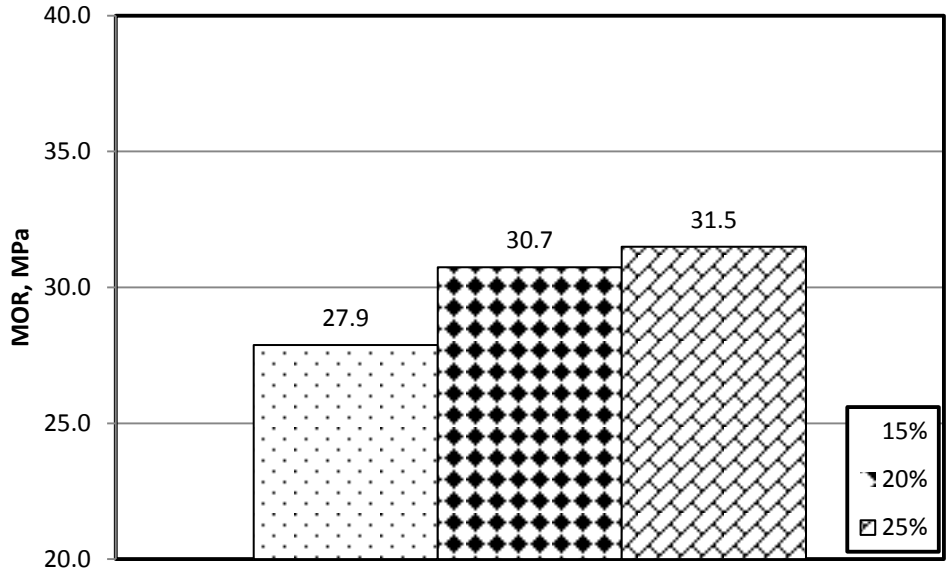

Figure 4.44: MOR of RPC specimens prepared with w/b of 0.20; CC of 1000 kg/m^3.

Figure 4.45 shows the MOR of the RPC specimens with w/b of 0.20, cement content of 1100 kg/m^3 and silica fume content varying from 15 to 25%, as replacement of sand. The MOR increased with the quantity of silica fume. The MOR of 15%, 20 % and 25% silica fume RPC specimens was 23.0, 25.7 and 27.1 MPa, respectively.

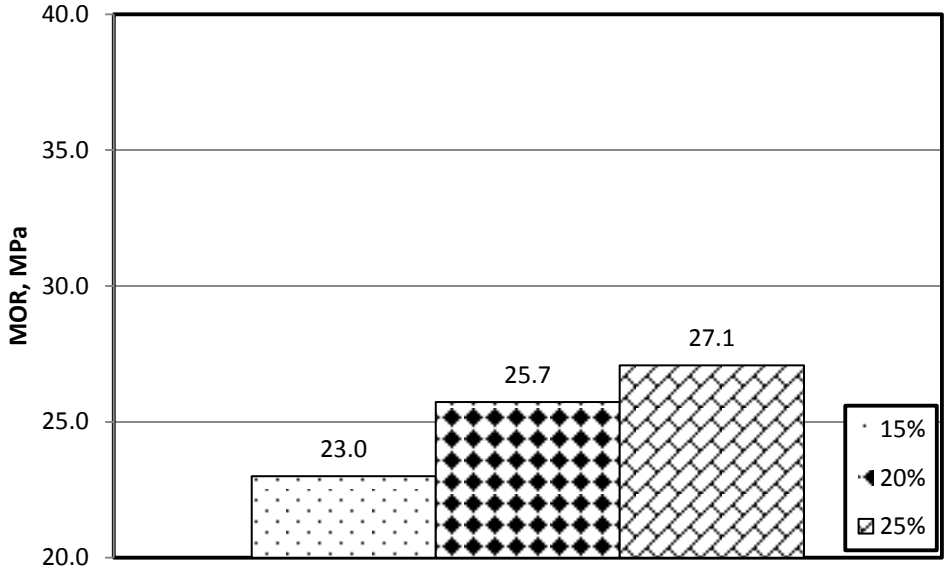

Figure 4.45: MOR of RPC specimens prepared with w/b of 0.20; CC of 1100 kg/m^3.

The MOR of the RPC specimens prepared with w/b of 0.20, cement content of 1200 kg/m^3 and silica fume content varying from 15 to 25%, as replacement of sand, is depicted in Figure 4.46. RPC mixture containing 25% silica fume showed higher MOR than the 15%, 20% silica fume RPC mixtures. The MOR of 15%, 20 % and 25% silica fume RPC specimens was 25, 26 and 26 MPa, respectively.

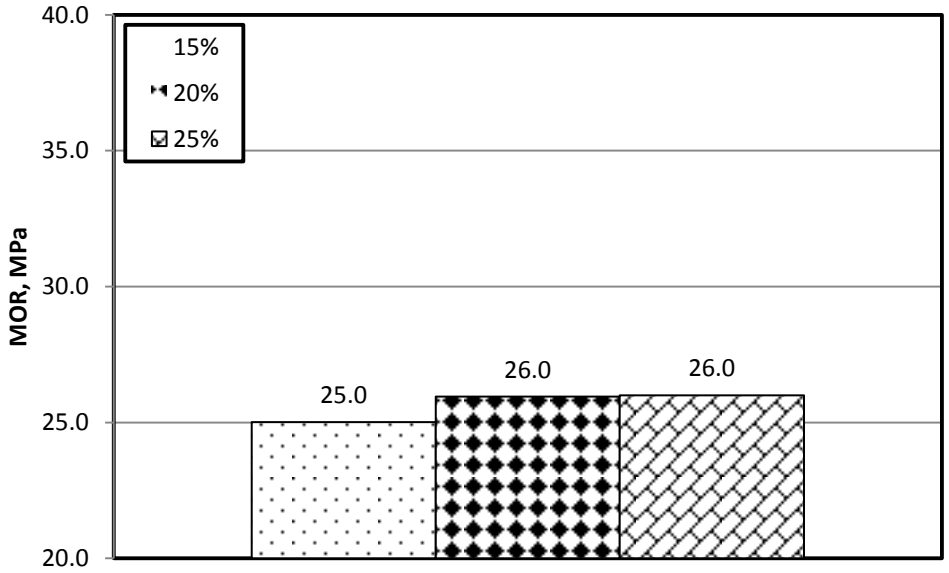

Figure 4.46: MOR of RPC specimens prepared with w/b of 0.20; CC of 1200 kg/m^3.

The MOR of RPC specimens with cement content of 1000 kg/m^3, different w/b ratios, and silica fume content varying from 15 to 25%, as replacement of sand, is depicted in Figure 4.47. While there is small difference in the MOR of specimens prepared with w/b ratio of 0.15 and 0.175, there was significant change between those prepared with w/b ratio of 0.175 and 0.20. The MOR of RPC specimens with w/b ratio of 0.15 was in the range of 33 to 37 MPa while the values in the specimens with w/b ratio 0.175 were in the range of 32 to 35 MPa. The modulus of elasticity of RPC specimens prepared with w/b ratio of 0.20 was in the range of 28 to 32 MPa.

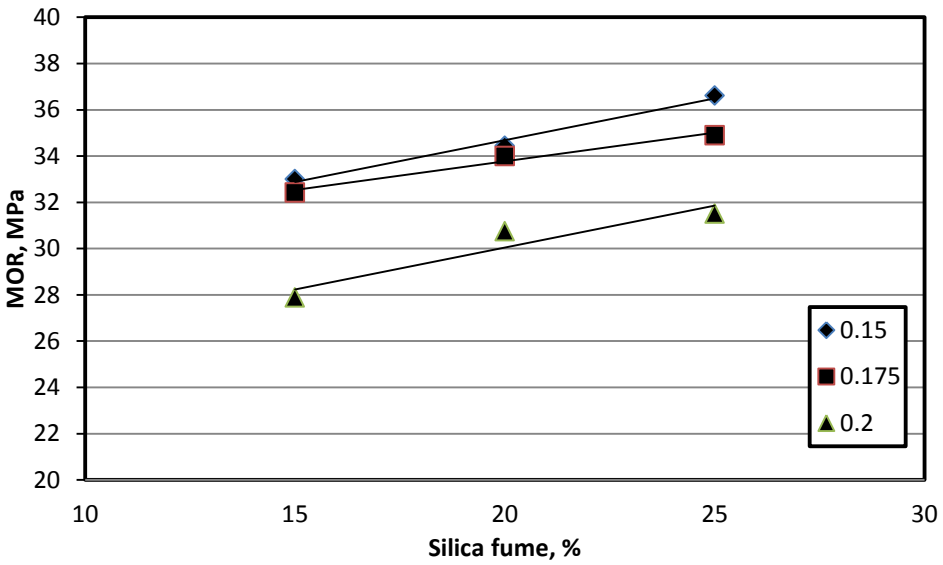

Figure 4.47: 28 day MOR for CC: 1000 kg/m^3 for different w/b ratios and silica fume.

Figure 4.48 shows the MOR of RPC specimens with cement content of 1100 kg/m^3, different w/b ratios, and silica fume content varying from 15 to 25%, as replacement of sand. While there is marginal difference in the MOR of specimens prepared with w/b ratio of 0.15 and 0.175, there was significant change between those prepared with w/b ratio of 0.175 and 0.20. The MOR of RPC specimens with w/b ratio of 0.15 was in the range of 28 to 33 MPa while the values in the specimens with w/b ratio 0.175 were in the

range of 24 to 28 MPa. The modulus of elasticity of RPC specimens prepared with w/b ratio of 0.20 was in the range of 23 to 27 MPa.

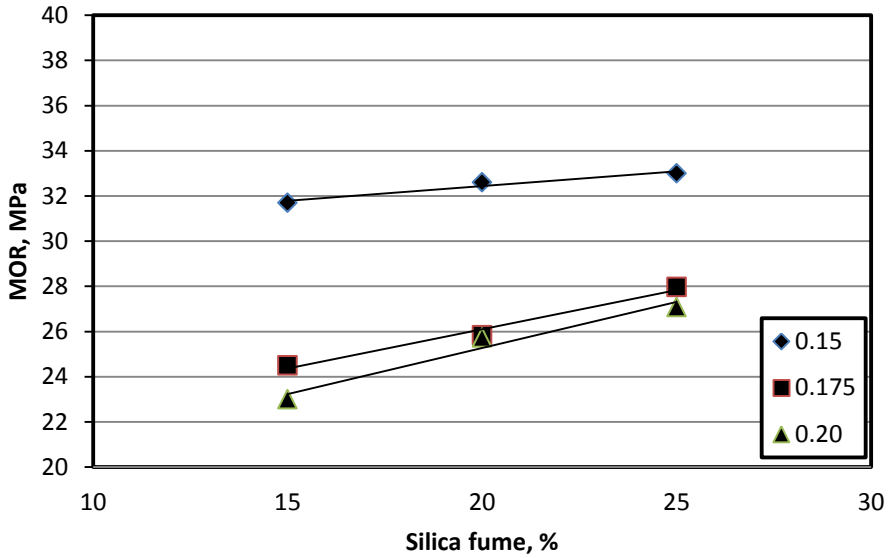

Figure 4.48: 28 day MOR for CC: 1100 kg/m^3 for different w/b ratios and silica fume.

The MOR of RPC specimens with cement content of 1200 kg/m^3, different w/b ratios, and silica fume content varying from 15 to 25%, as replacement of sand, is depicted in Figure 4.49. While there is marginal difference in the MOR of specimens prepared with w/b ratio of 0.15 and 0.175, there was significant change between those prepared with w/b ratio of 0.175 and 0.20. The MOR of RPC specimens with w/b ratio of 0.15 was in the range of 26 to 35 MPa while the values in the specimens with w/b ratio 0.175 were in the range of 25 to 28 MPa. The modulus of elasticity of RPC specimens prepared with w/b ratio of 0.20 was in the range of 25 to 27 MPa.

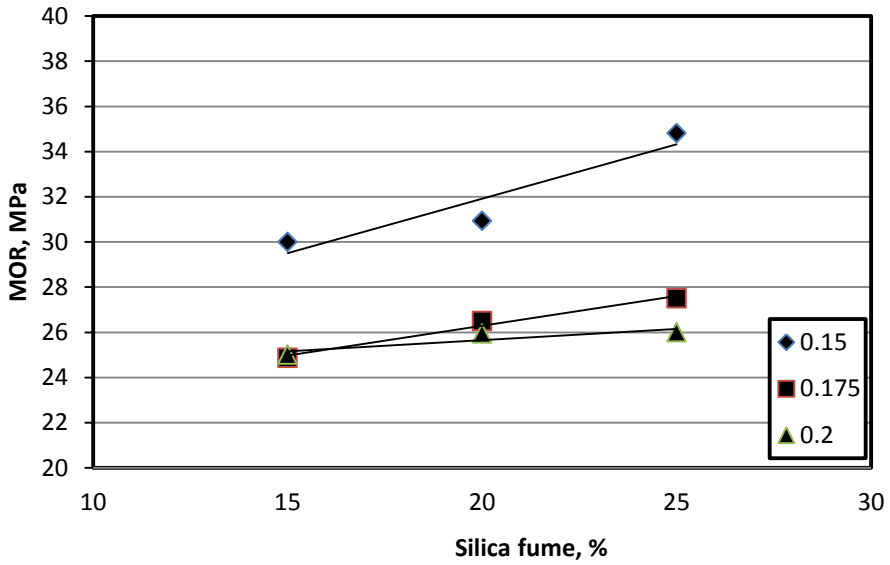

Figure 4.49: 28 day MOR for CC: 1200 kg/m^3 for different w/b ratios and silica fume.

4.5 DRYING SHRINKAGE

The drying shrinkage was measured over a period of about 90 days on prism specimens after 14 days of water curing. The average results of the drying shrinkage for w/b of 0.15, 0.175 and 0.20 are presented in Table 4-7, Table 4-8 and Table 4-9 respectively.

Table 4-7: Average drying shrinkage of RPC specimens prepared for w/b of 0.15.

Exposure Period, Days	Average Drying Shrinkage (µm)								
	M 1	M 2	M 3	M 4	M 5	M 6	M 7	M 8	M 9
3	150	209	244	208	258	272	303	317	320
7	225	274	275	309	338	345	378	385	398
14	267	344	354	342	385	387	427	437	449
21	303	405	408	405	420	432	463	481	492
28	368	438	441	459	467	471	505	509	520
42	417	471	474	529	538	542	547	552	555
56	443	485	486	579	580	591	596	601	604
90	450	492	493	590	592	603	606	608	614

Table 4-8: Average drying shrinkage in RPC specimens prepared for w/b of 0.175.

Exposure Period, Days	Average Drying Shrinkage (μm)								
	M 10	M 11	M 12	M 13	M 14	M 15	M 16	M 17	M 18
3	198	225	235	242	254	277	314	326	338
7	259	288	289	322	333	352	396	402	413
14	303	364	376	357	404	406	443	448	455
21	355	415	423	430	453	456	476	486	499
28	383	481	491	475	493	496	509	524	527
42	421	509	517	533	552	559	551	556	560
56	454	539	541	583	587	594	600	615	607
90	470	544	552	594	596	606	609	627	631

Table 4-9: Average drying shrinkage in RPC specimens prepared for w/b of 0.20.

Exposure Period, Days	Average Shrinkage (μm)								
	M 19	M 20	M 21	M 22	M 23	M 24	M 25	M 26	M 27
3	222	251	277	289	303	306	329	338	345
7	289	317	345	350	362	380	427	434	437
14	367	397	427	452	467	507	528	528	561
21	423	453	479	517	535	578	596	601	622
28	504	526	547	570	582	613	634	645	662
42	548	568	591	605	636	657	676	695	702
56	577	596	624	644	655	676	697	711	719
90	596	617	631	679	686	688	716	727	730

4.5.1 Shrinkage variation with age

The drying shrinkage in the RPC specimens prepared with w/b of 0.15, cement content of 1000 kg/m^3 and silica fume content varying from 15 to 25%, as replacement of sand, is depicted in Figure 4.50. The drying shrinkage strain increased with age in all the RPC specimens. The drying shrinkage strain increased with age in all the RPC specimens. The drying shrinkage strains development in the 20 and 25% silica fume was almost similar and more than that in the specimens with 15% silica fume. After 90 days of exposure, the drying shrinkage strains of 15%, 20 % and 25% silica fume RPC specimens was 450, 492, 493 μm, respectively.

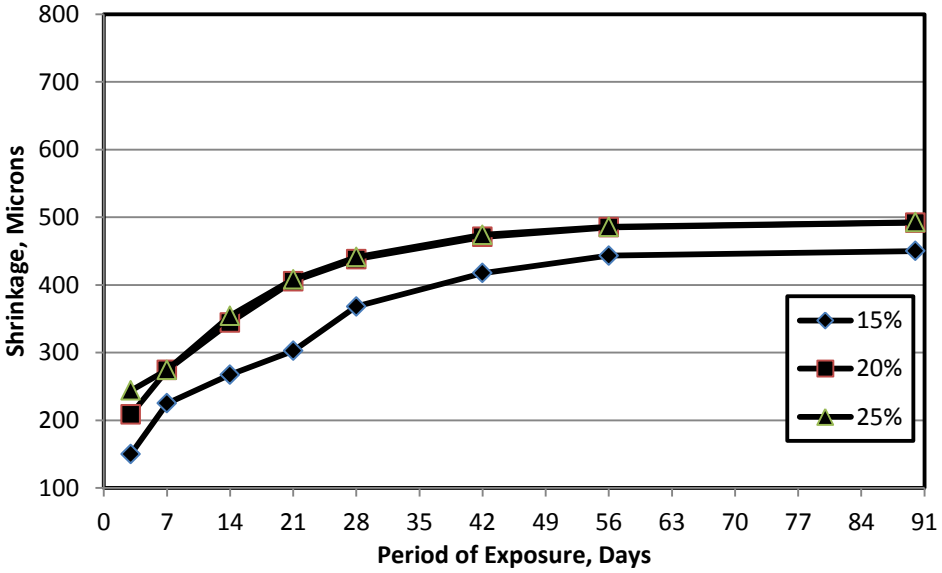

Figure 4.50: Drying shrinkage strain in RPC specimens prepared with different percentages of silica fume, w/b of 0.15 and CC of 1000 kg/m^3.

Figure 4.51 shows the drying shrinkage in the RPC specimens prepared with w/b of 0.15, cement content of 1100 kg/m^3 and silica fume content varying from 15 to 25%, as replacement of sand. The drying shrinkage strain increased with age in all the RPC specimens. The drying shrinkage strains development in the 20 and 25% silica fume was almost similar and more than that in the specimens with 15% silica fume. After 90 days of exposure, the drying shrinkage strain of 15%, 20 % and 25% silica fume RPC specimens was 590, 592 and 603 µm, respectively.

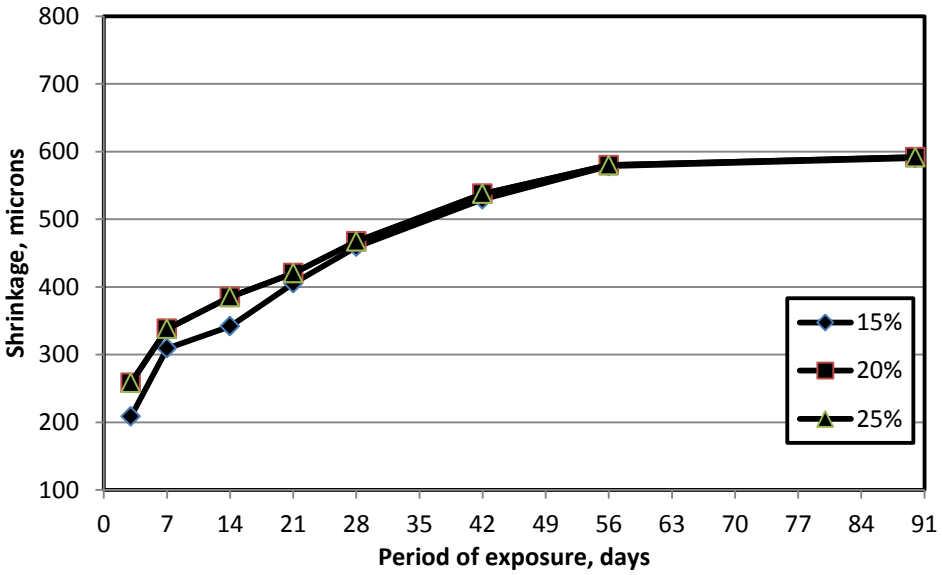

Figure 4.51: Drying shrinkage strain in RPC specimens prepared with different percentages of silica fume, w/b of 0.15 and CC of 1100 kg/m^3.

The drying shrinkage strain increased with age in all the RPC specimens. The drying shrinkage strain development in the 20 and 25% silica fume was almost similar and more than that in the specimens with 15% silica fume. The drying shrinkage in the RPC specimens prepared with w/b of 0.15, cement content of 1200 kg/m^3 and silica fume content varying from 15 to 25%, as replacement of sand, is depicted in Figure 4.52. After 90 days of exposure, the drying shrinkage strain of 15%, 20 % and 25% silica fume RPC specimens was 606, 608, 614 µm, respectively.

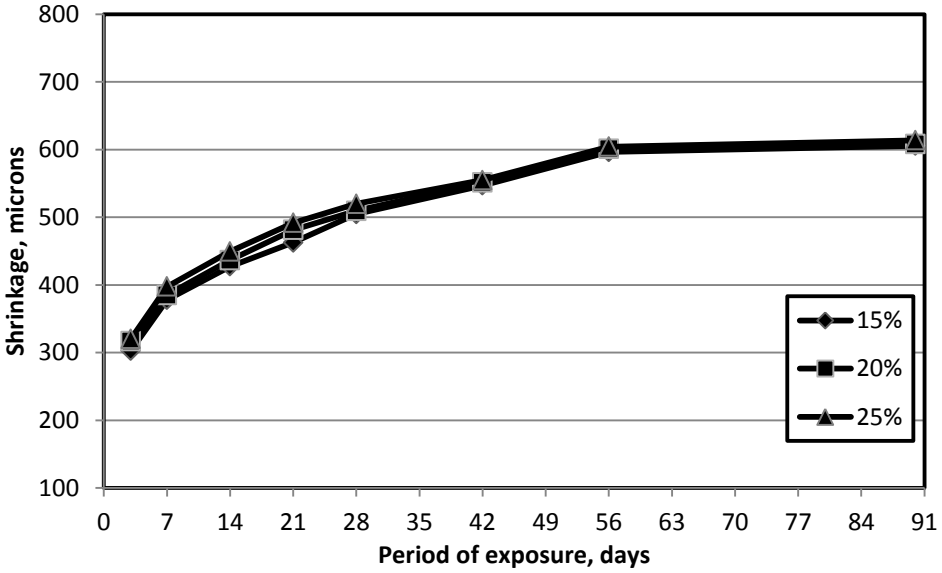

Figure 4.52: Drying shrinkage strain in RPC specimens prepared with different percentages of silica fume, w/b of 0.15 and CC of 1200 kg/m^3.

The drying shrinkage in the RPC specimens prepared with w/b of 0.175, cement content of 1000 kg/m^3 and silica fume content varying from 15 to 25%, as replacement of sand, is depicted in Figure 4.53. The drying shrinkage strains increased with age in all the RPC specimens. The drying shrinkage strain increased with age in all the RPC specimens. The drying shrinkage strains development in the 20 and 25% silica fume was almost similar and more than that in the specimens with 15% silica fume. After 90 days of exposure, the drying shrinkage strain of 15%, 20 % and 25% silica fume RPC specimens was 470, 544, 572 μm, respectively.

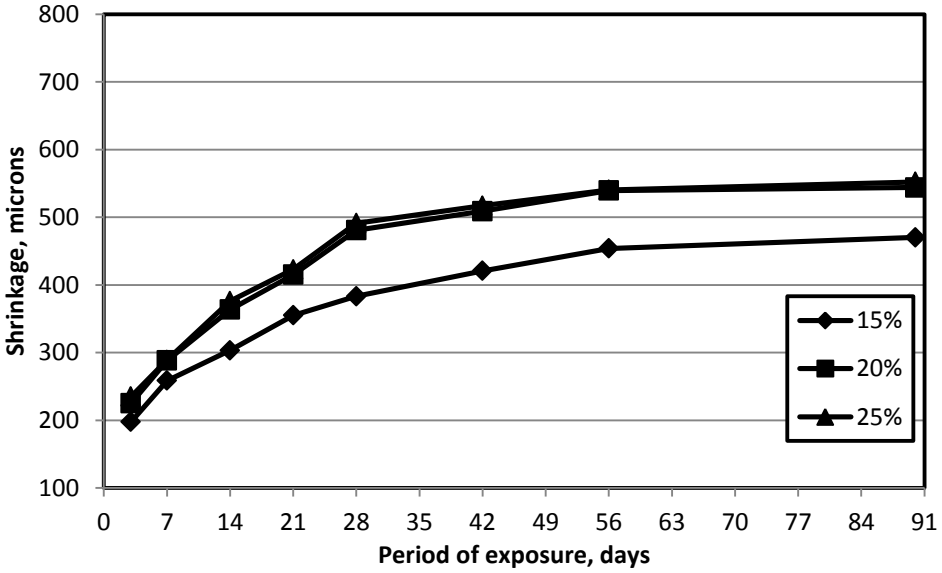

Figure 4.53: Drying shrinkage strain in RPC specimens prepared with different percentages of silica fume, w/b of 0.175 and CC of 1000 kg/m^3.

Figure 4.54 shows the drying shrinkage in the RPC specimens prepared with w/b of 0.175, cement content of 1100 kg/m^3 and silica fume content varying from 15 to 25%, as replacement of sand. The drying shrinkage strains increased with age in all the RPC specimens. The drying shrinkage strain increased with age in all the RPC specimens. The drying shrinkage strains development in the 20 and 25% silica fume was almost similar and more than that in the specimens with 15% silica fume. After 90 days of exposure, the drying shrinkage strain of 15%, 20 % and 25% silica fume RPC specimens was 594, 596 and 606 µm, respectively.

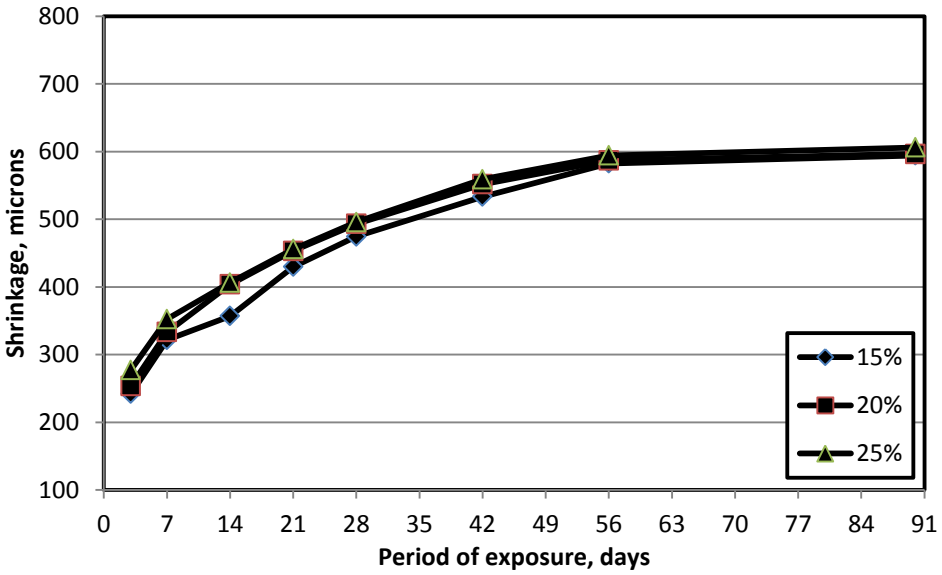

Figure 4.54: Drying shrinkage strain in RPC specimens prepared with different percentages of silica fume, w/b of 0.175 and CC of 1100 kg/m^3.

The drying shrinkage strain increased with age in all the RPC specimens. The drying shrinkage strains development in the 20 and 25% silica fume was almost similar and more than that in the specimens with 15% silica fume. The drying shrinkage in the RPC specimens prepared with w/b of 0.175, cement content of 1200 kg/m^3 and silica fume content varying from 15 to 25%, as replacement of sand, is depicted in Figure 4.55. After 90 days of exposure, the drying shrinkage strain of 15%, 20 % and 25% silica fume RPC specimens was 609, 627 and 631 µm, respectively.

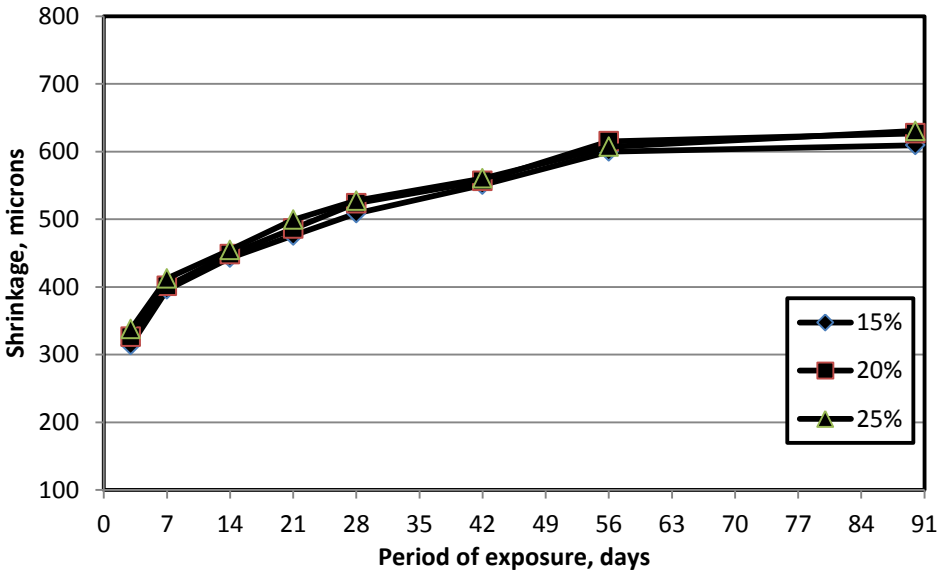

Figure 4.55: Drying shrinkage strain in RPC specimens prepared with different percentages of silica fume, w/b of 0.175 and CC of 1200 kg/m^3.

The drying shrinkage in the RPC specimens prepared with w/b of 0.20, cement content of 1000 kg/m^3 and silica fume content varying from 15 to 25%, as replacement of sand, is depicted in Figure 4.56. The drying shrinkage strains increased with age in all the RPC specimens. The drying shrinkage strain increased with age in all the RPC specimens. The drying shrinkage strains development in the 20 and 25% silica fume was almost similar and more than that in the specimens with 15% silica fume. After 90 days of exposure, the drying shrinkage strain of 15%, 20 % and 25% silica fume RPC specimens was 596, 617 and 631 µm, respectively.

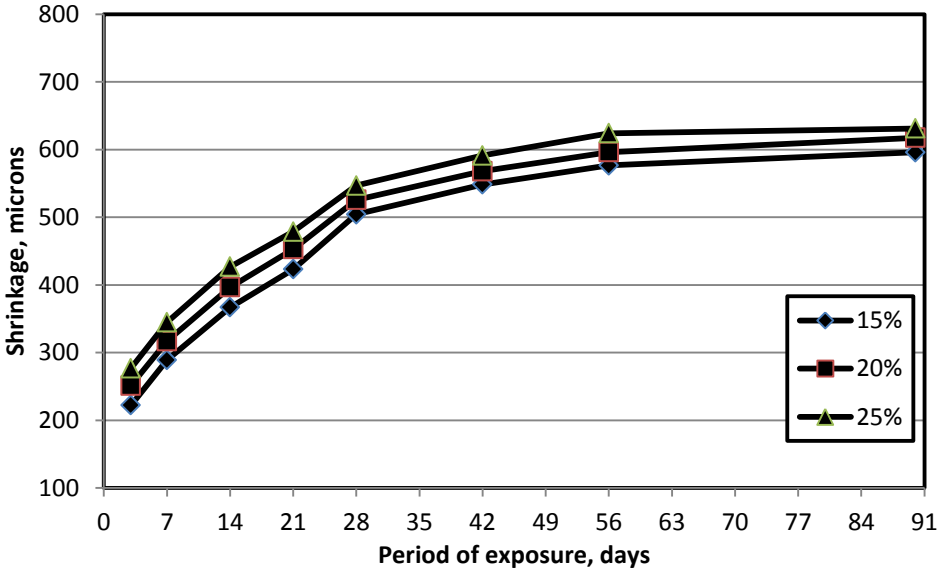

Figure 4.56: Drying shrinkage strain in RPC specimens prepared with different percentages of silica fume, w/b of 0.20 and CC of 1000 kg/m^3.

Figure 4.57 shows the drying shrinkage in the RPC specimens prepared with w/b of 0.20, cement content of 1100 kg/m^3 and silica fume content varying from 15 to 25%, as replacement of sand. The drying shrinkage strains increased with age in all the RPC specimens. The drying shrinkage strain increased with age in all the RPC specimens. The drying shrinkage strains development in the 20 and 25% silica fume was almost similar and more than that in the specimens with 15% silica fume. After 90 days of exposure, the drying shrinkage strain of 15%, 20 % and 25% silica fume RPC specimens was 679, 686 and 688 µm, respectively.

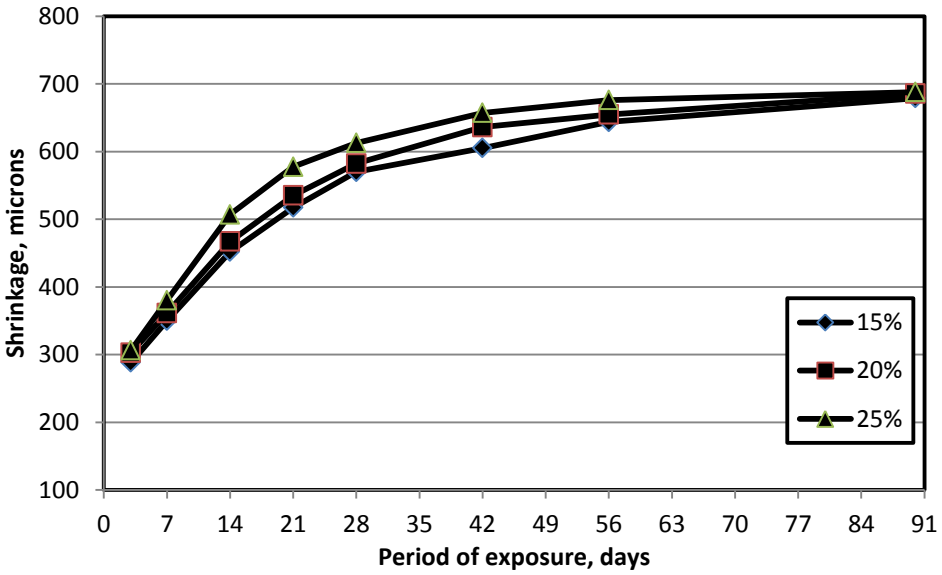

Figure 4.57: Drying shrinkage strain in RPC specimens prepared with different percentages of silica fume, w/b of 0.20 and CC of 1100 kg/m^3.

The drying shrinkage strains increased with age in all the RPC specimens. The drying shrinkage strain increased with age in all the RPC specimens. The drying shrinkage strains development in the 20 and 25% silica fume was almost similar and more than that in the specimens with 15% silica fume. The drying shrinkage in the RPC specimens prepared with w/b of 0.20, cement content of 1200 kg/m^3 and silica fume content varying from 15 to 25%, as replacement of sand, is depicted in Figure 4.58. After 90 days of exposure, the drying shrinkage strain of 15%, 20 % and 25% silica fume RPC specimens was 716, 727 and 730 µm, respectively.

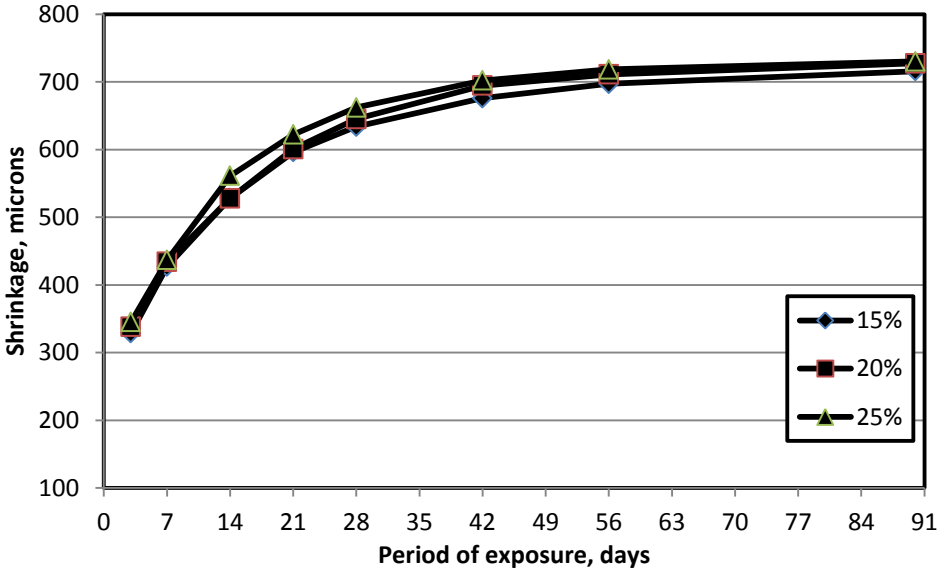

Figure 4.58: Drying shrinkage strain in RPC specimens prepared with different percentages of silica fume, w/b of 0.20 and CC of 1200 kg/m^3.

4.5.2 Ultimate shrinkage variation with mixture variables

The ultimate drying shrinkage strain (at 90 days) in the RPC specimens prepared with w/b of 0.15, cement content of 1000 kg/m^3 and silica fume content varying from 15 to 25%, as replacement of sand, is depicted in Figure 4.59. The ultimate drying in 20% and 25% silica fume RPC mixtures was almost similar and more than that of 15% silica fume RPC specimens. After 90 days of exposure, the ultimate drying shrinkage strain of 15%, 20 % and 25% silica fume RPC specimens was 450, 492 and 493 µm, respectively.

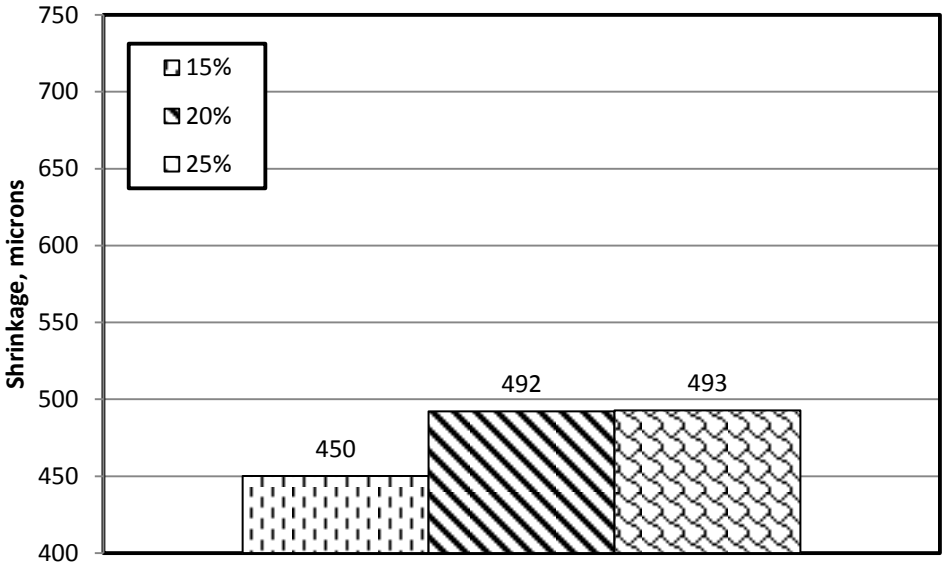

Figure 4.59: 90-day Drying shrinkage strain in RPC specimens prepared with different percentages of silica fume, w/b of 0.15 and CC of 1000 kg/m^3.

Figure 4.60 shows the ultimate drying shrinkage strain (at 90 days) in the RPC specimens with w/b of 0.15, cement content of 1100 kg/m^3 and silica fume content varying from 15 to 25%, as replacement of sand. The ultimate drying in 20% and 25% silica fume RPC mixtures was almost similar and more than that of 15% silica fume RPC specimens. After 90 days of exposure, the ultimate drying shrinkage strain of 15%, 20 % and 25% silica fume RPC specimens was 590, 592 and 603 µm, respectively.

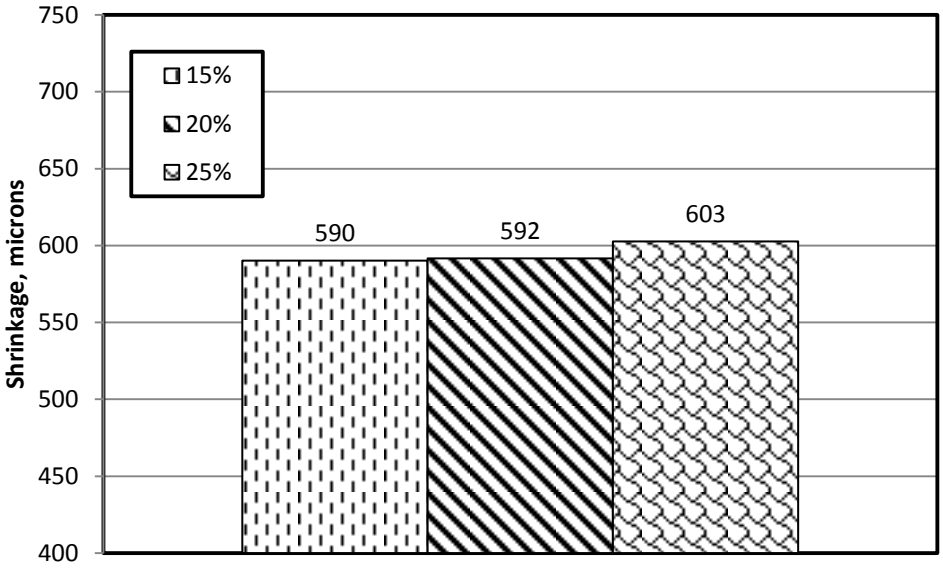

Figure 4.60: 90-day Drying shrinkage strain in RPC specimens prepared with different percentages of silica fume, w/b of 0.15 and CC of 1100 kg/m^3.

The ultimate drying in 20% and 25% silica fume RPC mixtures was almost similar and more than that of 15% silica fume RPC specimens. The ultimate drying shrinkage strain (at 90 days) in the RPC specimens prepared with w/b of 0.15, cement content of 1200 kg/m^3 and silica fume content varying from 15 to 25%, as replacement of sand, is depicted in Figure 4.61. After 90 days of exposure, the ultimate drying shrinkage strain of 15%, 20 % and 25% silica fume RPC specimens was 606, 608 and 614 µm, respectively.

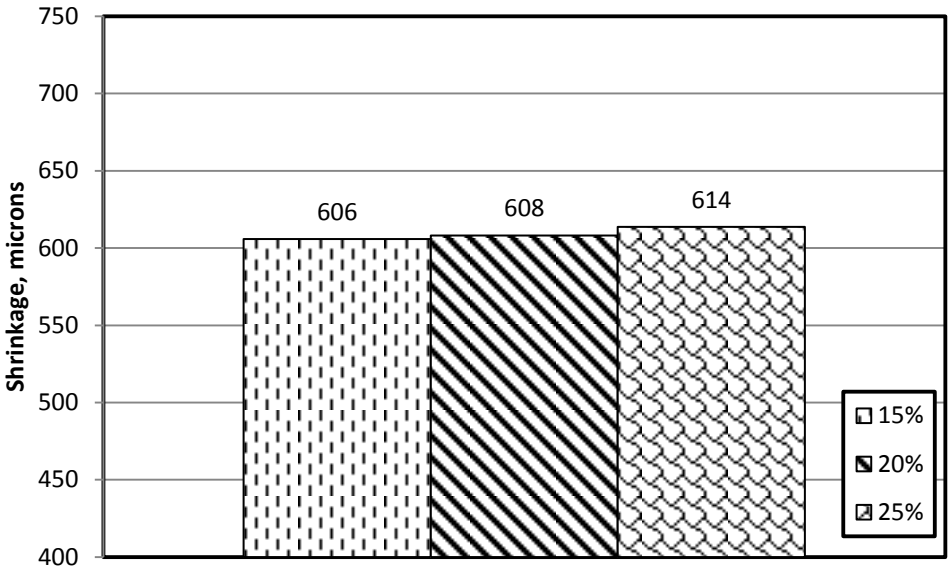

Figure 4.61: 90-day Drying shrinkage strain in RPC specimens prepared with different percentages of silica fume, w/b of 0.15 and CC of 1200 kg/m^3.

The ultimate drying shrinkage strain at 90 days in the RPC specimens prepared with w/b of 0.175, cement content of 1000 kg/m^3 and silica fume content varying from 15 to 25%, as replacement of sand, is depicted in Figure 4.62. The ultimate drying in 20% and 25% silica fume RPC mixtures was almost similar and more than that of 15% silica fume RPC specimens. After 90 days of exposure, the ultimate drying shrinkage strain of 15%, 20 % and 25% silica fume RPC specimens was 470, 544 and 552 µm, respectively.

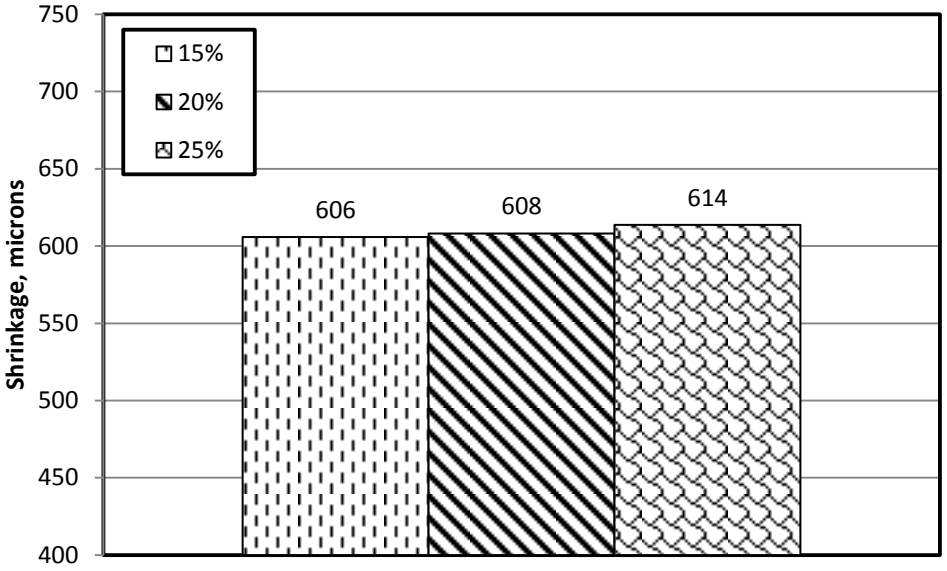

Figure 4.62: 90-day Drying shrinkage strain in RPC specimens prepared with different percentages of silica fume, w/b of 0.175 and CC of 1000 kg/m^3.

Figure 4.63 shows the ultimate drying shrinkage strain at 90 days in the RPC specimens prepared with w/b of 0.175, cement content of 1100 kg/m^3 and silica fume content varying from 15 to 25%, as replacement of sand. The ultimate drying in 20% and 25% silica fume RPC mixtures was almost similar and more than that of 15% silica fume RPC specimens. After 90 days of exposure, the ultimate drying shrinkage strain of 15%, 20 % and 25% silica fume RPC specimens was 594, 596 and 606 µm, respectively.

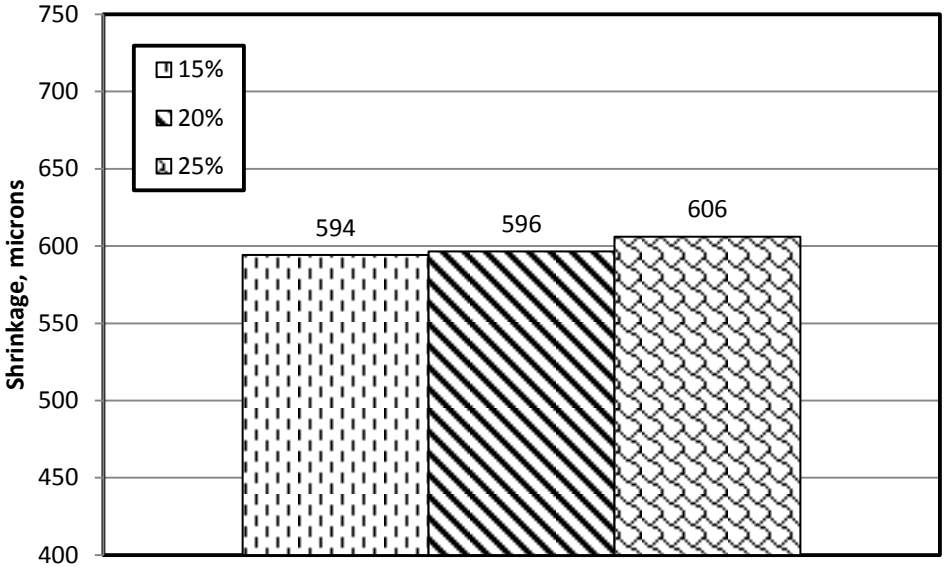

Figure 4.63: 90-day Drying shrinkage strain in RPC specimens prepared with different percentages of silica fume, w/b of 0.175 and CC of 1100 kg/m^3.

The ultimate drying in 20% and 25% silica fume RPC mixtures was almost similar and more than that of 15% silica fume RPC specimens. The ultimate drying shrinkage strain at 90 days in the RPC specimens with w/b of 0.15, cement content of 1200 kg/m^3 and silica fume content varying from 15 to 25%, as replacement of sand, is depicted in Figure 4.64. After 90 days of exposure, the ultimate drying shrinkage strain of 15%, 20 % and 25% silica fume RPC specimens was 609, 627 and 631 µm, respectively.

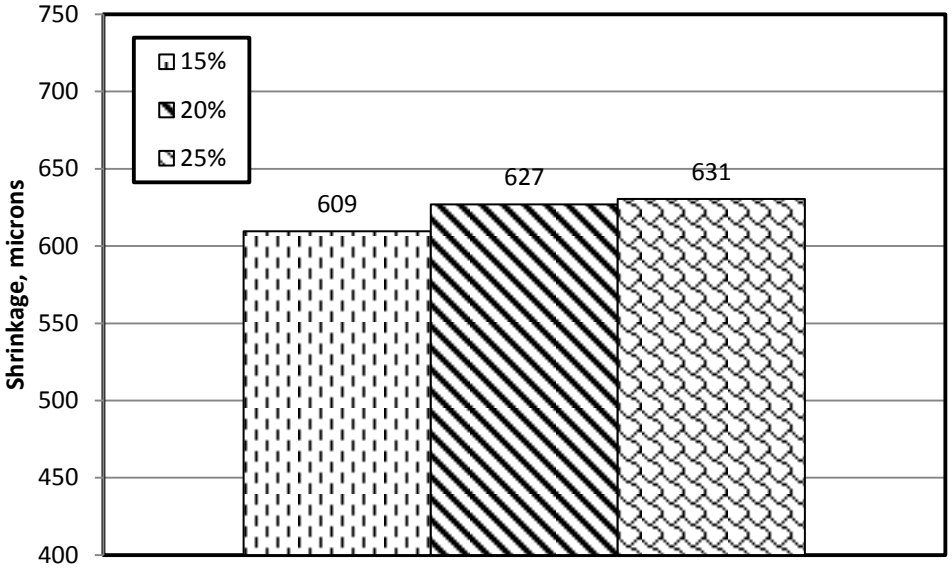

Figure 4.64: 90-day Drying shrinkage strain in RPC specimens prepared with different percentages of silica fume, w/b of 0.175 and CC of 1200 kg/m^3.

The ultimate drying shrinkage strain at 90 days in the RPC specimens prepared with w/b of 0.20, cement content of 1000 kg/m^3 and silica fume content varying from 15 to 25%, as replacement of sand, is depicted in Figure 4.65 The ultimate drying in 20% and 25% silica fume RPC mixtures was almost similar and more than that of 15% silica fume RPC specimens. After 90 days of exposure, the ultimate drying shrinkage strain of 15%, 20 % and 25% silica fume RPC specimens was 596, 617 and 631 µm, respectively.

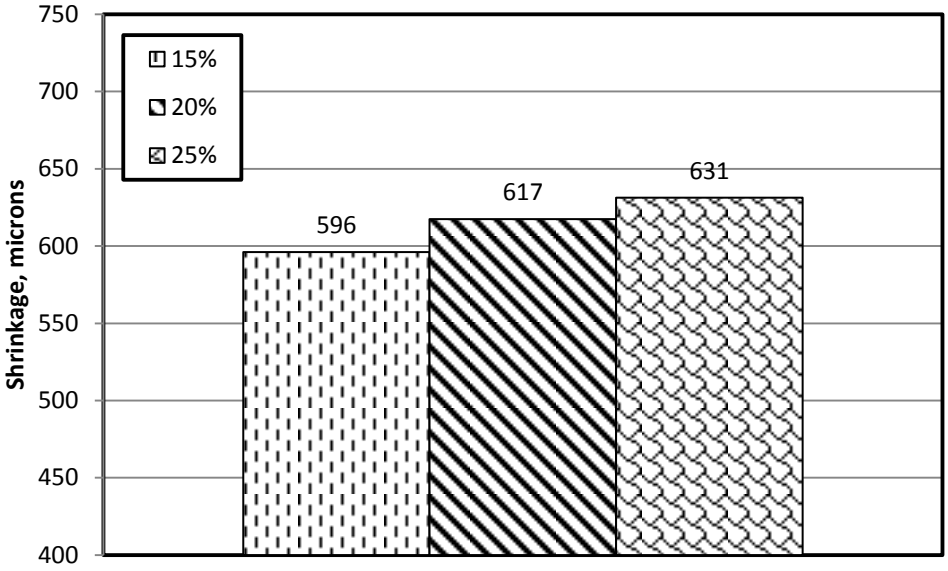

Figure 4.65: 90-day Drying shrinkage strain in RPC specimens prepared with different percentages of silica fume, w/b of 0.20 and CC of 1000 kg/m^3.

Figure 4.66 shows the ultimate drying shrinkage strain at 90 days in the RPC specimens prepared with w/b of 0.20, cement content of 1100 kg/m^3 and silica fume content varying from 15 to 25%, as replacement of sand. The ultimate drying in 20% and 25% silica fume RPC mixtures was almost similar and more than that of 15% silica fume RPC specimens. After 90 days of exposure, the ultimate drying shrinkage strain of 15%, 20 % and 25% silica fume RPC specimens was 679, 686 and 688 μm, respectively.

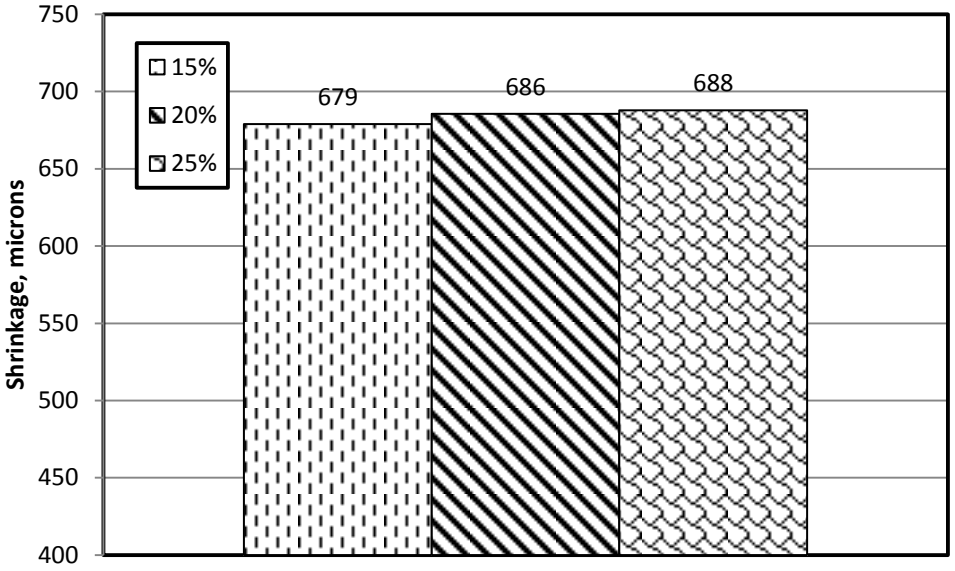

Figure 4.66: 90-day Drying shrinkage strain in RPC specimens prepared with different percentages of silica fume, w/b of 0.20 and CC of 1100 kg/m^3.

The ultimate drying in 20% and 25% silica fume RPC mixtures was almost similar and more than that of 15% silica fume RPC specimens. The ultimate drying shrinkage strain at 90 days in the RPC specimens prepared with w/b of 0.15, cement content of 1200 kg/m^3 and silica fume content varying from 15 to 25%, as replacement of sand, is depicted in Figure 4.67. After 90 days of exposure, the ultimate drying shrinkage strain of 15%, 20 % and 25% silica fume RPC specimens was 716, 727 and 730 µm, respectively.

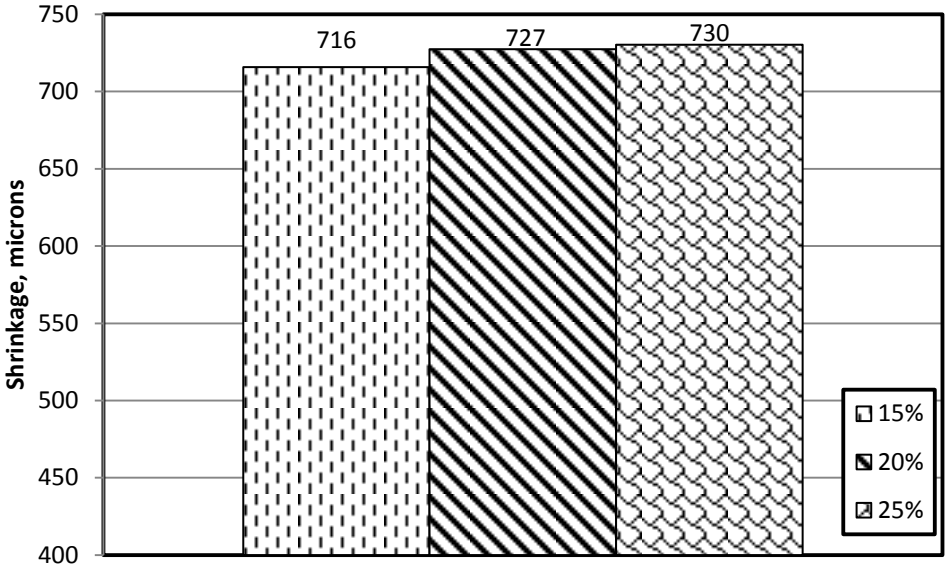

Figure 4.67: 90-day Drying shrinkage strain in RPC specimens prepared with different percentages of silica fume, w/b of 0.20 and CC of 1200 kg/m^3.

4.6 FRACTURE TOUGHNESS

The typical loading and unloading response for one of the selected specimens is presented in Figure 4.68. A total of 12 specimens were tested and the load-displacement curves similar to Figure 4.67 were developed.

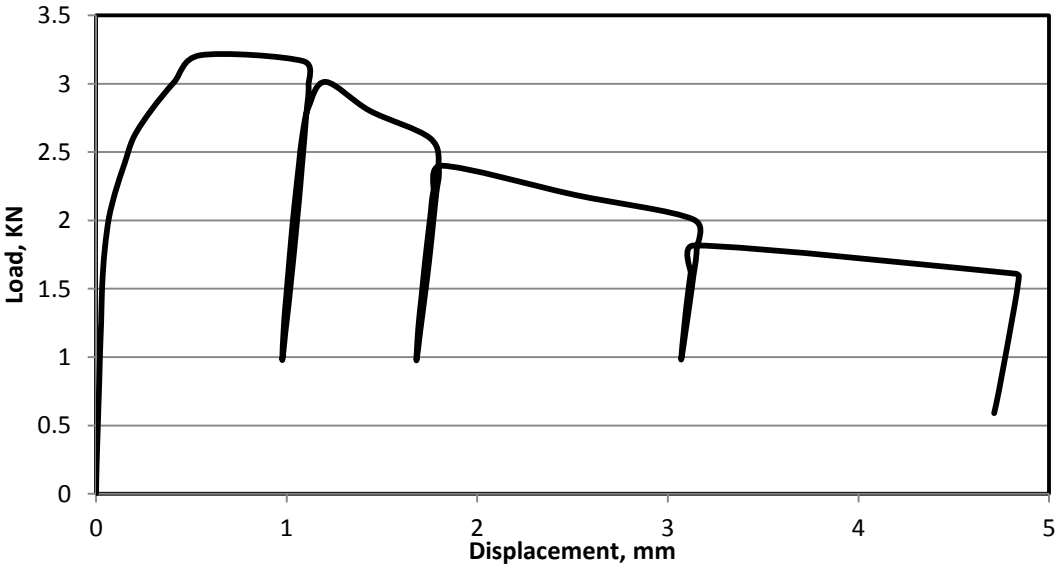

Figure 4.68: Loading and unloading response of notched RPC specimen with w/b of 0.20, CC of 1000 kg/m^3 and 15% silica fume.

Table 4-10 lists the values of K_{ic} and G_f of RPC specimens belonging to different mixes.

Table 4-10: Fracture Toughness test results for RPC specimens.

MIX #	Ci (mm/KN)	Cu (mm/KN)	ac (mm)	Pc (N)	K_{ic} (MPa√m)	K_{ic} ($KNm^{-3/2}$)	G_f (N/m)
1	0.008	0.057	27.064	2500	4.90	4898	470
3	0.012	0.069	25.500	3200	5.27	5267	523
7	0.022	0.049	19.300	5900	5.58	5579	676
9	0.017	0.071	23.590	4200	5.72	5716	680
10	0.013	0.036	21.000	4300	4.66	4658	452
12	0.017	0.059	22.384	4100	5.00	4999	499
16	0.015	0.0627	23.596	3900	5.31	5311	655
18	0.022	0.074	22.210	4500	5.40	5403	663
19	0.022	0.052	19.726	4600	4.50	4496	439
21	0.017	0.075	23.938	3400	4.78	4783	497
25	0.012	0.065	25.198	3200	5.10	5104	651
27	0.016	0.088	25.200	3300	5.26	5264	644

The K_{ic} values in the RPC specimens prepared with w/b of 0.15 and total cementitious content varying from 1150 kg/m^3 to 1500 kg/m^3 is depicted in Figure 4.69. The K_{ic} of RPC specimens show increase with increase in cementitious content. The K_{ic} values for RPC specimens were 4.90, 5.27, 5.58, 5.72 MPa√m, respectively.

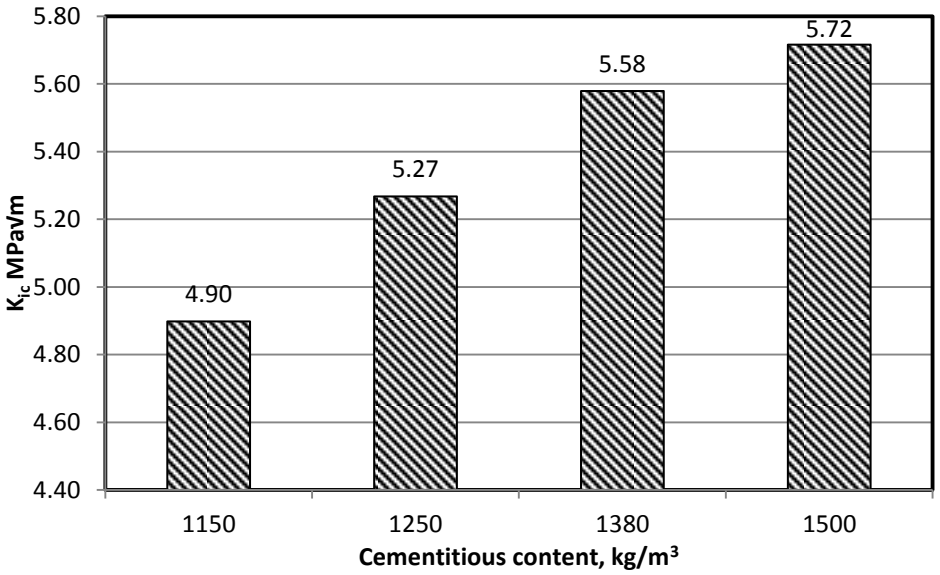

Figure 4.69: K_{ic} in RPC Specimens Prepared with Different cementitious content, and w/b of 0.15.

The K_{ic} increases with an increase in cementitious content. The K_{ic} values for RPC specimens prepared with w/b of 0.175 and total cementitious content varying from 1150 kg/m^3 to 1500 kg/m^3 is depicted in Figure 4.70. The values for K_{ic} for RPC specimens were 4.60, 5.00, 5.31, 5.40 MPa√m, respectively.

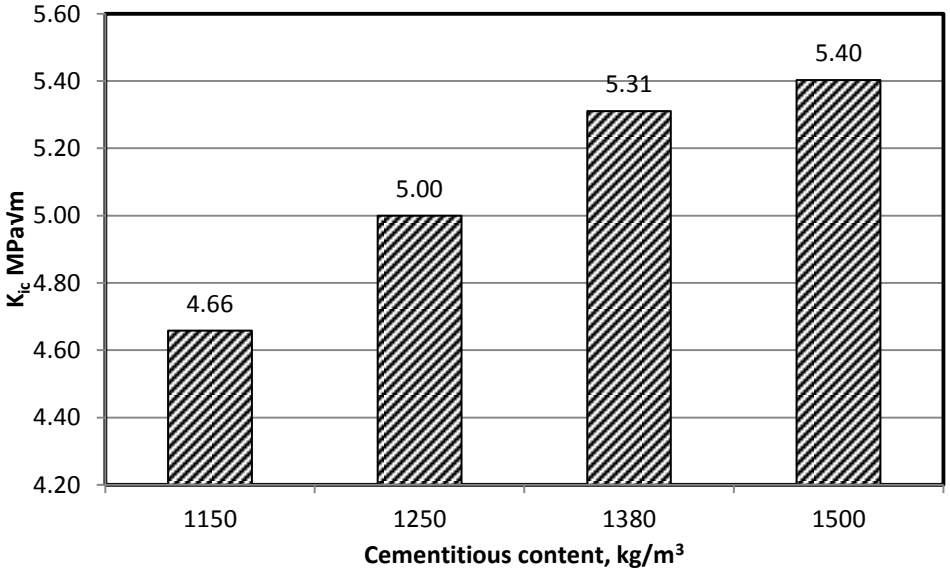

Figure 4.70: K_{ic} in RPC Specimens Prepared with Different cementitious content, and w/b of 0.175.

The K_{ic} values for RPC specimens prepared with w/b of 0.15 and total cementitious content varying from 1150 kg/m^3 to 1500 kg/m^3 is depicted in Figure 4.71. The K_{ic} increases with an increase in cementitious content. The values for K_{ic} for RPC specimens was 4.50, 4.78, 5.10, 5.26 MPa√m, respectively.

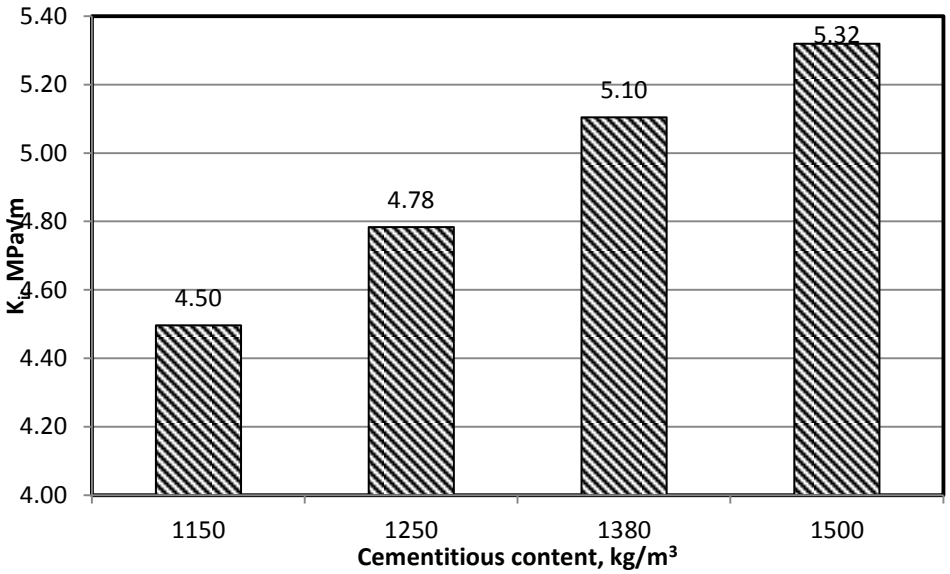

Figure 4.71: K_{ic} in RPC Specimens Prepared with Different cementitious content, and w/b of 0.20.

The K_{ic} values of the RPC specimens with total cementitious material content varying from 1150 kg/m^3 to 1500 kg/m^3 and different w/b ratios is depicted in Figure 4.72. These values increased with an increase in cementitious material content. Also, the K_{ic} values of RPC increased with decrease in w/b ratio. However, there is a significant increase in K_{ic} values for RPC mixtures with a w/b of 0.15 as compared to those prepared with w/b of 0.175 and 0.20.

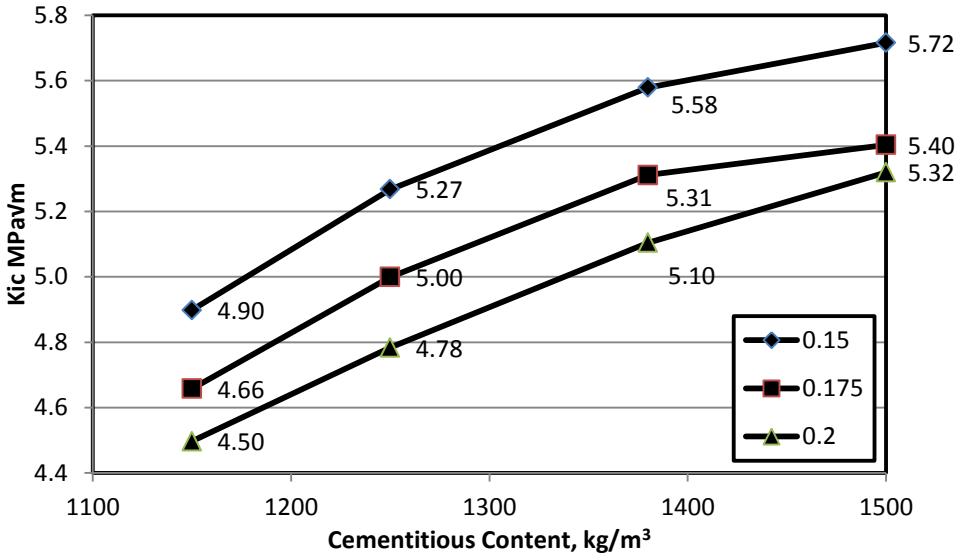

Figure 4.72: 28 day K_{ic} values for varying cementitious content for different w/b.

The G_f values for the RPC specimens prepared with w/b of 0.15 and total cementitious material content varying from 1150 kg/m^3 to 1500 kg/m^3 is depicted in Figure 4.73. The G_f increases with an increase in cementitious material content. The values for G_f for RPC specimens was 470, 524, 677, 681 N/m, respectively.

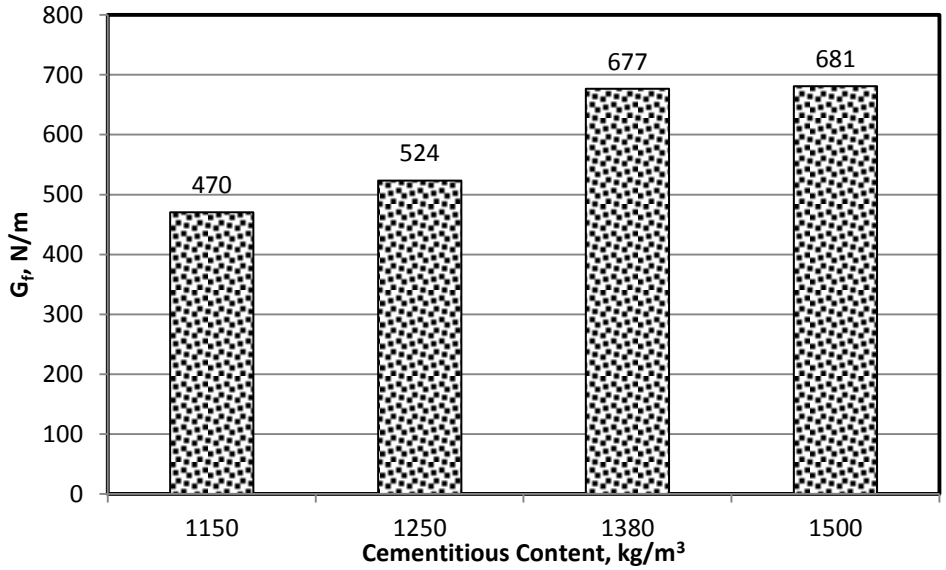

Figure 4.73: G_f in RPC Specimens Prepared with Different cementitious content, and w/b of 0.15.

The G_f values for the RPC specimens prepared with w/b of 0.175 and total cementitious material content varying from 1150 kg/m^3 to 1500 kg/m^3 is depicted in Figure 4.74. The G_f increases with an increase in cementitious material content. The values for G_f for RPC specimens were 452, 500, 656 and 664 N/m, respectively.

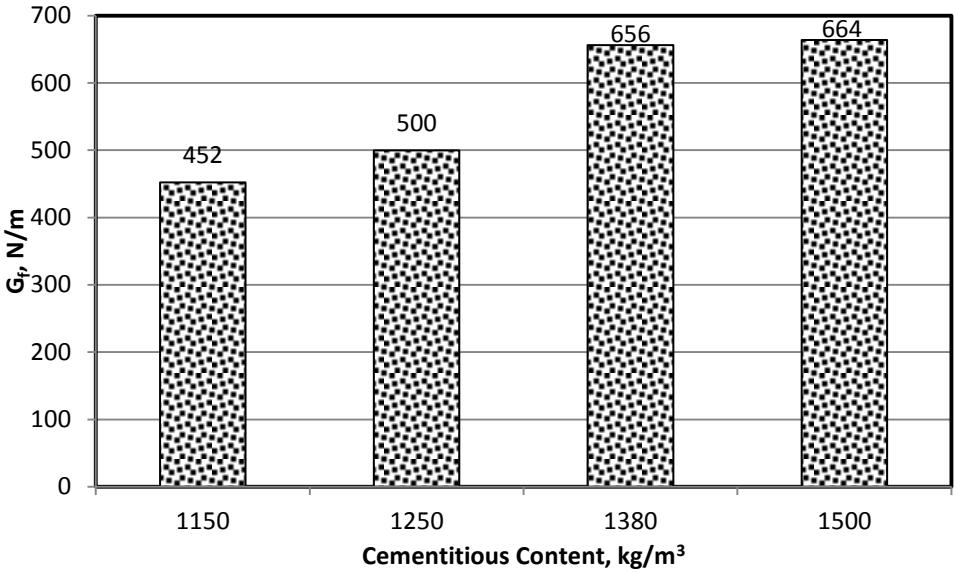

Figure 4.74: G_f in RPC Specimens Prepared with Different cementitious content, and w/b of 0.175.

The G_f values for the RPC specimens prepared with w/b of 0.20 and total cementitious material content varying from 1150 kg/m^3 to 1500 kg/m^3 is depicted in Figure 4.75.The G_f increases with an increase in cementitious material content. The values for G_f for RPC specimens was 440, 497, 651, 658 N/m, respectively.

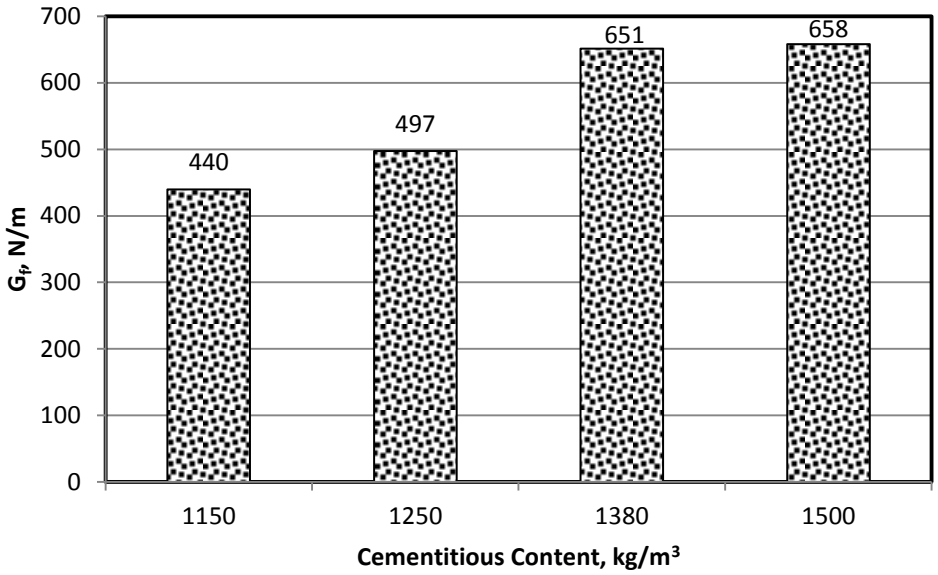

Figure 4.75: G_f in RPC Specimens Prepared with Different cementitious content, and w/b of 0.20.

The G_f at 28 days in the RPC specimens prepared with total cementitious material content varying from 1150 kg/m^3 to 1500 kg/m^3 and different w/b ratios is depicted in Figure 4.75. These values increased with increase in cementitious material content. Also, the G_f of RPC increased with a decrease in w/b ratio. However, there is a significant increase in K_{ic} values for RPC mixtures with w/b of 0.15 as compared to those prepared with w/b of 0.175 and 0.20.

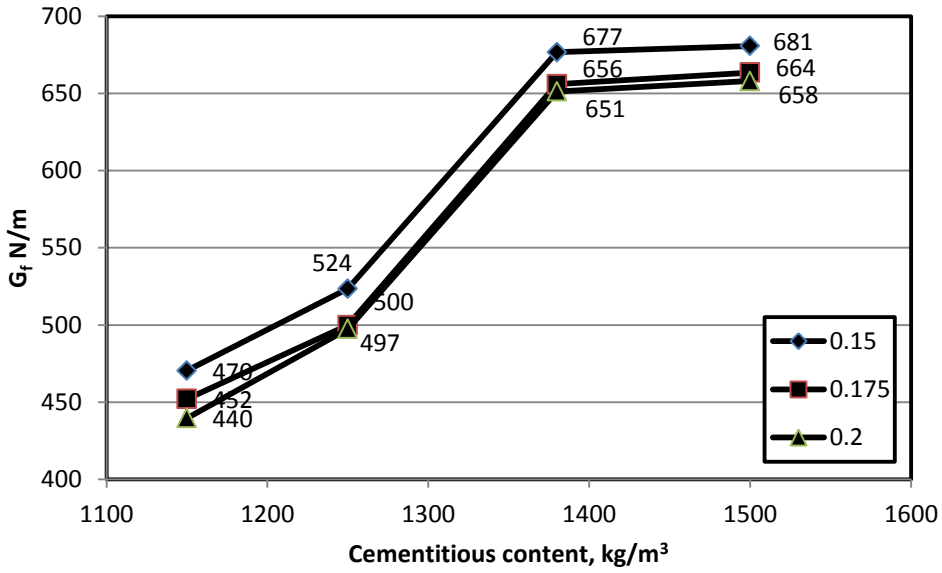

Figure 4.76: G_f values for varying cementitious content for different w/b.

4.7 STATISTICAL ANALYSIS OF EXPERIMENTAL DATA

A statistical analysis of the test results was carried out to develop models relating the mechanical properties of the developed RPC mixtures. Analysis of variance (ANOVA) was first carried out to assess the effect of mixture variables, such as w/b ratio, cement content, silica fume content on all the five mechanical properties of the RPC mixtures using simple software namely, MINITAB. Secondly, based on the ANOVA results, the models for compressive strength (for all 5 curing durations), elastic modulus, modulus of rupture, critical stress intensity factor, and critical fracture energy were developed using the *least squares* method. In the ANOVA as well as in the regression models, the notations used for independent variables were as follows:

W: Water/cementitious materials ratio by mass, cementitious materials means mixture of cement and silica fume

C: Cement content in kg/m^3

S: Silica fume content (as % of the cement content)

4.7.1 Statistical Analysis for Compressive strength

Data was utilized to develop relationship between the parameter and w/b ratio, cementitious material content and silica fume content. The ANOVA for compressive strength at 3 days, for which a general linear model was developed, is given below:

ANOVA for f_c' @ 3days, F vs. W, C, S

General Linear Model: F versus W, C, S

```
Factor  Type   Levels  Values
W       fixed       3  0.150, 0.175, 0.200
C       fixed       3  1000, 1100, 1200
S       fixed       3  15, 20, 25


Analysis of Variance for F, using Adjusted SS for Tests

Source  DF    Seq SS   Adj SS   Adj MS      F      P
W        2   224.003  224.003  112.002  13.62  0.003
C        2   135.581  135.581   67.791   8.24  0.011
S        2   359.680  359.680  179.840  21.87  0.001
W*C      4   331.557  331.557   82.889  10.08  0.003
C*S      4    10.218   10.218    2.554   0.31  0.863
W*S      4   107.007  107.007   26.752   3.25  0.073
Error    8    65.778   65.778    8.222
Total   26  1233.824


S = 2.86745   R-Sq = 94.67%   R-Sq(adj) = 82.67%
```

From above it is clear that parameters W, C, S and W*C have significant effect on the 3-day compressive strength results.

The regression equation relating the 3-day compressive strength to the w/b ratio, cementitious material content, and silica fume content is given below.

$$f'_{c,\,3d} = 136 - 176\ W - 0.0181\ C + 0.752\ S$$

A good fit of this model is noted by a $R^2 = 0.9467$.

Data was utilized to develop relationship between the parameter and w/b ratio, cementitious material content and silica fume content. The ANOVA for compressive strength at 7 days, for which a general linear model was developed, is given below:

ANOVA for f_c' @ 7days, F vs. W, C, S

General Linear Model: F versus W, C, S

```
Factor  Type   Levels  Values
W       fixed       3  0.150, 0.175, 0.200
C       fixed       3  1000, 1100, 1200
S       fixed       3  15, 20, 25

Analysis of Variance for F, using Adjusted SS for Tests

Source  DF   Seq SS   Adj SS   Adj MS      F      P
W        2  396.675  396.675  198.337  44.74  0.000
C        2   40.670   40.670   20.335   4.59  0.047
S        2  284.210  284.210  142.105  32.05  0.000
W*C      4  116.916  116.916   29.229   6.59  0.012
C*S      4   16.036   16.036    4.009   0.90  0.505
W*S      4   53.944   53.944   13.486   3.04  0.085
Error    8   35.466   35.466    4.433
Total   26  943.916


S = 2.10553   R-Sq = 96.24%   R-Sq(adj) = 87.79%
```

The regression equation relating the 3-day compressive strength to the w/b ratio, cementitious material content, and silica fume content is given below.

$$f'_{c,\,7d} = 136 - 141\ W - 0.0129\ C + 0.673\ S$$

A good fit of this model is noted by a R^2 of 0.9624.

Data was utilized to develop relationship between the parameter and w/b ratio, cementitious material content and silica fume content. The ANOVA for compressive strength at 14 days, for which a general linear model was developed, is given below:

ANOVA for f_c' @ 14days, F vs. W, C, S

General Linear Model: F versus W, C, S

```
Factor  Type   Levels  Values
W       fixed       3  0.150, 0.175, 0.200
C       fixed       3  1000, 1100, 1200
S       fixed       3  15, 20, 25


Analysis of Variance for F, using Adjusted SS for Tests

Source  DF   Seq SS   Adj SS   Adj MS      F      P
W        2  268.656  268.656  134.328  40.46  0.000
C        2  134.905  134.905   67.453  20.32  0.001
S        2  204.408  204.408  102.204  30.78  0.000
W*C      4   85.551   85.551   21.388   6.44  0.013
C*S      4   19.674   19.674    4.918   1.48  0.294
W*S      4    8.839    8.839    2.210   0.67  0.633
Error    8   26.560   26.560    3.320
Total   26  748.592


S = 1.82209   R-Sq = 96.45%   R-Sq(adj) = 88.47%
```

The regression equation relating the 14-day compressive strength to the w/b ratio, cementitious material content, and silica fume content is given below.

$$f'_{c,\,14d} = 169 - 168\ W - 0.0275\ C + 0.596\ S$$

A good fit of this model is noted by a R^2 of 0.9645.

Data was utilized to develop relationship between the parameter and w/b ratio, cementitious material content and silica fume content. The ANOVA for compressive strength at 28 days, for which a general linear model was developed, is given below:

ANOVA for f_c' @ 28days, F vs. W, C, S

General Linear Model: F versus W, C, S

```
Factor  Type   Levels  Values
W       fixed       3  0.150, 0.175, 0.200
C       fixed       3  1000, 1100, 1200
S       fixed       3  15, 20, 25


Analysis of Variance for F, using Adjusted SS for Tests

Source  DF   Seq SS   Adj SS   Adj MS       F      P
W        2  260.902  260.902  130.451  234.40  0.000
C        2   39.699   39.699   19.850   35.67  0.000
S        2  145.253  145.253   72.627  130.50  0.000
W*C      4   52.771   52.771   13.193   23.71  0.000
C*S      4    1.551    1.551    0.388    0.70  0.615
W*S      4    0.692    0.692    0.173    0.31  0.863
Error    8    4.452    4.452    0.557
Total   26  505.321


S = 0.746004   R-Sq = 99.12%   R-Sq(adj) = 97.14%
```

The regression equation relating the 3-day compressive strength to the w/b ratio, cementitious material content, and silica fume content is given below.

$$f'_{c,\,28d} = 133 - 151\ W + 0.0123\ C + 0.564\ S$$

A good fit of this model is noted by a R^2 of 0.9912

Data was utilized to develop relationship between the parameter and w/b ratio, cementitious material content and silica fume content. The ANOVA for compressive strength at 90 days, for which a general linear model was developed, is given below:

ANOVA for f_c' @ 90days, F vs. W, C, S

General Linear Model: F versus W, C, S

```
Factor  Type   Levels  Values
W       fixed       3  0.150, 0.175, 0.200
C       fixed       3  1000, 1100, 1200
S       fixed       3  15, 20, 25


Analysis of Variance for F, using Adjusted SS for Tests

Source  DF   Seq SS  Adj SS  Adj MS      F      P
W        2   229.68  229.68  114.84   6.62  0.020
C        2    19.54   19.54    9.77   0.56  0.591
S        2   531.74  531.74  265.87  15.32  0.002
W*C      4   178.15  178.15   44.54   2.57  0.120
C*S      4    14.18   14.18    3.54   0.20  0.929
W*S      4    21.51   21.51    5.38   0.31  0.864
Error    8   138.85  138.85   17.36
Total   26  1133.65


S = 4.16608   R-Sq = 87.75%   R-Sq(adj) = 60.19%
```

The regression equation relating the 3-day compressive strength to the w/b ratio, cementitious material content, and silica fume content is given below.

$$f'_{c,\,90d} = 160 - 121\,W - 0.0154\,C + 0.980\,S$$

A good fit of this model is noted by a R^2 of 0.8775

4.7.2 Statistical Analysis for Modulus of Elasticity

Data was utilized to develop relationship between the parameter and w/b ratio, cementitious material content and silica fume content. The ANOVA for secant modulus of elasticity at 28 days, for which a general linear model was developed, is given below:

ANOVA for E vs. W, C, S

General Linear Model: E versus W, C, S

```
Factor  Type   Levels  Values
W       fixed       3  0.150, 0.175, 0.200
C       fixed       3  1000, 1100, 1200
S       fixed       3  15, 20, 25


Analysis of Variance for E, using Adjusted SS for Tests

Source  DF   Seq SS   Adj SS  Adj MS       F      P
W        2  194.852  194.852  97.426  175.64  0.000
C        2   94.201   94.201  47.100   84.91  0.000
S        2   31.899   31.899  15.949   28.75  0.000
W*C      4   30.439   30.439   7.610   13.72  0.001
C*S      4    1.386    1.386   0.347    0.62  0.658
W*S      4    0.561    0.561   0.140    0.25  0.900
Error    8    4.438    4.438   0.555
Total   26  357.775

S = 0.744782   R-Sq = 98.76%   R-Sq(adj) = 95.97%
```

The regression equation relating the 28-day modulus of elasticity to the w/b ratio, cementitious material content, and silica fume content is given below.

E = 85.8 - 132 W - 0.0206 C + 0.266 S

A good fit of this model is noted by a R^2 of 0.9876.

4.7.3 Statistical Analysis of Modulus of Rupture

Data was utilized to develop relationship between the parameter and w/b ratio, cementitious material content and silica fume content. The ANOVA for modulus of Rupture, for which a general linear model was developed, is given below:

ANOVA for MOR vs. W, C, S

General Linear Model: M versus W, C, S

```
Factor  Type   Levels  Values
W       fixed       3  0.150, 0.175, 0.200
C       fixed       3  1000, 1100, 1200
S       fixed       3  15, 20, 25


Analysis of Variance for M, using Adjusted SS for Tests

Source  DF   Seq SS   Adj SS  Adj MS      F      P
W        2  107.748  107.748  53.874  44.72  0.000
C        2  180.882  180.882  90.441  75.08  0.000
S        2   67.709   67.709  33.855  28.10  0.000
W*C      4   13.251   13.251   3.313   2.75  0.104
C*S      4    1.191    1.191   0.298   0.25  0.903
W*S      4    9.633    9.633   2.408   2.00  0.188
Error    8    9.637    9.637   1.205
Total   26  390.052
S = 1.09755   R-Sq = 97.53%   R-Sq(adj) = 91.97%
```

The regression equation relating the 28-day modulus of rupture to the w/b ratio, cementitious material content, and silica fume content is given below.

MOR = 69.6 - 85.6 W - 0.0293 C + 0.332 S

A good fit of this model is noted by a R^2 of 0.9753.

4.7.4 Statistical Analysis for Ultimate Shrinkage

Data was utilized to develop relationship between the parameter and w/b ratio, cementitious material content and silica fume content. The ANOVA for ultimate shrinkage at 90 days, for which a general linear model was developed, is given below:

ANOVA for Ultimate Shrinkage SH vs. W, C, S

General Linear Model: SH versus W, C, S

```
Factor  Type   Levels  Values
W       fixed       3  0.150, 0.175, 0.200
C       fixed       3  1000, 1100, 1200
S       fixed       3  150, 200, 250


Analysis of Variance for X, using Adjusted SS for Tests

Source  DF    Seq SS   Adj SS   Adj MS       F      P
W        2   67027.4  67027.4  33513.7  358.68  0.000
C        2   62146.7  62146.7  31073.4  332.56  0.000
S        2    3029.3   3029.3   1514.6   16.21  0.002
W*C      4    2353.7   2353.7    588.4    6.30  0.014
C*S      4    2332.9   2332.9    583.2    6.24  0.014
W*S      4     313.6    313.6     78.4    0.84  0.537
Error    8     747.5    747.5     93.4
Total   26  137951.0


S = 9.66623   R-Sq = 99.46%   R-Sq(adj) = 98.24%
```

The regression equation relating the ultimate drying shrinkage to the w/b ratio, cementitious material content, and silica fume content is given below.

SH = - 445 + 2401 W + 0.529 C + 0.247 S

A good fit of this model is noted by a R^2 of 0.9946.

4.7.5 Statistical Analysis for Critical Stress Intensity Factor

Data was utilized to develop relationship between the parameter and w/b ratio, cementitious material content and silica fume content. The ANOVA for K_{ic}, for which a general linear model was developed, is given below:

ANOVA for Critical Stress Intensity Factor K vs. W, C, S

General Linear Model: K versus W, C, S

```
Factor  Type   Levels  Values
W       fixed       3  0.150, 0.175, 0.200
C       fixed       2  1000, 1200
S       fixed       2  15, 25


Analysis of Variance for K, using Adjusted SS for Tests

Source  DF   Seq SS   Adj SS   Adj MS       F      P
W        2  0.42432  0.42432  0.21216   43.40  0.000
C        1  0.88563  0.88563  0.88563  181.18  0.000
S        1  0.15870  0.15870  0.15870   32.47  0.001
Error    7  0.03422  0.03422  0.00489
Total   11  1.50287


S = 0.0699149   R-Sq = 97.72%   R-Sq(adj) = 96.42%
```

The regression equation relating the ultimate drying shrinkage to the w/b ratio, cementitious material content, and silica fume content is given below.

$$K_{ic} = 3.27625 - 9.15\ W + 0.00271667\ C + 0.023\ S$$

A good fit of this model is noted by a R^2 of 0.9642.

4.7.6 Statistical Analysis for Critical Fracture Energy

Data was utilized to develop relationship between the parameter and w/b ratio, cementitious material content and silica fume content. The ANOVA for G_f for which a general linear model was developed, is given below:

ANOVA for Critical Fracture Energy G vs. W, C, S

General Linear Model: G versus W, C, S

```
Factor  Type   Levels  Values
W       fixed       3  0.150, 0.175, 0.200
C       fixed       2  1000, 1200
S       fixed       2  15, 25

Analysis of Variance for G, using Adjusted SS for Tests

Source  DF  Seq SS  Adj SS  Adj MS       F      P
W        2    1814    1814     907    3.10  0.109
C        1   98827   98827   98827  337.55  0.000
S        1    2214    2214    2214    7.56  0.029
Error    7    2049    2049     293
Total   11  104904

S = 17.1106   R-Sq = 98.05%   R-Sq(adj) = 96.93%
```

The regression equation relating the critical fracture energy to the w/b ratio, cementitious material content, and silica fume content is given below:

$$G_f = -378.583 - 590\ W + 0.9075\ C + 2.71667\ S$$

A good fit of this model is noted by a R^2 of 0.9798.

4.7.7 Summary of all regression equations

Table 4-11 gives the summary of all the regression equations and their corresponding R^2 values, obtained utilizing the experimental data generated through the present work based on the statistical experiment design.

Table 4-11: Summary of all regression equations.

Curing duration (days)	Fitted equation	R^2
3	$f'_c = 136 - 176\ W - 0.0181\ C + 0.752\ S$	0.95
7	$f'_c = 136 - 141\ W - 0.0129\ C + 0.673\ S$	0.96
14	$f'_c = 169 - 168\ W - 0.0275\ C + 0.596\ S$	0.96
28	$f'_c = 133 - 151\ W + 0.0123\ C + 0.564\ S$	0.99
90	$f'_c = 160 - 121\ W - 0.0154\ C + 0.980\ S$	0.88
28	$E = 85.8 - 132\ W - 0.0206\ C + 0.266\ S$	0.98
28	$MOR = 69.6 - 85.6\ W - 0.0293\ C + 0.332\ S$	0.97
28	$K_{ic} = 3.27625 - 9.15\ W + 0.00271667\ C + 0.023\ S$	0.96
28	$G_f = -378.583 - 590\ W + 0.9075\ C + 2.71667\ S$	0.98
28	$SH = - 445 + 2401\ W + 0.529\ C + 0.247\ S$	0.99

4.8 CORRELATION BETWEEN COMPRESSIVE STRENGTH AND OTHER MECHANICAL PROPERTIES

28-days compressive strength, modulus of elasticity and MOR of all the 27 RPC mixtures are presented in Table 4-12. 28-days K_{ic} and G_f values of 12 selected mixtures of RPC are given in Table 4-13.

Table 4-12: Summary of Compressive strength, modulus of elasticity and modulus of rupture after 28 days of curing.

Mix #	f'_c (MPa)	E (GPa)	MOR (MPa)
M 1	132.0	51.0	33.0
M 2	135.6	52.5	34.4
M 3	136.9	53.0	36.6
M 4	132.0	44.8	27.8
M 5	136.3	46.5	29.8
M 6	138.9	47.6	32.9
M 7	132.8	45.7	26.0
M 8	135.0	47.8	30.9
M 9	137.0	48.4	34.8
M 10	129.4	48.3	32.4
M 11	133.3	49.2	34.0
M 12	135.0	50.0	34.9
M 13	128.4	42.9	24.5
M 14	130.0	44.4	25.8
M 15	133.0	45.0	28.0
M 16	130.0	41.2	24.9
M 17	134.0	42.4	26.5
M 18	136.0	45.7	27.5
M 19	121.5	40.3	27.9
M 20	126.2	43.2	30.7
M 21	128.0	44.5	31.5
M 22	123.3	41.6	23.0
M 23	125.7	42.0	25.7
M 24	128.3	43.0	27.1
M 25	128.0	40.0	25.0
M 26	132.2	41.0	26.0
M 27	135.0	42.5	26.0

Table 4-13: Summary of K_{ic} and G_f values

Mix #	K_{ic} MPa√m	G_f N/m
1	4.90	470
3	5.27	523
7	5.58	676
9	5.72	680
10	4.66	452
12	5.00	499
16	5.31	655
18	5.40	663
19	4.50	439
21	4.78	497
25	5.10	651
27	5.26	644

The data presented in Table 4-12 and Table 4-13 were utilized to obtain regression equations correlating compressive strength with other four mechanical properties of RPC. The fitted correlation equations are presented in Table 4-14 along with their R^2 values.

Table 4-14: Summary of co-relationships developed with f_c and other mechanical properties

Fitted correlation equations	R^2
$E = 4.36\sqrt{f`c}$	0.85
$MOR = 3.08\sqrt{f`c}$	0.86
$K_{ic} = 0.0017 f`_c^{1.6464}$	0.86
$G_f = 9.5498e^{0.0312f`c}$	0.97

As observed from Table 4-14, the coefficient for modulus of elasticity for RPC is 4.36, which is very close to the value of the coefficient (4.70) for normal concrete [36]. However, the coefficient for modulus of rupture for RPC is 3.08, whereas the coefficient for normal concrete is 0.99 [37]. This indicates that for same compressive strength the inclusion of steel fibers in the RPC has no significant effect on modulus of elasticity but

has increased the flexural capacity of RPC by more than three times as compared to conventional concrete.

The correlation equations presented in Table 4-14 can be used to calculate the values of *E*, *MOR*, K_{ic}, and G_f by substituting the experimentally measured value of f'_c.

4.9 UTILIZATION OF THE DERIVED REGRESSION MODELS

The regression models obtained for the five mechanical properties (f'_c, *E*, *MOR*, K_{ic}, *and* G_f) and ultimate shrinkage (*SH*) of RPC mixtures, as presented in Table 4-11, can be utilized for the purpose of obtaining an optimum mixture proportion. The mixture optimization for achieving a target compressive strength for a given curing duration (within minimum and maximum range of compressive strength as given in Table 4-4) can be carried out using Excel-Solver by considering the regression model for the given curing period as objective function and considering the models for other properties as constraints. If the strength requirement is less than or equal to the minimum value of strength at given period of curing, the mixture optimization can be carried out corresponding to a minimum total unit cost of the mixture.

CHAPTER 5

CONCLUSIONS AND

RECOMMENDATIONS

5.1 CONCLUSIONS

Several trial mixtures were carried out to optimize the various constituents of RPC. Firstly, the trials were carried out to determine the optimum sand grading. Preliminary results show that the natural grading of sand available in Saudi Arabia is yielding best results. Secondly, trials were carried out to optimize the superplasticizer dosage. It was found that the optimum superplasticizer dosage was 3.6% by the cementitious material for mixtures with a w/b ratio of 0.15. For mixtures with w/b ratio of 0.175, optimum super plasticizer dosage was in the range of 1.5% to 2% of the cementitious material. The optimum dosage of superplasticizer was in the range of 1% to 1.5% in the RPC with w/b ratio of 0.20. It is evident that the quantity of superplasticizer increases with a decrease in the w/b ratio.

Curing period and mixture variables both were found to have combined effect on compressive strength of the RPC mixtures. It was found that there is significant increase

in compressive strength with increase in the curing period. Out of three mix variables considered, the w/b ratio was found to have most significant effect on compressive strength. The silica fume content was next to the w/b ratio to show the positive effect on compressive strength. However, the cement content has not shown considerable effect on compressive strength. For mixtures with similar silica fume content the compressive strength increased with decreasing w/b ratio. The compressive strength of mixtures with a w/b ratio of 0.15 was in the range of 128 to 139 MPa, while it was in the range of 128 to 123 MPa in the mixtures prepared with a w/b ratio of 0.175. The compressive strength of RPC mixtures prepared with w/b ratio of 0.20 was in the range of 123 to 129 MPa. The effect of the mix variables is highest at 3-days curing period and lowest for 28-days curing period because the difference in minimum and maximum values are 31% and 14%, respectively for 3-days and 28-days curing period. Effect of mix variables for 28-days curing period is almost half of that for 3-days cuing period. For other curing durations (7, 14, and 90 days) the difference in minimum and maximum values is almost same (around 20%).

The modulus of elasticity of the RPC mixtures with cement content of 1000, 1100, 1200 kg/m^3, different w/b ratios, and silica fume content varying from 15 to 25%, as replacement of sand. While there is small marginal difference in the secant modulus of mixtures prepared with w/b ratio of 0.15 and 0.175 there was significant change between those prepared with w/b ratio of 0.175 and 0.20. The 28-day modulus of elasticity of RPC mixtures with w/b ratio of 0.15 was in the range of 46 to 53 GPa while the values in the mixtures with w/b ratio were in the range of 41 to 49.5 GPa. The modulus of elasticity of RPC mixtures prepared with w/b ratio of 0.20 was in the range of 40 to 45 GPa.

The *MOR* of RPC mixtures with cement content of 1000, 1100, 1200 kg/m^3, different w/b ratios, and silica fume content varying from 15 to 25%, as replacement of sand. While there is small marginal difference in the *MOR* of mixtures prepared with w/b ratio of 0.15 and 0.175 there was significant change between those prepared with w/b ratio of 0.175 and 0.20. The 28-day *MOR* of RPC mixtures with w/b ratio of 0.15 were in the range of 26 to 37 MPa while the values in the mixtures with w/b ratio 0.175 were in the range of 25 to 36 MPa. The modulus of elasticity of RPC mixtures prepared with w/b ratio of 0.20 was in the range of 24 to 32 MPa.

The drying shrinkage strain increased with age in all the RPC mixtures. The drying shrinkage strains development in the 20 and 25% silica fume was almost similar and more than that in the mixtures with 15% silica fume. The drying shrinkage in the RPC mixtures prepared with w/b of 0.15, 0.175, 0.20 cement content of 1000, 1100, 1200 kg/m^3 and silica fume content varying from 15 to 25%, as replacement of sand. After 90 days of exposure, the drying shrinkage strains of 15%, 20 % and 25% silica fume RPC mixtures were 716, 727 and 730 μm, respectively.

The 28-day K_{ic} values of the RPC mixtures with total cementitious material content varying from 1150 kg/m^3 to 1500 kg/m^3 and different w/b ratios were determined. These values increased with an increase in cementitious material content. Also, the K_{ic} values of RPC increased with decrease in w/b ratio. However, there is a significant increase in K_{ic} values for RPC mixtures with a w/b of 0.15 as compared to those prepared with w/b of 0.175 and 0.20.

The G_f at 28 days in the RPC mixtures prepared with total cementitious material content varying from 1150 kg/m^3 to 1500 kg/m^3 and different w/b ratios. These values increased

with increase in cementitious material content. Also, the G_f of RPC increased with a decrease in w/b ratio. However, there is a significant increase in K_{ic} values for RPC mixtures with w/b of 0.15 as compared to those prepared with w/b of 0.175 and 0.20.

The regression models obtained for all five mechanical properties and ultimate shrinkage of the RPC mixtures can be utilized to carry out optimum design of the RPC mixtures for a given curing period within the ranges of mixture variables considered in this study.

The equation showing correlation between compressive strength and *MOR* for RPC mixtures has indicated that for the same compressive strength value, the RPC has three times more *MOR* than a normal concrete. The equations correlating compressive strength with other four mechanical properties of the RPC mixtures can be useful for predicting the values of modulus of elasticity, modulus of rupture, critical stress intensity factor, and critical fracture energy by substituting the experimentally measured values of compressive strength into the correlation equations.

5.2 RECOMMENDATIONS

- A study on durability of RPC should to be conducted for ensuring the adoptability of RPC in the aggressive exposure conditions.
- There is a need to explore the possibility of developing RPC using industrial waste materials for achieving economy.

REFERENCES

1. Yanni, V.Y.G., *"Multi-scale Investigation of Tensile Creep of Ultra High Performance Concrete for Bridge Applications"*. 2009, Georgia Institute of Technology.
2. VandeVoort, T., M. Suleiman, and S. Sritharan, *"Design and Performance Verification of UHPC Piles for Deep Foundations"*, in *'Use of Ultra-High Performance Concrete in Geotechnical and Substructure Applications'*. 2008.
3. Richard, P. and M. Cheyrezy, *"Composition of reactive powder concretes"*. Cement and Concrete Research, 1995. **25**(7): p. 1501-1511.
4. Skazlic´, M. and D. Bjegovic´, *"Toughness Testing of Ultra-high Performance Fibre Reinforced Concrete".* Materials and Structures/Materiaux et Constructions, 2009. **42**: p. 1025-1038.
5. Graybeal, B.A., *"Material Property Characterization of Ultra-High Performance Concrete"*, in *FHWA-HRT-06-103*, F.H. Administration, Editor. 2006: Washington, D.C.
6. Graybeal, B.A., *"Characterization of the Behavior of Ultra-High Performance Concrete"*. 2005, Faculty of the Graduate School of the University of Maryland.
7. Ma, J. and H. Schneider, *"Properties of Ultra-High Performance Concrete"*. LACER, No.7, 2002: p. 25-32.
8. Vagelis G, P., *"Experimental investigation and theoretical modeling of silica fume activity in concrete"*. Cement and Concrete Research, 1999. **29**(1): p. 79-86.
9. Shah, S.P. and W.J. Weiss. *"Ultra High strength concrete; looking toward the future"*. in *ACI Special Proceedings from the Paul Zia Symposium*. 1998. Atlanta.
10. Long, G., X. Wang, and Y. Xie, *"Very-high-performance concrete with ultrafine powders"*. Cement and Concrete Research, 2002. **32**(4): p. 601-605.
11. Yazici, H., et al., *"Mechanical properties of reactive powder concrete containing high volumes of ground granulated blast furnace slag"*. Cement and Concrete Composites, 2010. **32**(8): p. 639-648.
12. de Larrard, F. and T. Sedran, *"Optimization of ultra-high-performance concrete by the use of a packing model"*. Cement and Concrete Research, 1994. **24**(6): p. 997-1009.
13. Konstantin, S., *"The development of a new method for the proportioning of high-performance concrete mixtures"*. Cement and Concrete Composites, 2004. **26**(7): p. 901-907.
14. Acker, P. and M. Behloul. *"Ductal Technology: a large spectrum of properties, a wide range of applications"*. in *Proceedings of the International Symposium on Ultra Reactive Powder Concrete*. 2004: Kassel University Press, Kassel, Germany, pp. 11-24.
15. Chan, Y.-W. and S.-H. Chu, *"Effect of silica fume on steel fiber bond characteristics in reactive powder concrete"*. Cement and Concrete Research, 2004. **34**(7): p. 1167-1172.

16. Hajar, Z., et al. *"Design and construtions of the world first ultra-high performance road bridges"*. in *Proceedings of the Interantional Symposium on Ultra Reactive Powder Concrete*. 2004: Kassel University Press, Kassel, Germany.
17. Kaufmann, J., F. Winnefeld, and D. Hesselbarth, *"Effect of the addition of ultrafine cement and short fiber reinforcement on shrinkage, rheological and mechanical properties of Portland cement pastes"*. Cement and Concrete Composites, 2004. **26**(5): p. 541-549.
18. Liu, J., S. Song, and L. Wang, *"Durability and micro-structure of reactive powder concrete"*. Journal Wuhan University of Technology, Materials Science Edition, 2009. **24**(3): p. 506-509.
19. Matte, V. and M. Moranville, *"Durability of reactive powder composites: Influence of silica fume on the leaching properties of very low water/binder pastes"*. Cement and Concrete Composites, 1999. **21**(1): p. 1-9.
20. Mazanec, O., D. Lowke, and P. Schiel, *"Mixing of high performance concrete: Effect of concrete composition and mixing intensity on mixing time"*. Materials and Structures/Materiaux et Constructions, 2010. **43**(3): p. 357-365.
21. Ng, K.M., C.M. Tam, and V.W.Y. Tam, *"Studying the production process and mechanical properties of reactive powder concrete: A Hong Kong study"*. Magazine of Concrete Research, 2010. **62**(9): p. 647-654.
22. Shmidt, M. and E. Fehling, *"Ultra-High Performance Concrete: Research. Development and Application in Europe"*, in *International Symposium on UHPC*. 2004: Kassel.
23. Tam, C.M., V.W.Y. Tam, and K.M. Ng, *"Optimal conditions for producing reactive powder concrete"*. Magazine of Concrete Research, 2010. **62**(10): p. 701-716.
24. Yazici, H., et al., *"Utilization of fly ash and ground granulated blast furnace slag as an alternative silica source in reactive powder concrete"*. Fuel, 2008. **87**(12): p. 2401-2407.
25. Garas, V.Y., L.F. Kahn, and K.E. Kurtis, *"Short-term tensile creep and shrinkage of ultra-high performance concrete"*. Cement and Concrete Composites, 2009. **31**(3): p. 147-152.
26. Tam, C.M., V.W.Y. Tam, and K.M. Ng, *"Assessing drying shrinkage and water permeability of reactive powder concrete produced in Hong Kong"*. Construction and Building Materials, 2012. **26**(1): p. 79-89.
27. Loukili, A., A. Khelidj, and P. Richard, *"Hydration Kinetics, Change of Relative Humidity, and Autogenous Shrinkage of Ultra-High-Strength Concrete",*. Cement and Concrete Research, 1999. **29**(4, April): p. 577-584.
28. Graybeal, B.A. and J.L. Hartmann, *"Strength and Durability of Ultra-High Performance Concrete"*, in *Concrete Bridge Conference*. 2003, Portland Cement Association.
29. Gilliland, S.K. *"Reactive Powder Concrete (RPC), A New Material for Prestressed Concrete Bridge Girders"*. in *Structures Congress – Proceedings, Building an International Community of Structural Engineers*. 1996.
30. Buitelaar, P. *"Heavy Reinforced Ultra-Reactive Powder Concrete"*. in *Proceedings of the International Symposium on Ultra Reactive Powder Concrete*. 2004: Kassel University Press, Kassel, Germany.

31. ASTM, *"Standard specification for steel fiber reinforced concrete"*, in *ASTM A 820-90*. 1990.
32. ASTM, *"Standard Test Method for Flow of Hydraulic Cement Mortar"*, in *ASTM C1437 - 07* 2007.
33. Jenq, Y. and S.P. Shah, *"Two Parameter Model for Concrete".* Journal of Engineering Mechanics, 1985. **111**(10): p. 1227-1241.
34. *ASTM C 39, "Standard Test Method for Compressive Strength of Cylindrical Concrete Specimens"*. Annual Book of ASTM Standards. Vol. 4.02. 2005, Philadelphia: American Society for Testing and Materials.
35. Gowripalan, N. and R.I. Gilbert, *"Design Guidelines for RPC Prestressed Concrete Beams"*. 2000, The University of New South Wales.
36. ACI, *"Building Code Requirements for Reinforced Concrete (ACI 318M-95) and Commentary (ACI 318RM-95),"* in *Committe 318*. 1995. p. 371 pp.
37. ASTM C78 / C78M - 10, "Standard Test Method for Flexural Strength of Concrete (Using Simple Beam with Third-Point Loading)". Annual Book of ASTM Standards.

APPENDICES

APPENDIX A

STRESS-STRAIN RESPONSES OF RPC SPECIMENS PREPARED WITH DIFFERENT MIX PROPORTIONS, FOR OBTAINING SECANT MODULUS OF ELASTICITY.

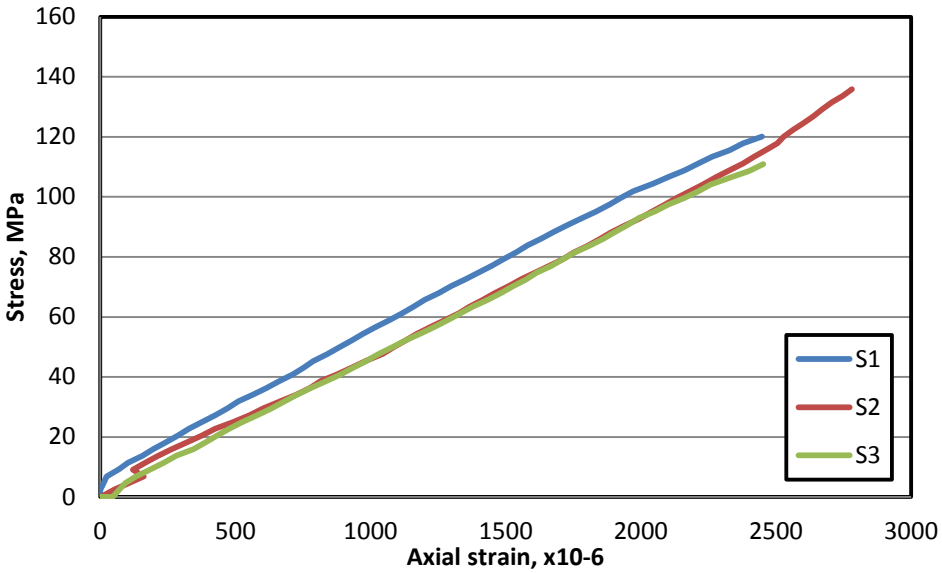

Figure 0A.1: Stress-strain response or RPC mixture M1.

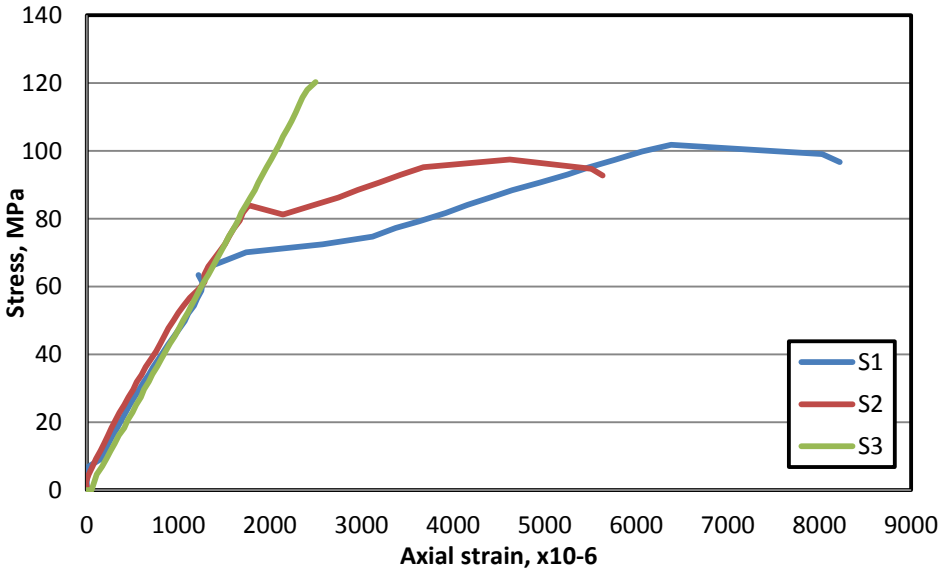

Figure A.2: Stress-strain response or RPC mixture M2.

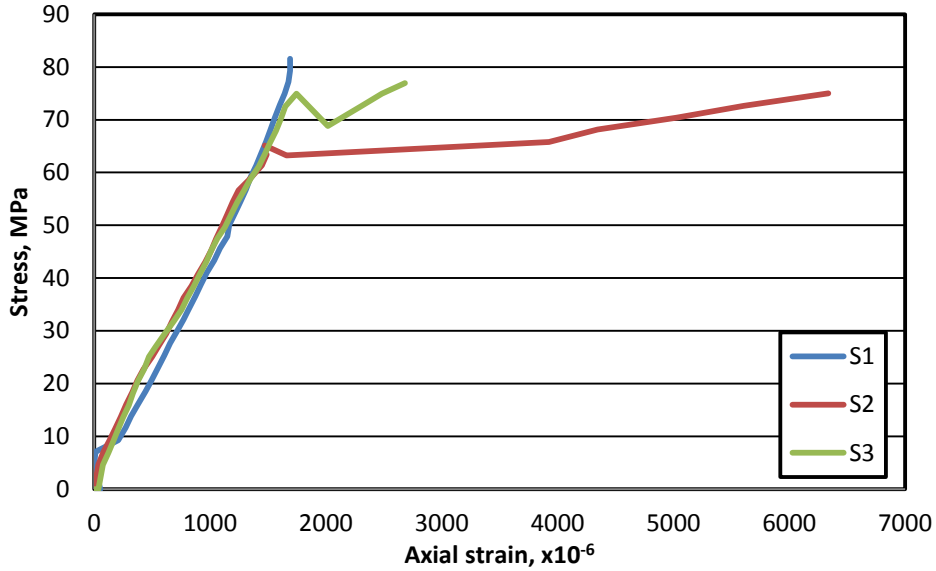

Figure A.3: Stress-strain response or RPC mixture M3.

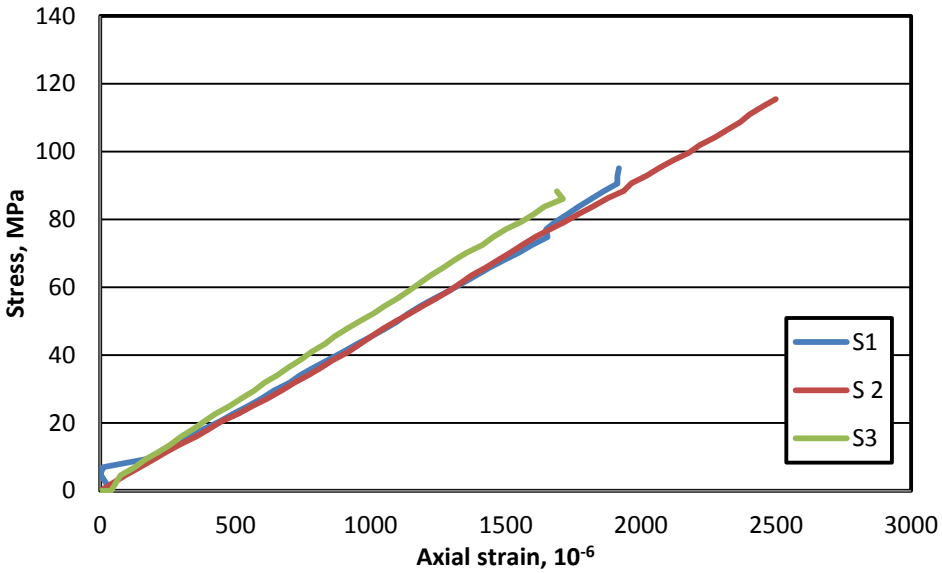

Figure A.4: Stress-strain response or RPC mixture M4.

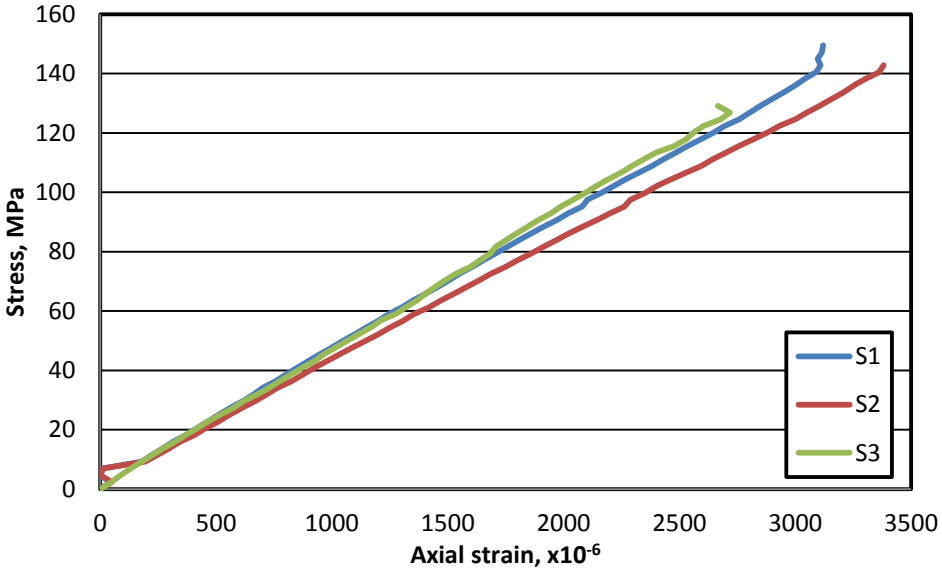

Figure A.5: Stress-strain response or RPC mixture M5.

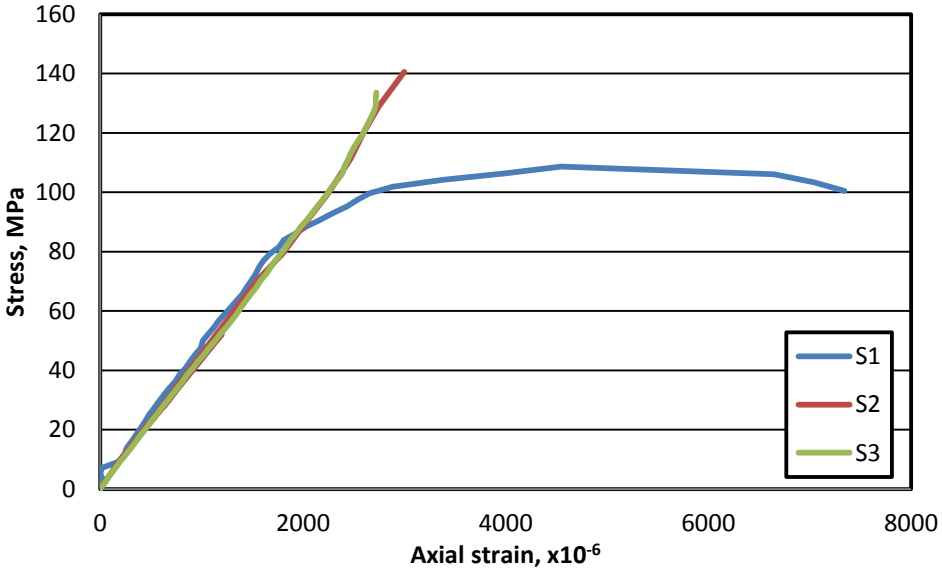

Figure A.6: Stress-strain response or RPC mixture M6.

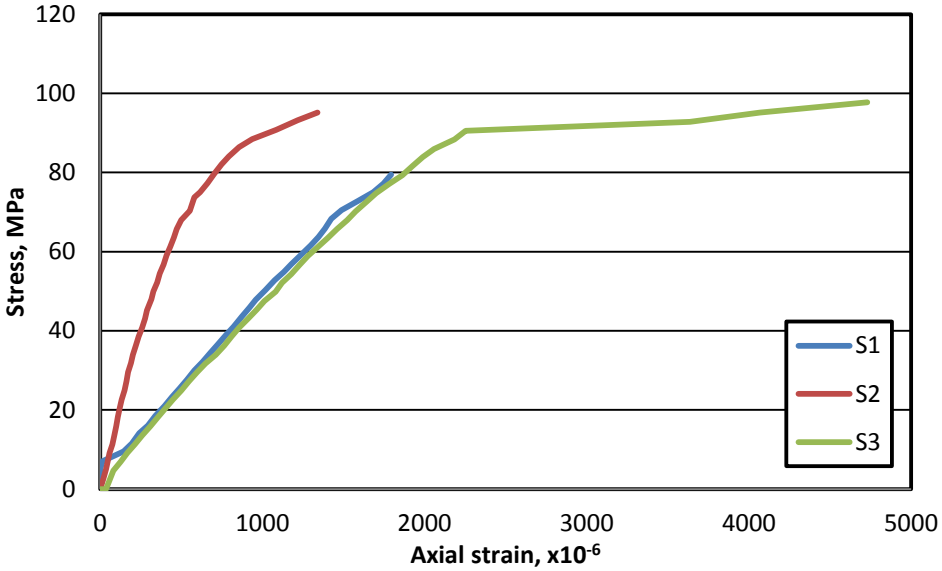

Figure A.7: Stress-strain response or RPC mixture M7.

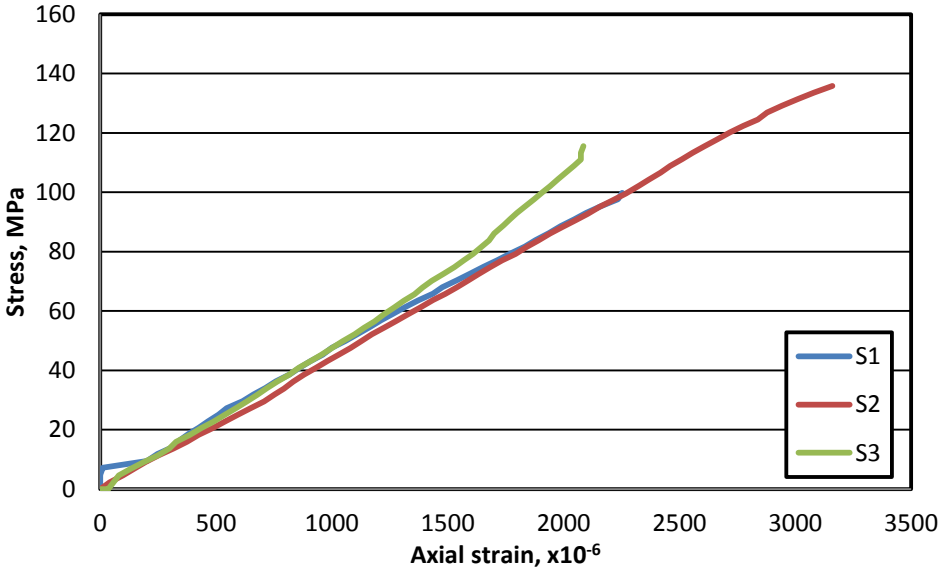

Figure A.8: Stress-strain response or RPC mixture M8.

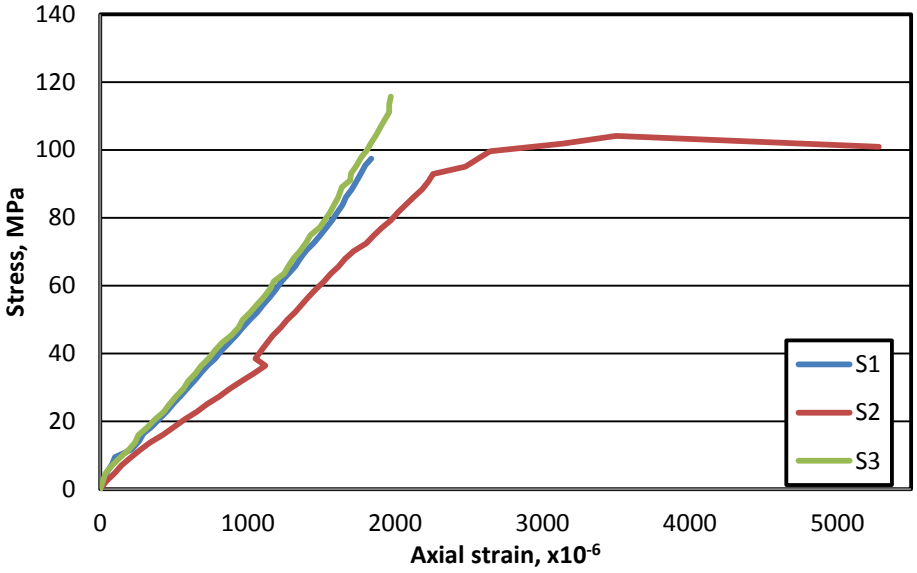

Figure A.9: Stress-strain response or RPC mixture M9.

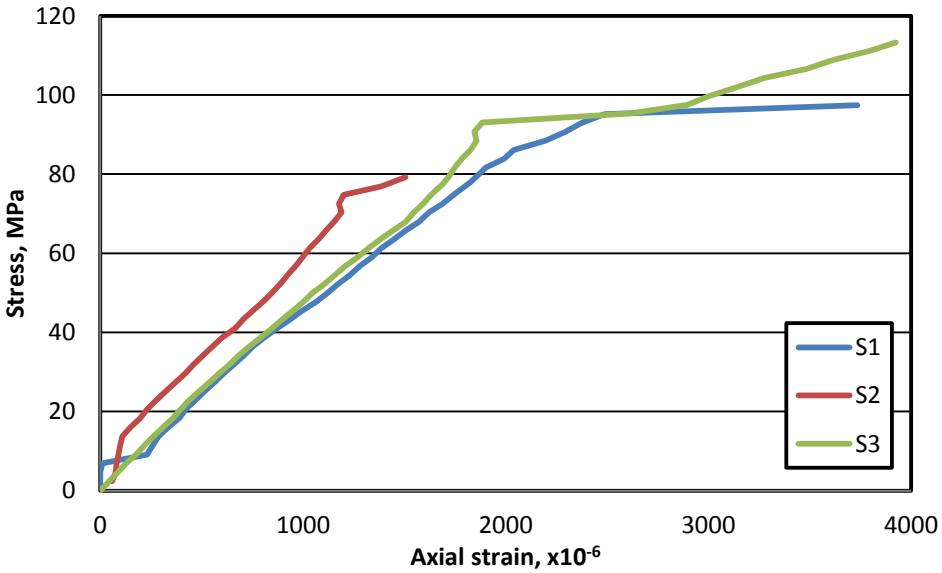

Figure A.10: Stress-strain response or RPC mixture M10.

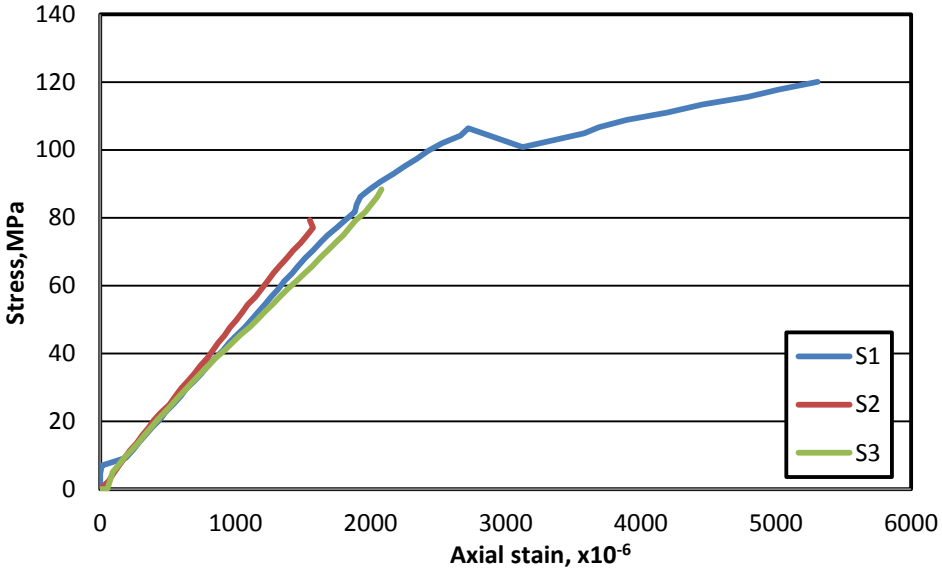

Figure A.11: Stress-strain response or RPC mixture M11.

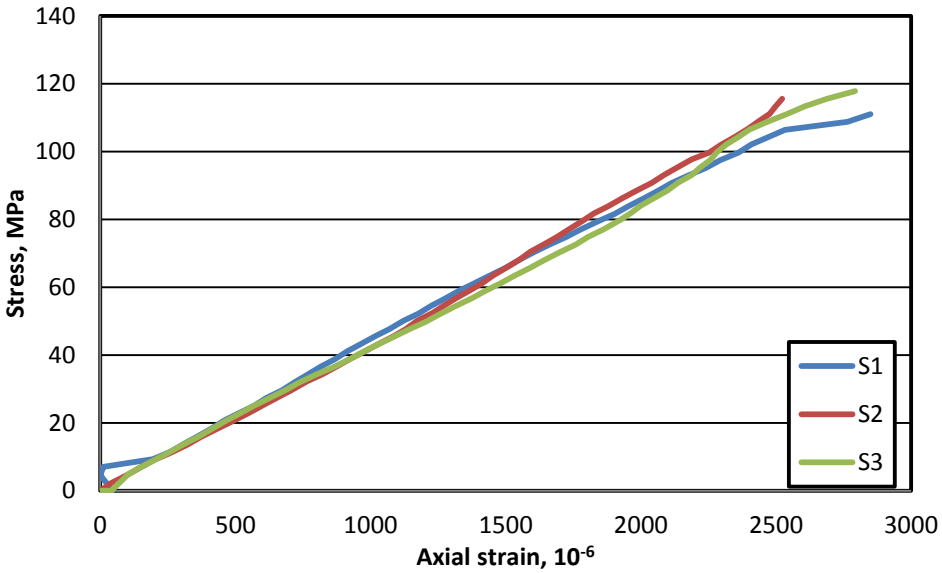

Figure A.12: Stress-strain response or RPC mixture M12.

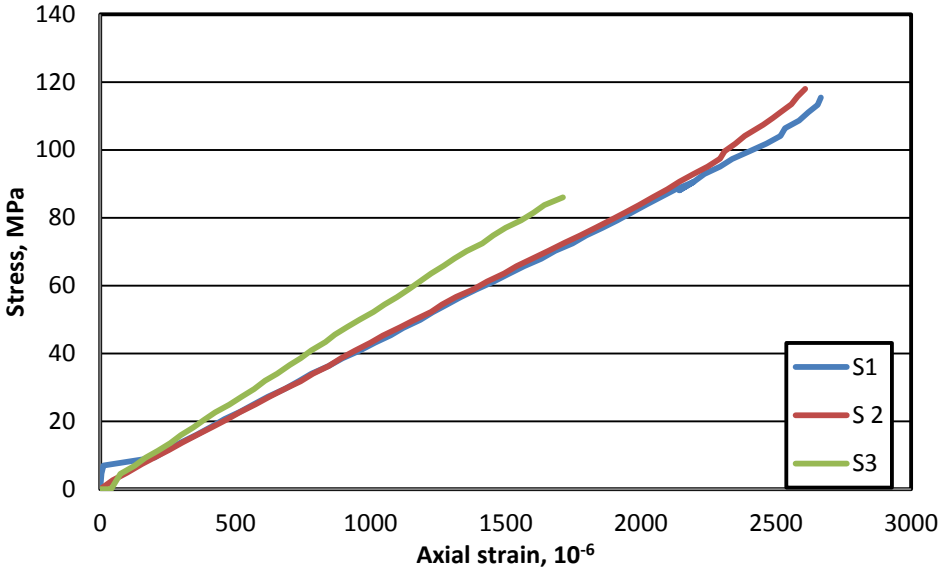

Figure A.13: Stress-strain response or RPC mixture M13.

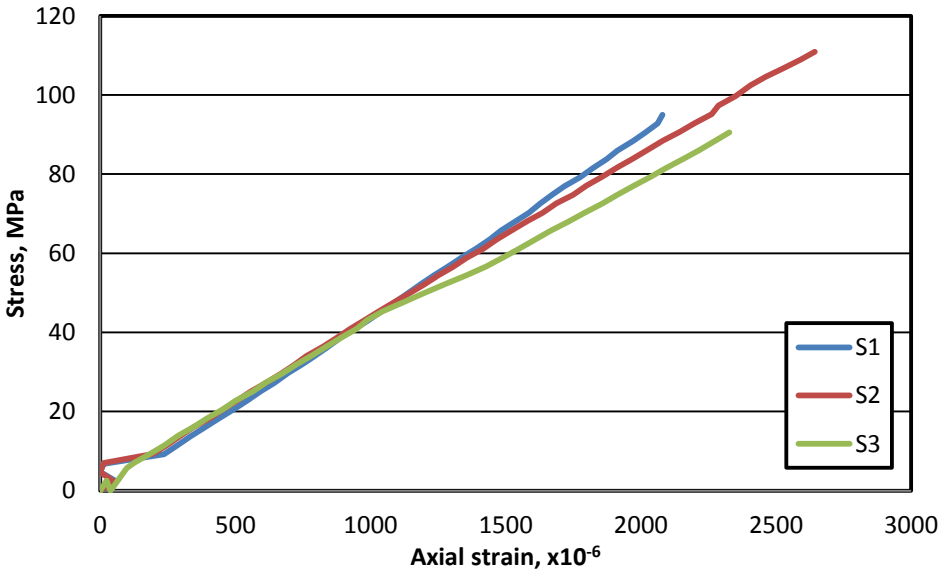

Figure A.14: Stress-strain response or RPC mixture M14.

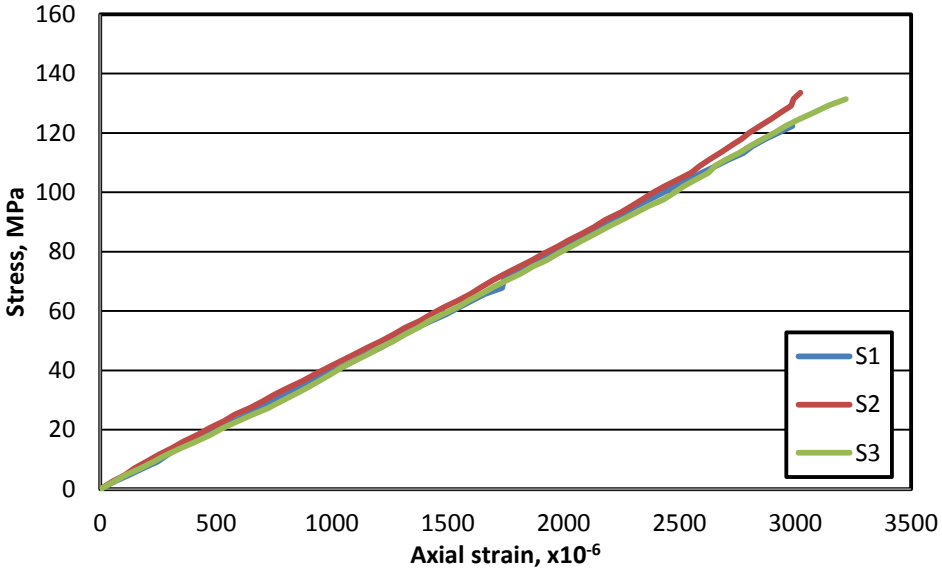

Figure A.15: Stress-strain response or RPC mixture M15.

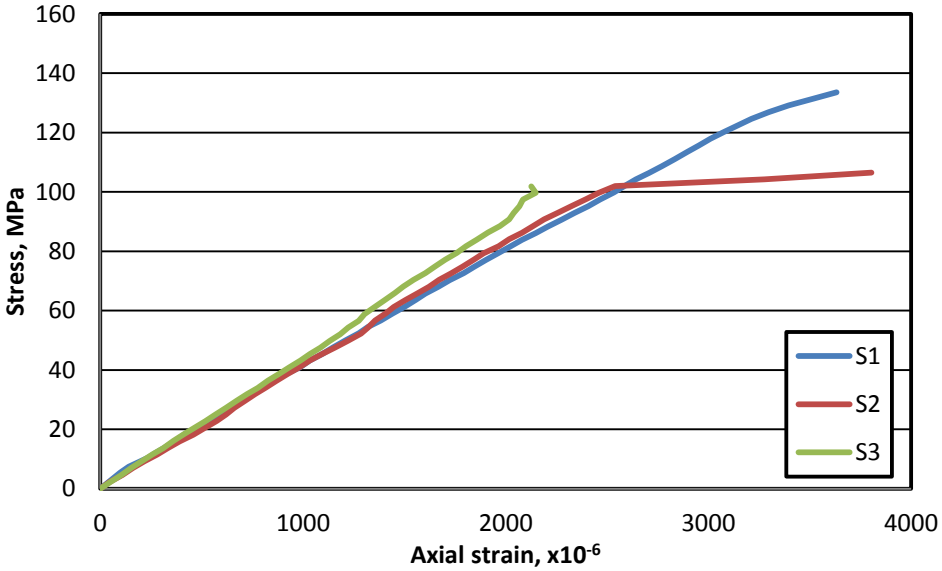

Figure A.16: Stress-strain response or RPC mixture M16.

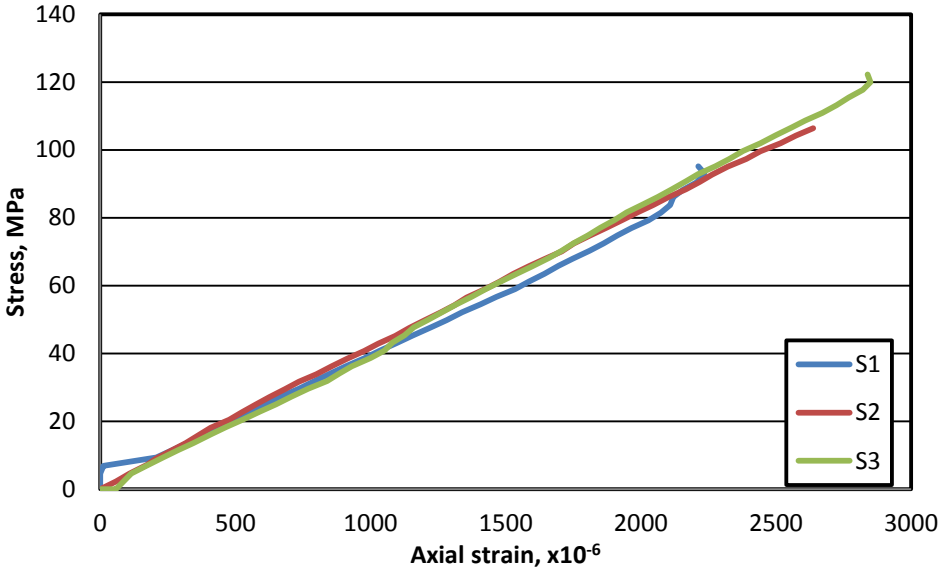

Figure A.17: Stress-strain response or RPC mixture M9.

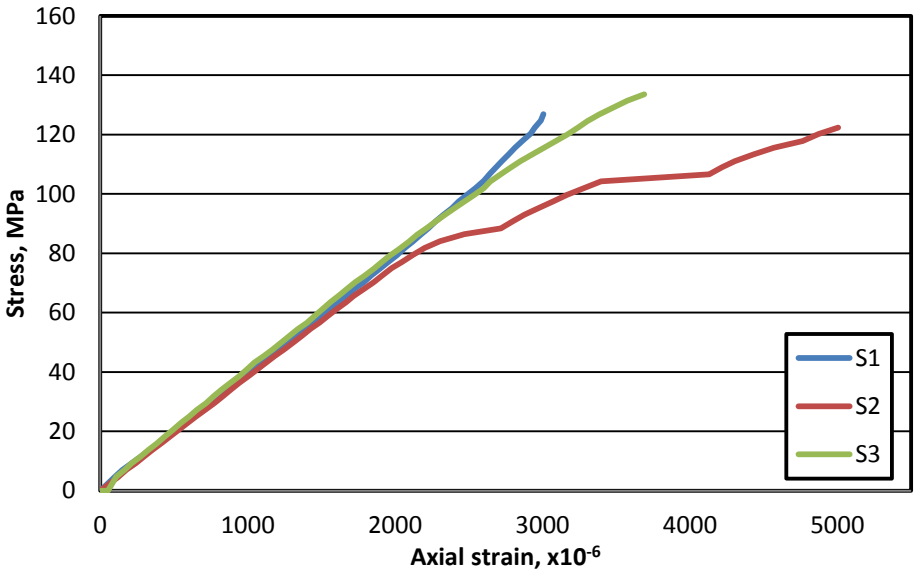

Figure A.18: Stress-strain response or RPC mixture M18.

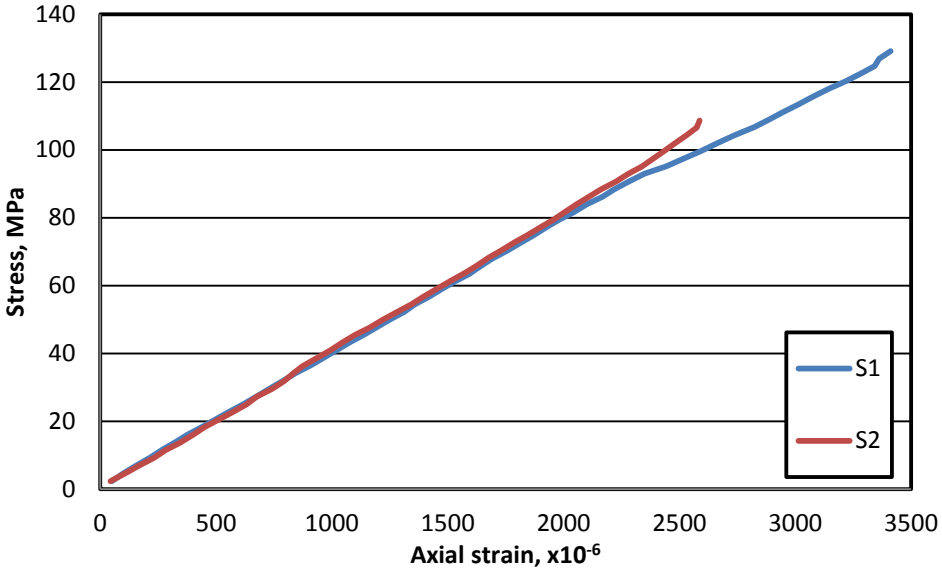

Figure A.19: Stress-strain response or RPC mixture M19.

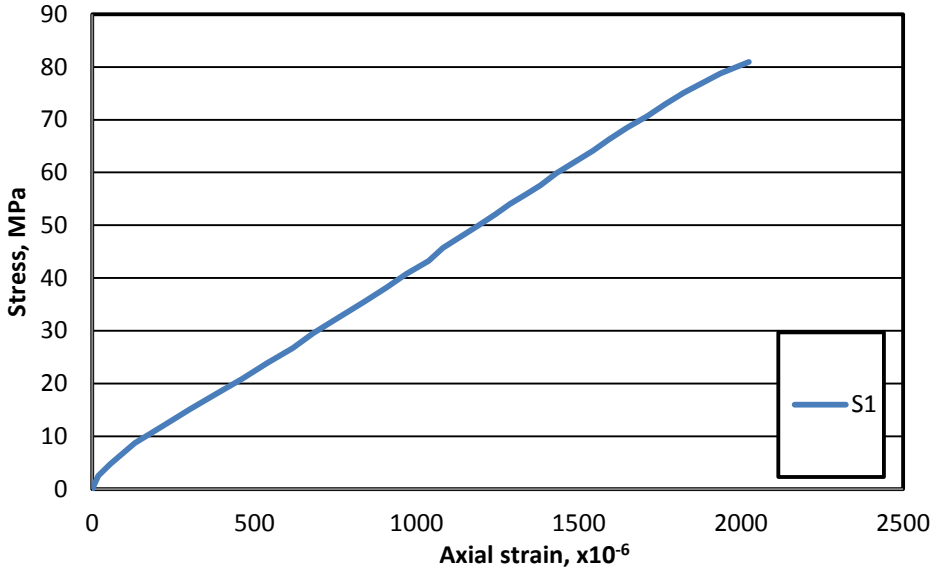

Figure A.20: Stress-strain response or RPC mixture M20.

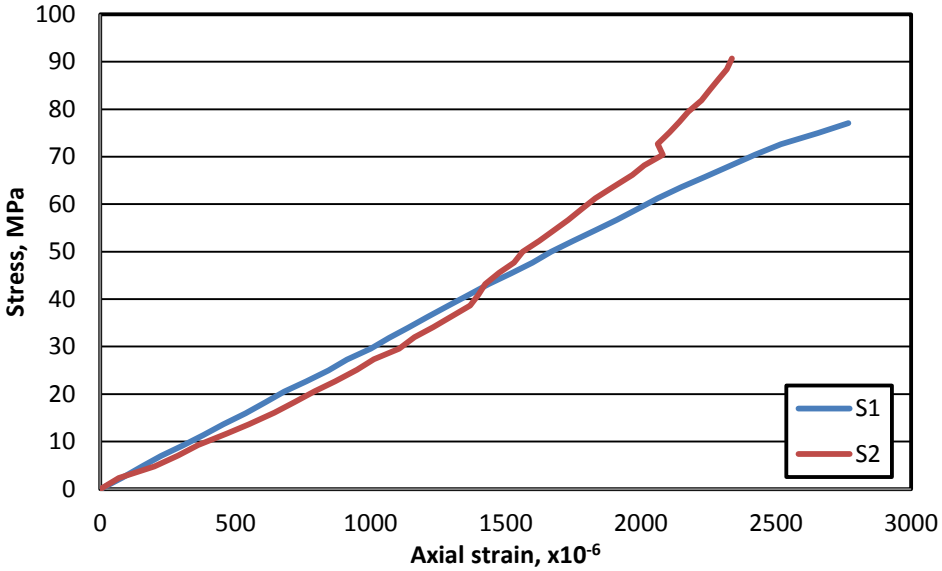

Figure A.21: Stress-strain response or RPC mixture M21.

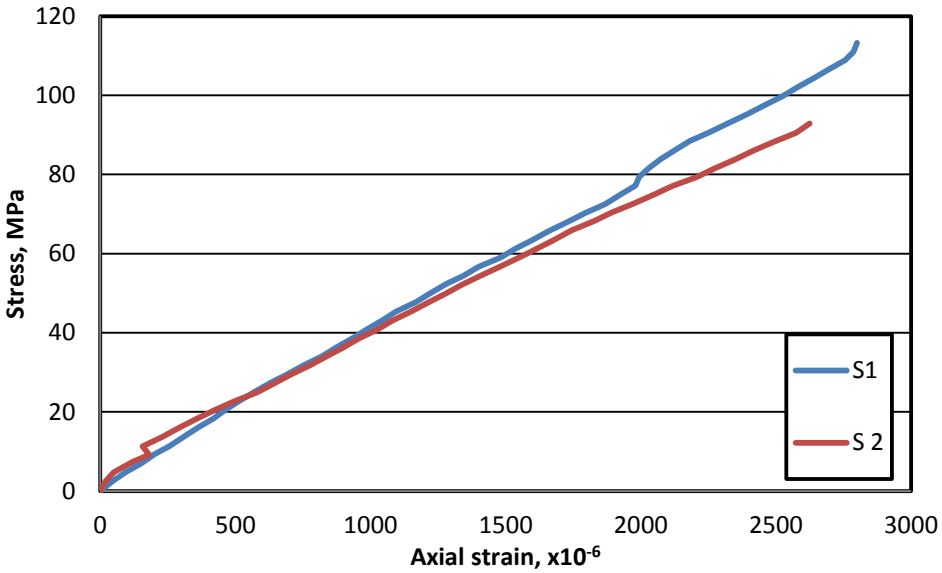

Figure A.22: Stress-strain response or RPC mixture M22.

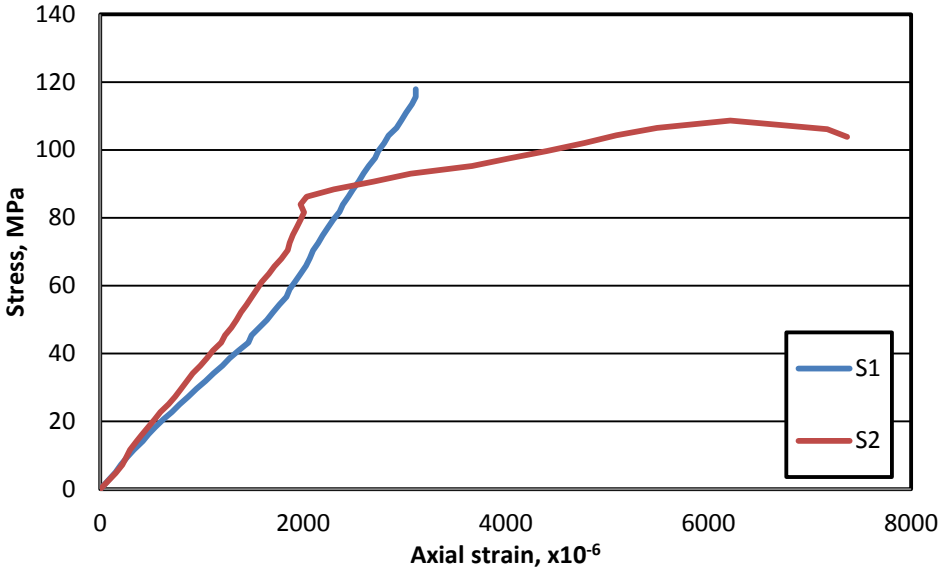

Figure A.23: Stress-strain response or RPC mixture M23.

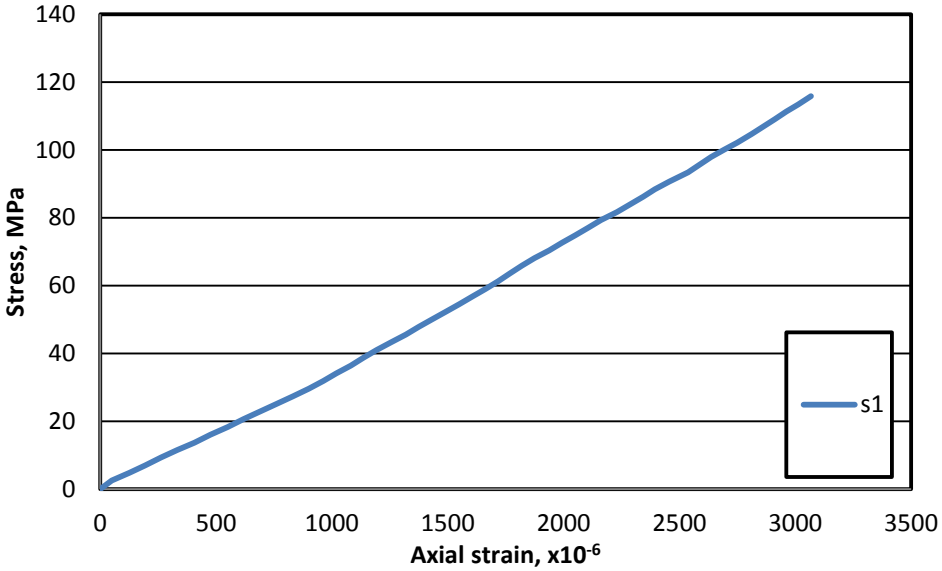

Figure A.24 Stress-strain response or RPC mixture M24.

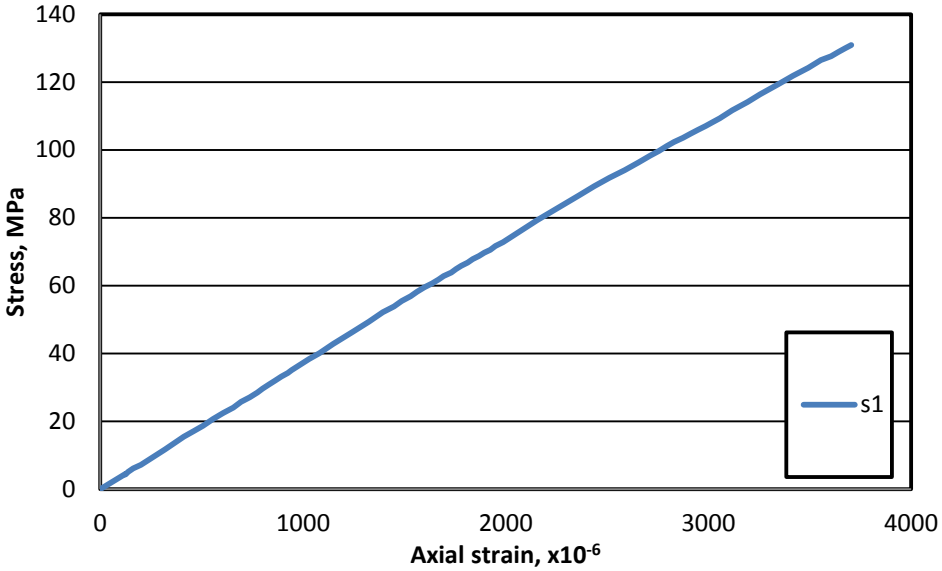

Figure A.25: Stress-strain response or RPC mixture M25.

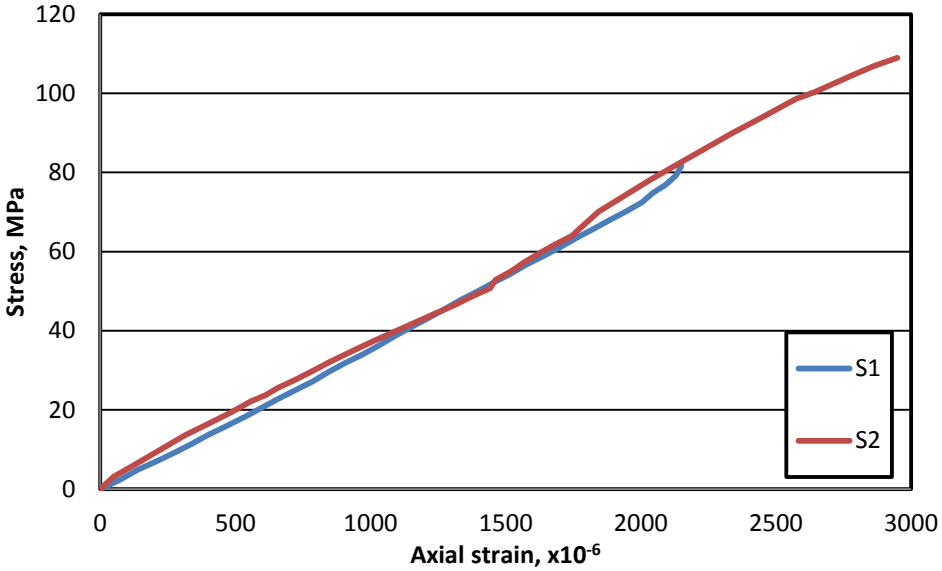

Figure A.26: Stress-strain response or RPC mixture M26.

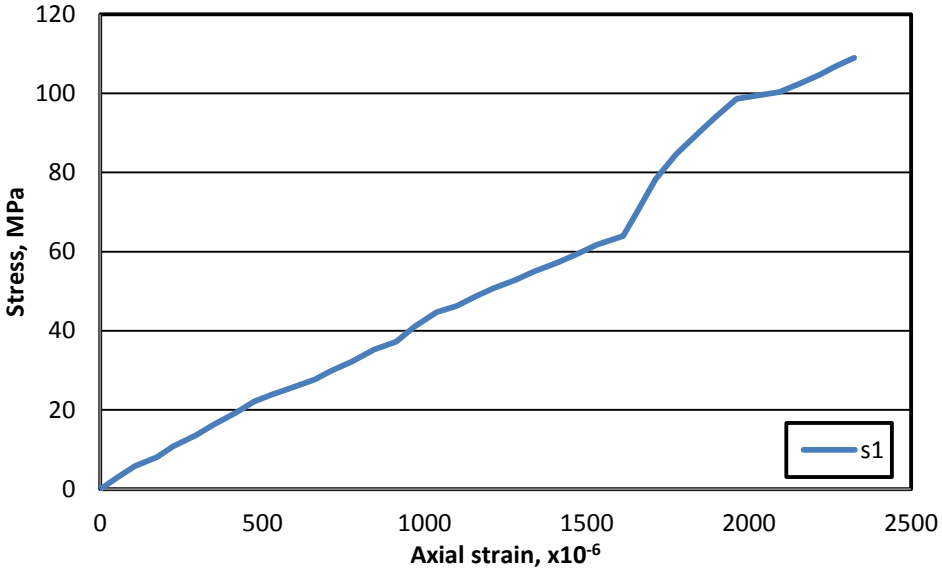

Figure A.27: Stress-strain response or RPC mixture M27.

APPENDIX B

LOAD-DEFLECTION PLOTS FOR RPC SPECIMENS PREPARED WITH VARIOUS MIX PROPORTIONS FOR OBTAINING MODULUS OF RUPTURE.

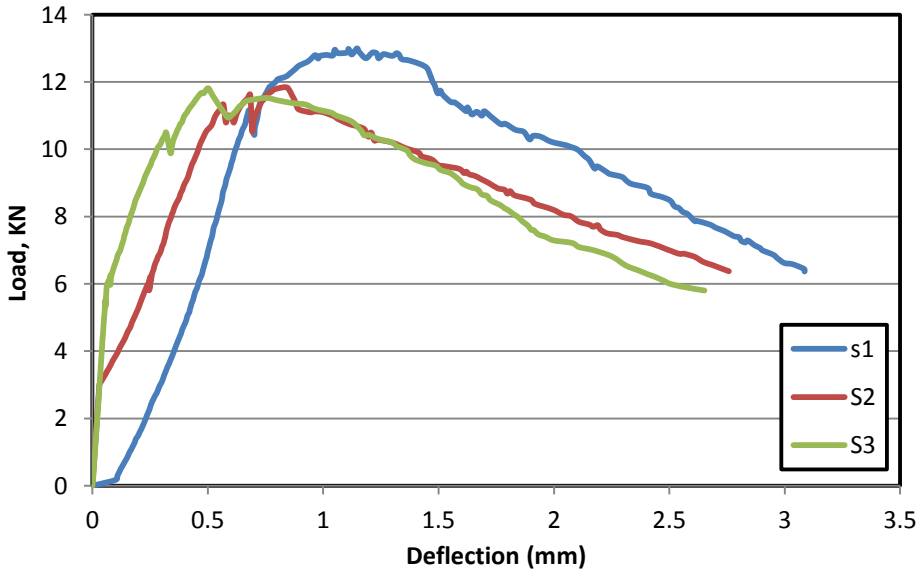

Figure B.1: Load-deflection response or RPC mixture M1.

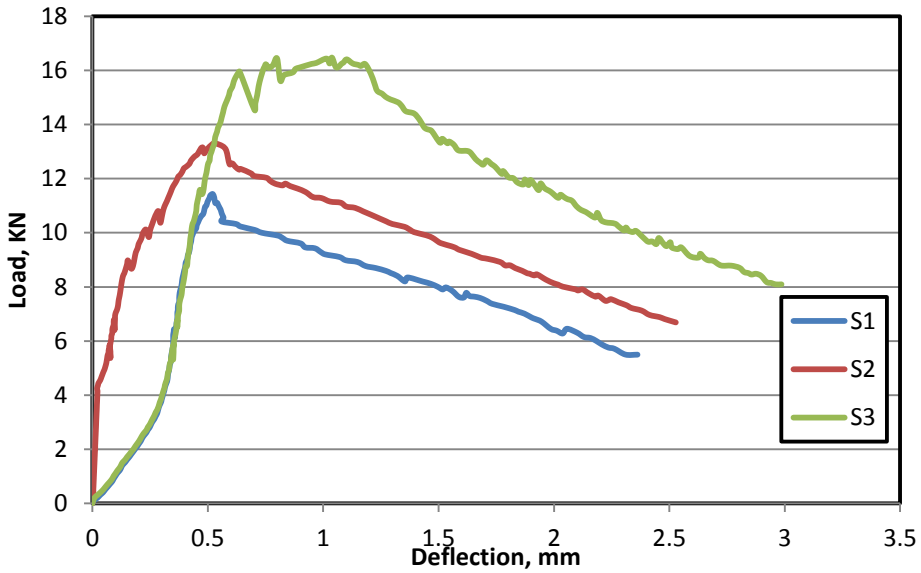

Figure B.2: Load-deflection response or RPC mixture M2.

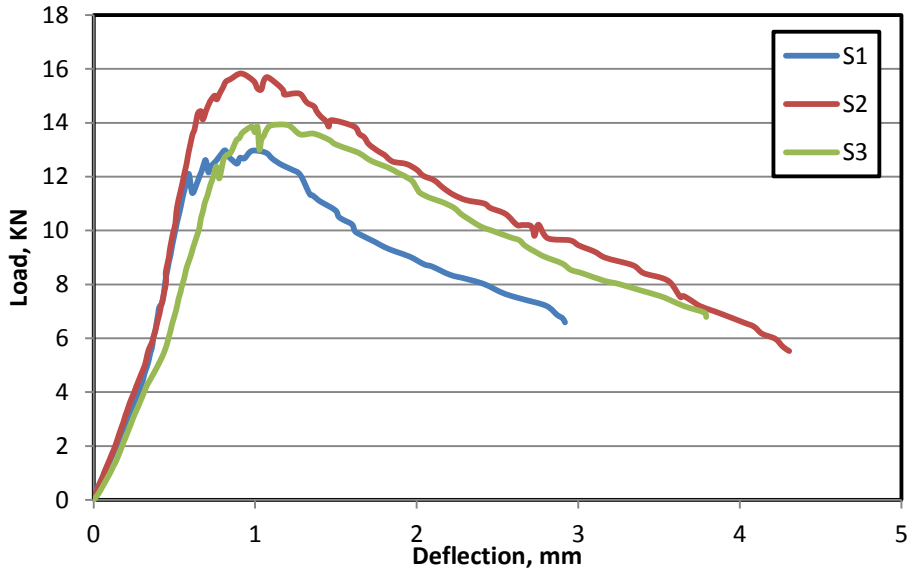

Figure B.3: Load-deflection response or RPC mixture M3.

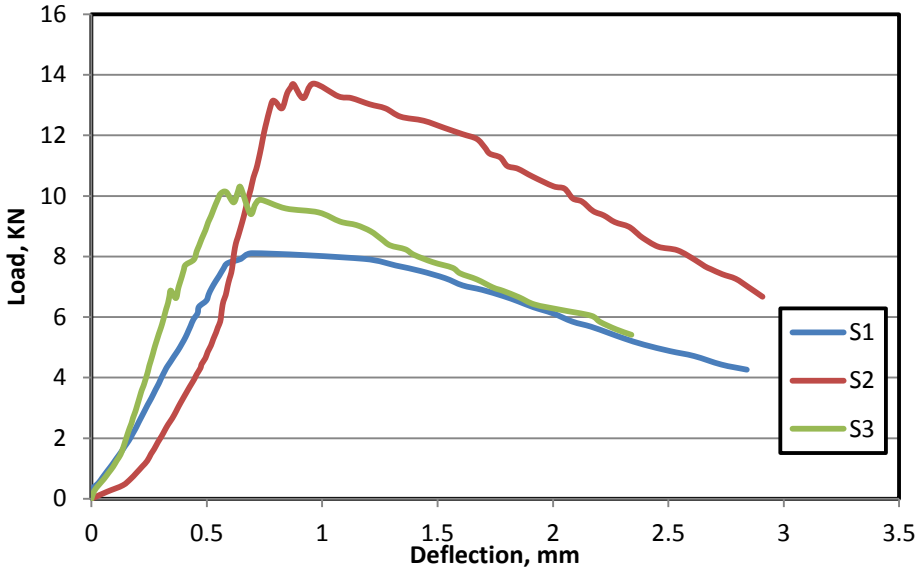

Figure B.4: Load-deflection response or RPC mixture M4.

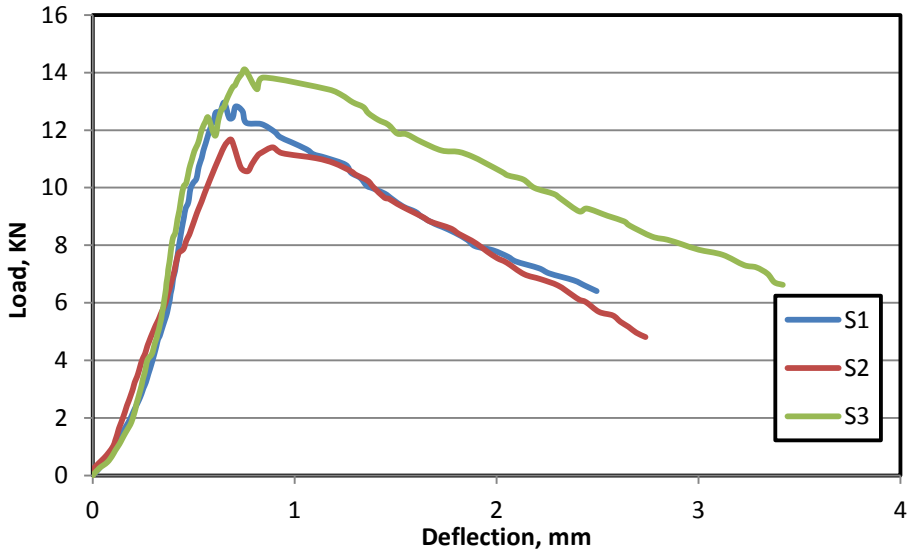

Figure B.5: Load-deflection response or RPC mixture M5.

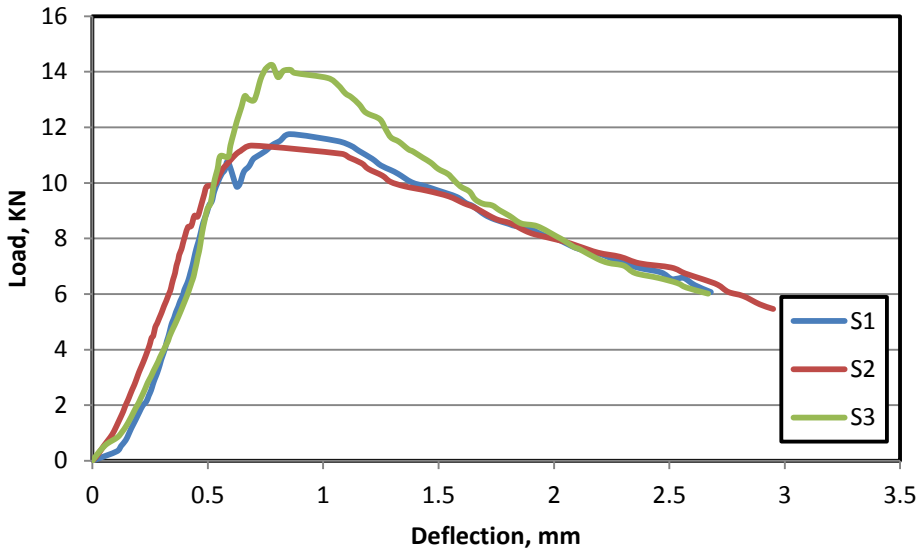

Figure B.6: Load-deflection response or RPC mixture M6.

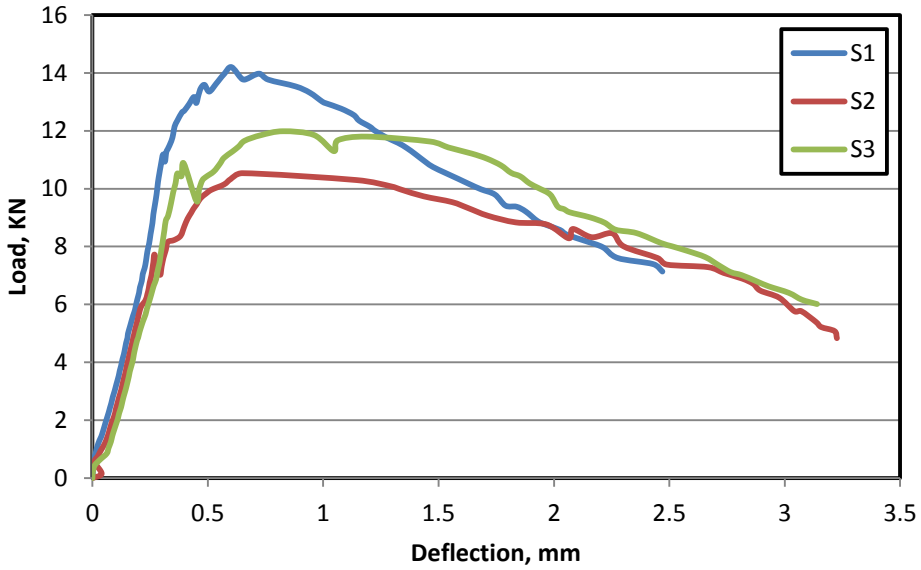

Figure B.7: Load-deflection response or RPC mixture M7.

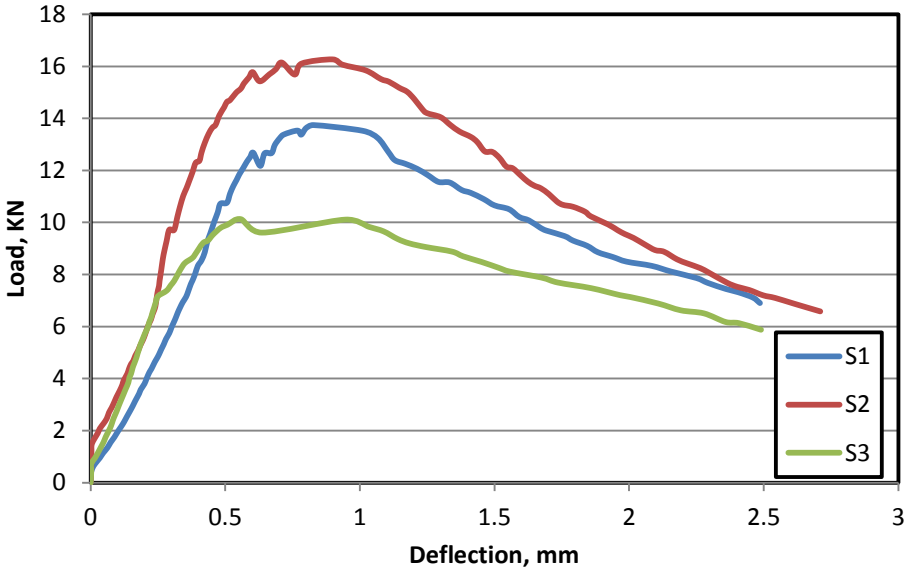

Figure B.8: Load-deflection response or RPC mixture M8.

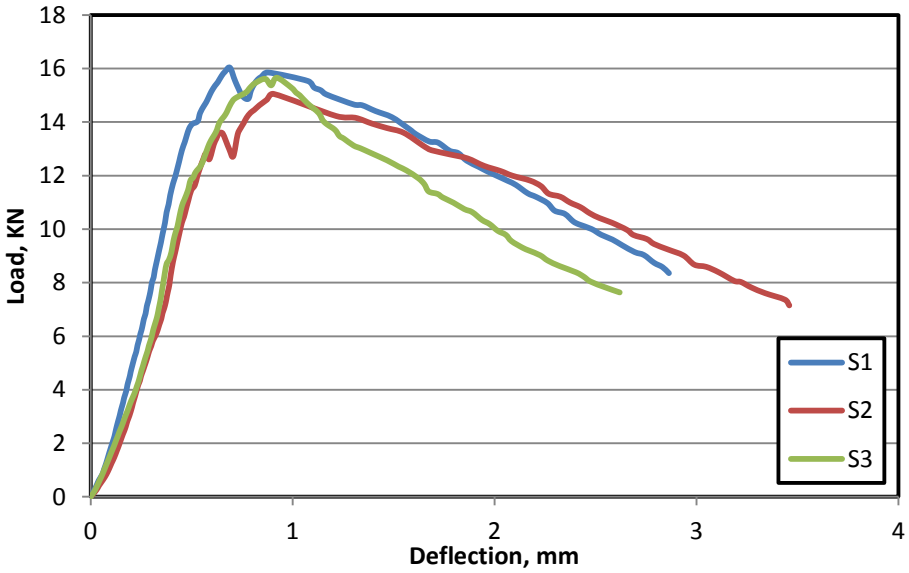

Figure B.9: Load-deflection response or RPC mixture M9.

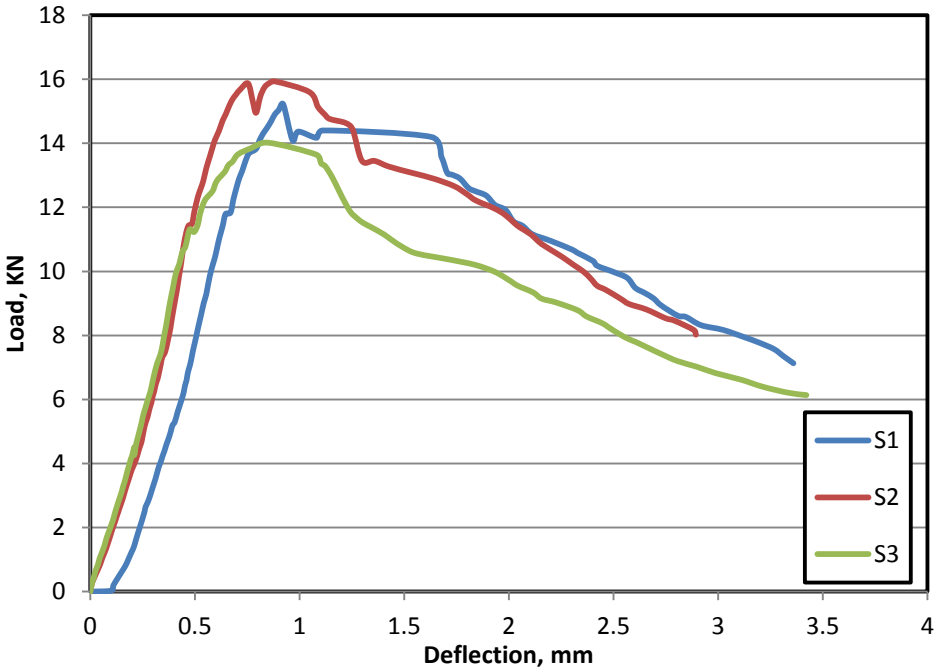

Figure B.10: Load-deflection response or RPC mixture M10.

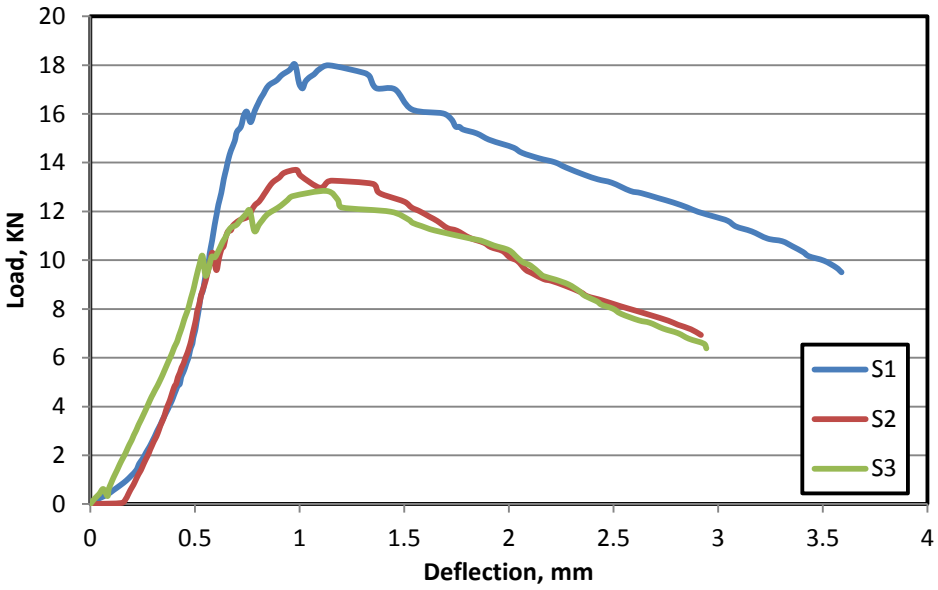

Figure B.11: Load-deflection response or RPC mixture M11.

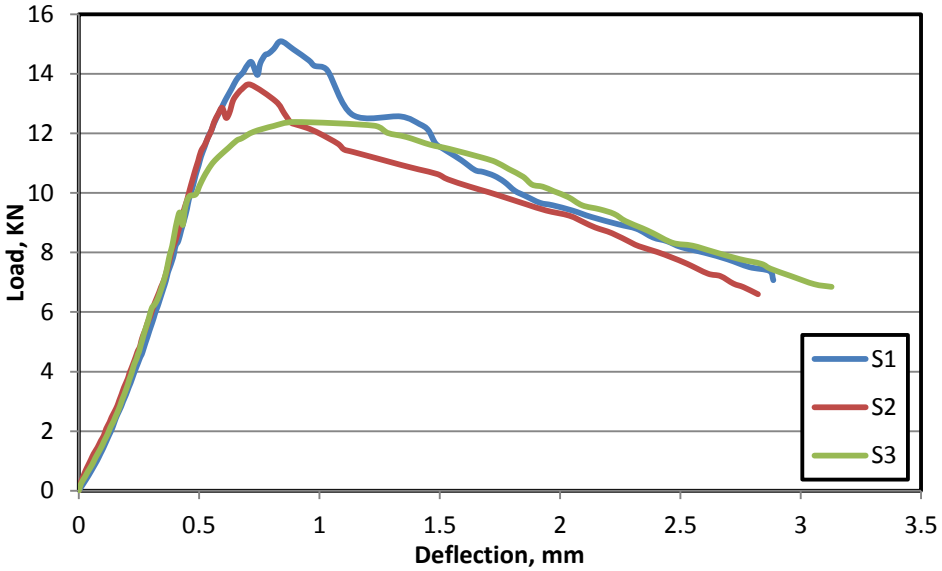

Figure B.12: Load-deflection response or RPC mixture M12.

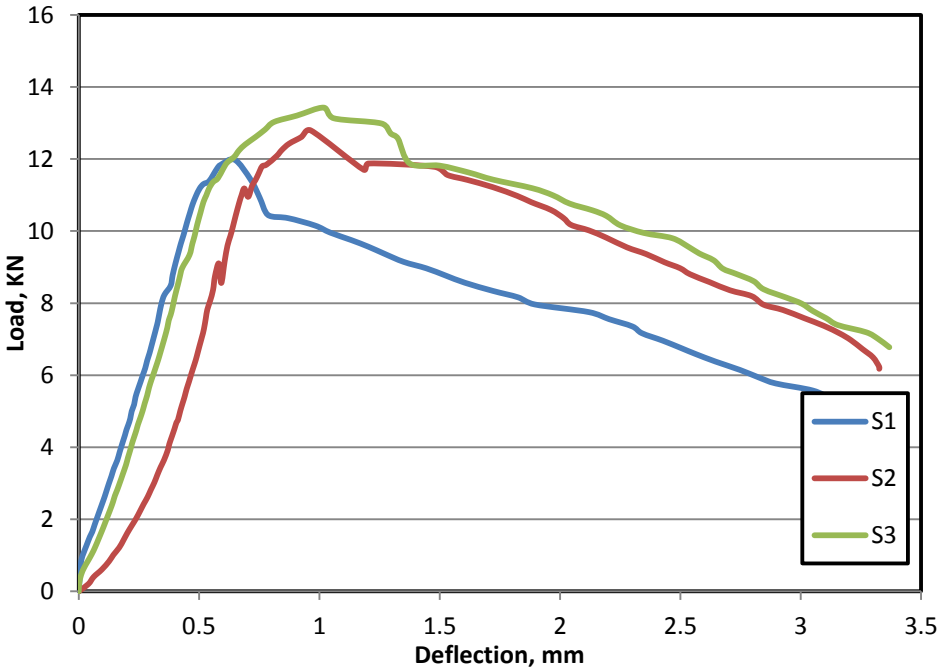

Figure B.13: Load-deflection response or RPC mixture M13.

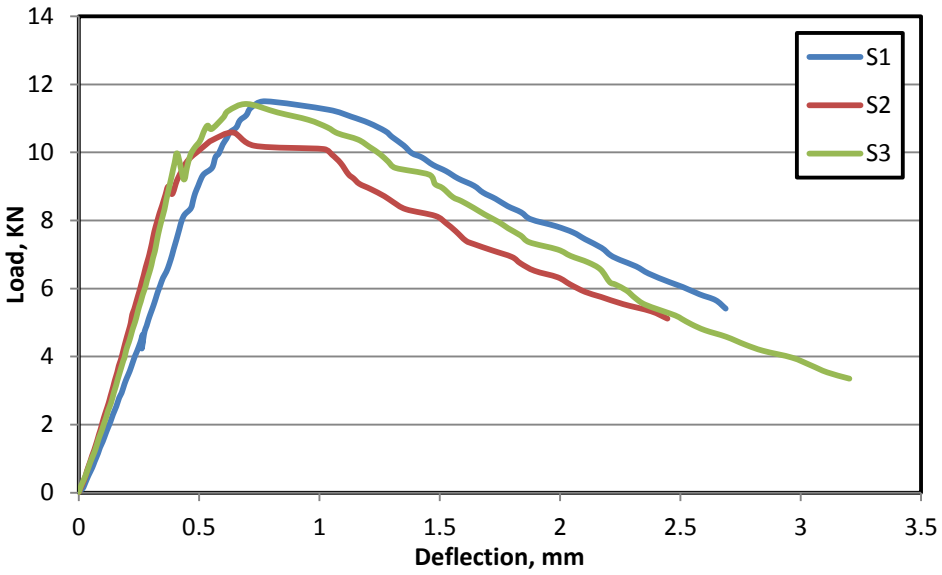

Figure B.14: Load-deflection response or RPC mixture M14.

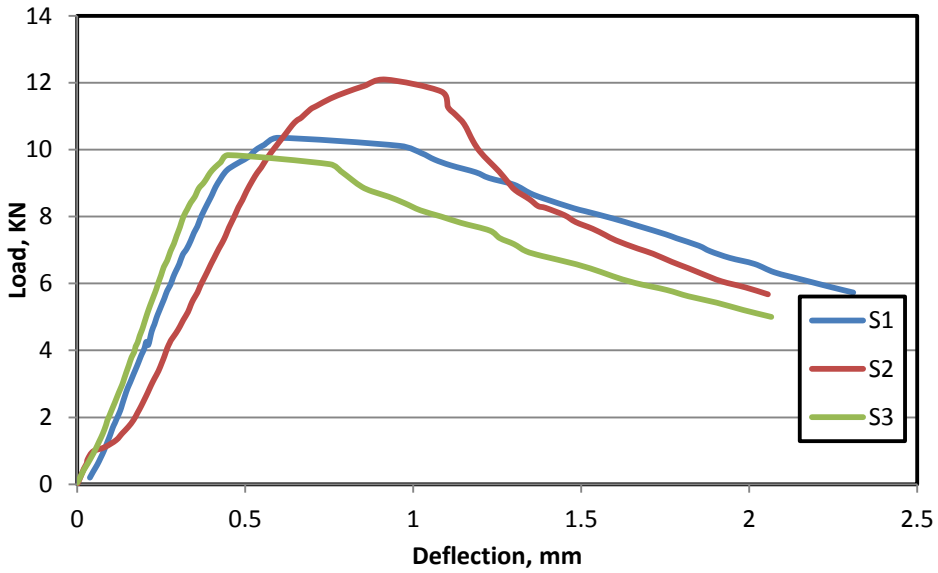

Figure B.15: Load-deflection response or RPC mixture M15.

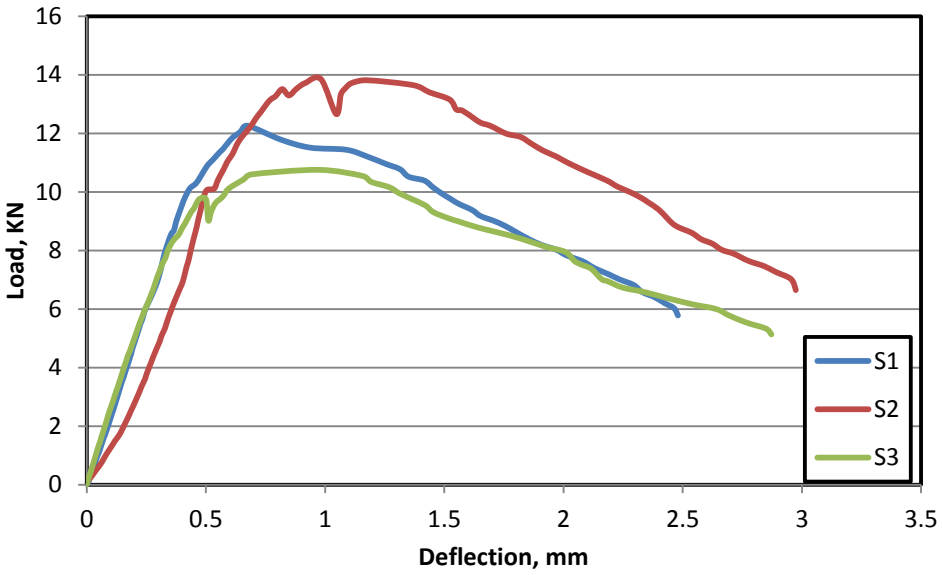

Figure B.16: Load-deflection response or RPC mixture M16.

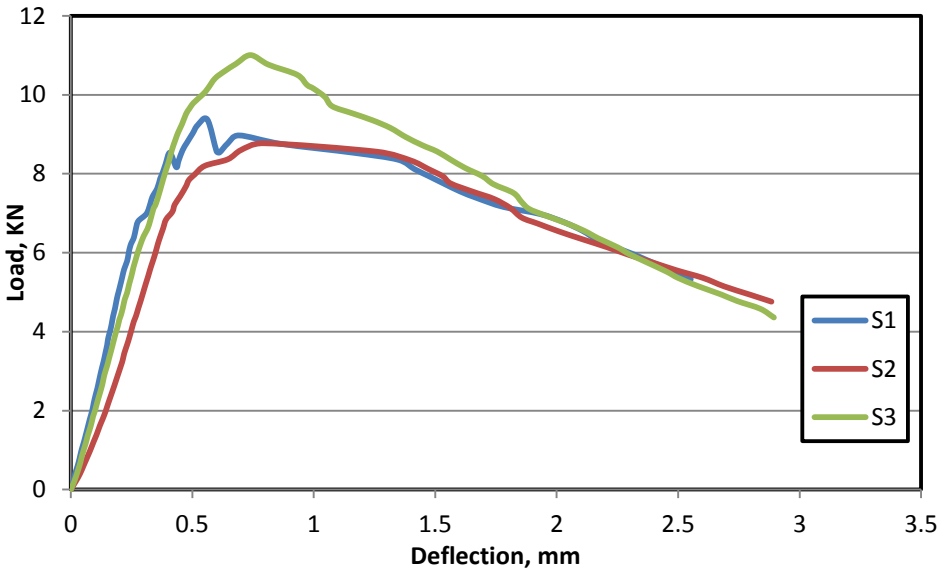

Figure B.17: Load-deflection response or RPC mixture M17.

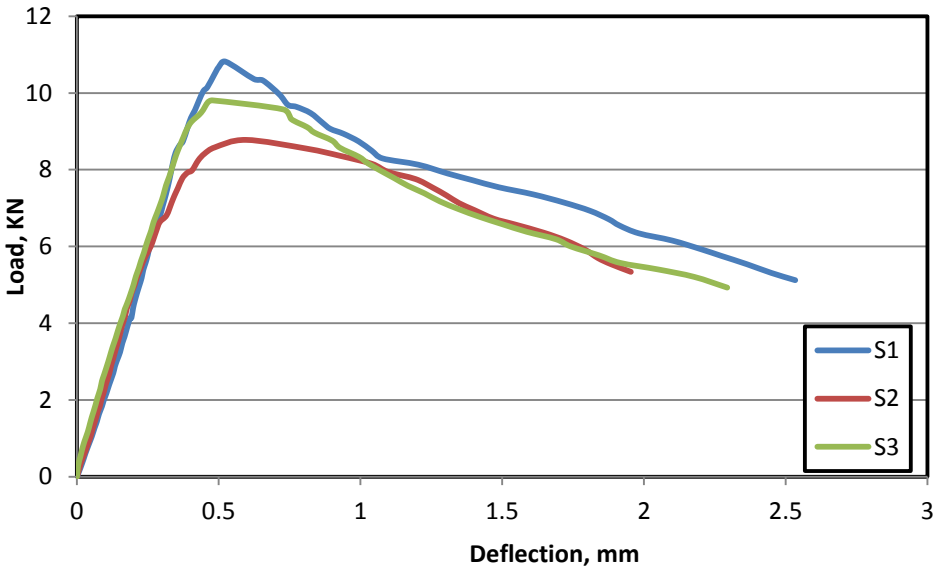

Figure B.18: Load-deflection response or RPC mixture M18.

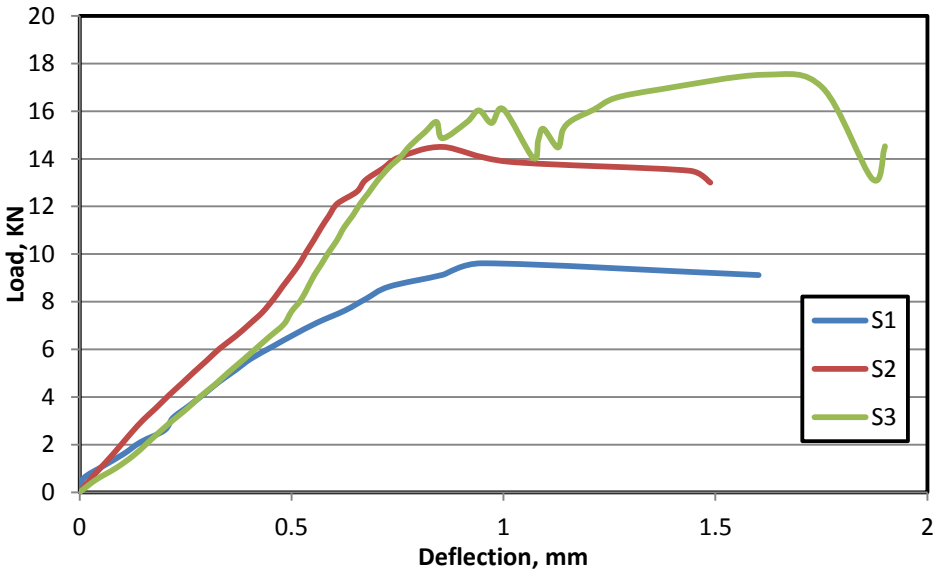

Figure B.19: Load-deflection response or RPC mixture M19.

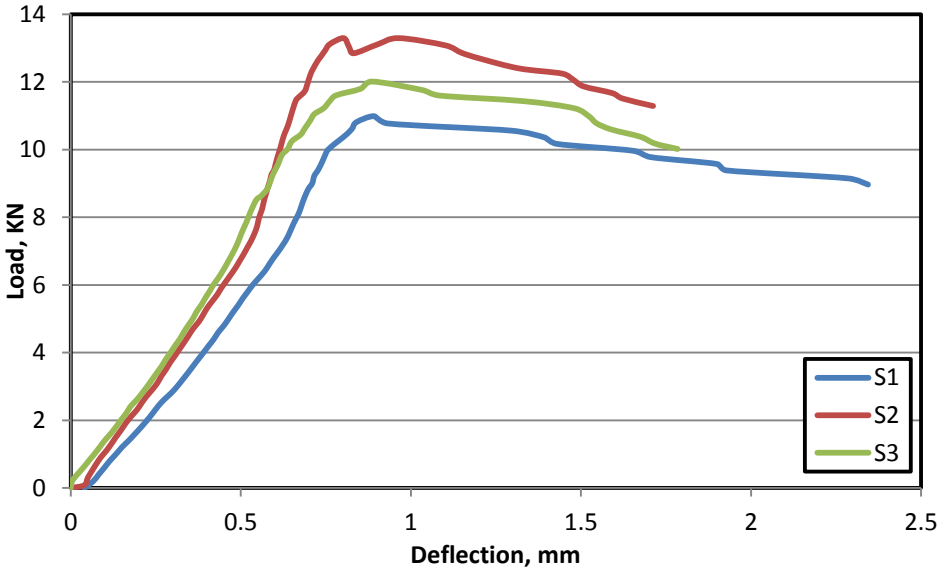

Figure B.20: Load-deflection response or RPC mixture M20.

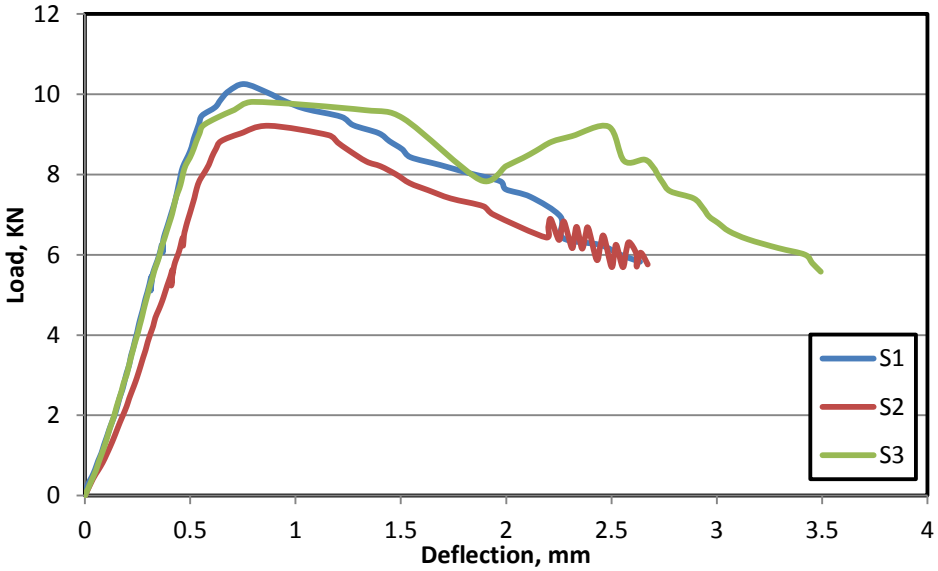

Figure B.21: Load-deflection response or RPC mixture M21.

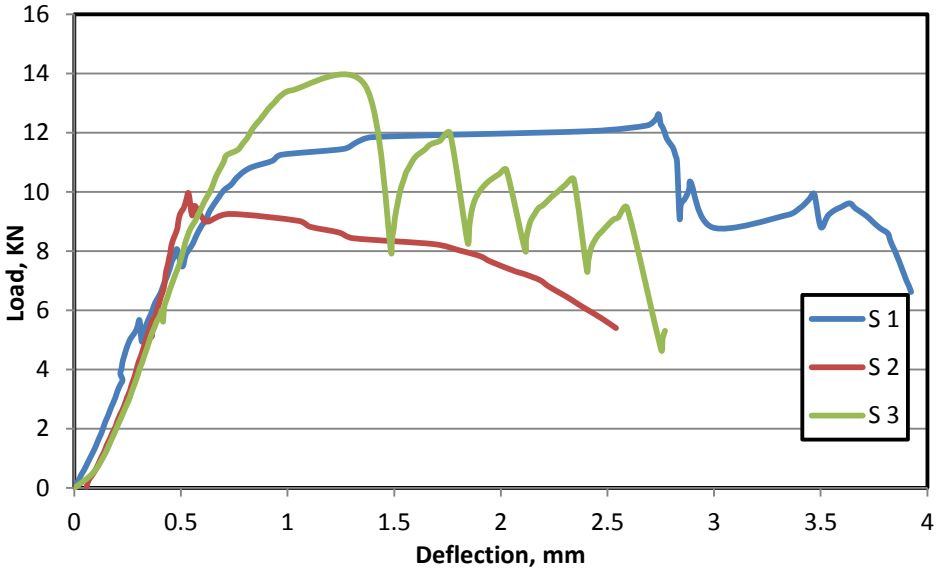

Figure B.22: Load-deflection response or RPC mixture M22.

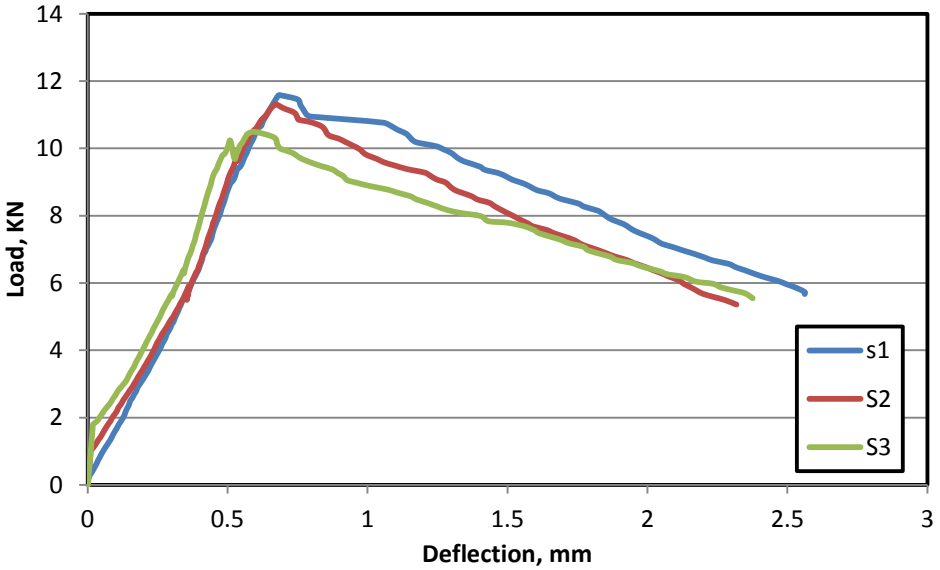

Figure B.23: Load-deflection response or RPC mixture M23.

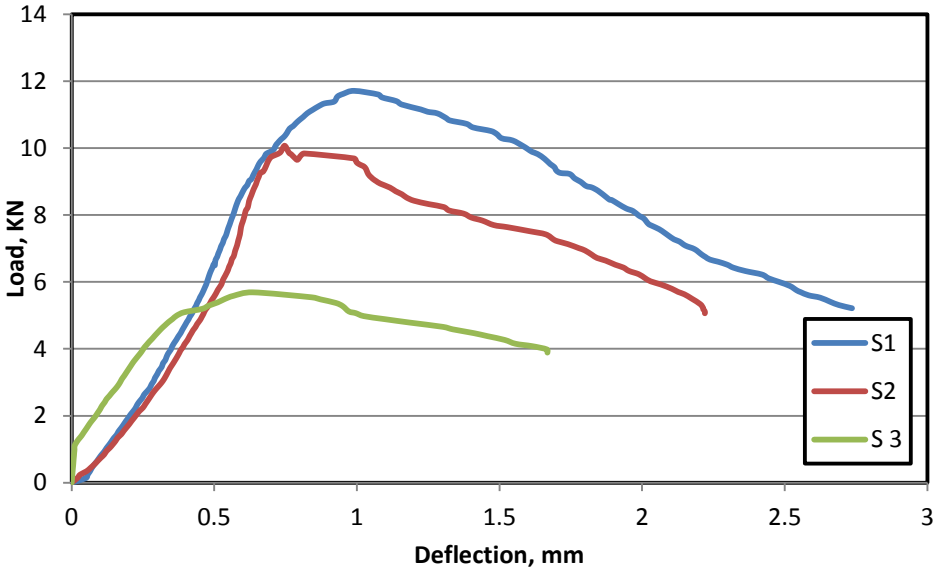

Figure B.24: Load-deflection response or RPC mixture M24.

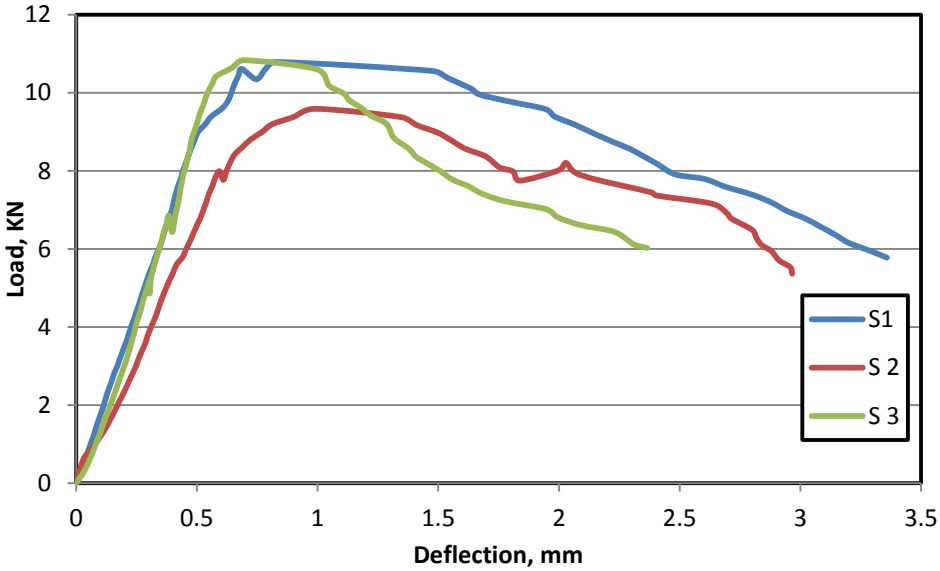

Figure B.25: Load-deflection response or RPC mixture M25.

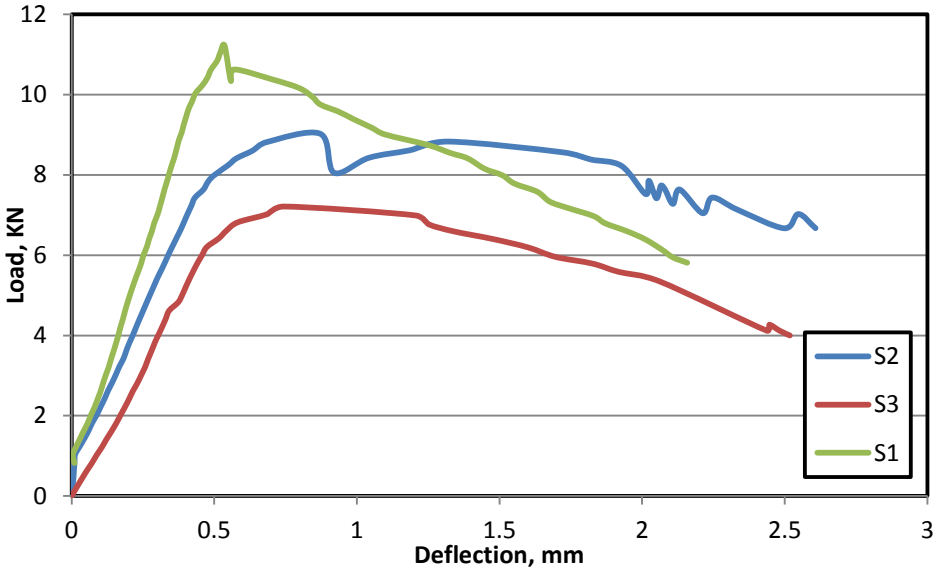

Figure B.26: Load-deflection response or RPC mixture M26.

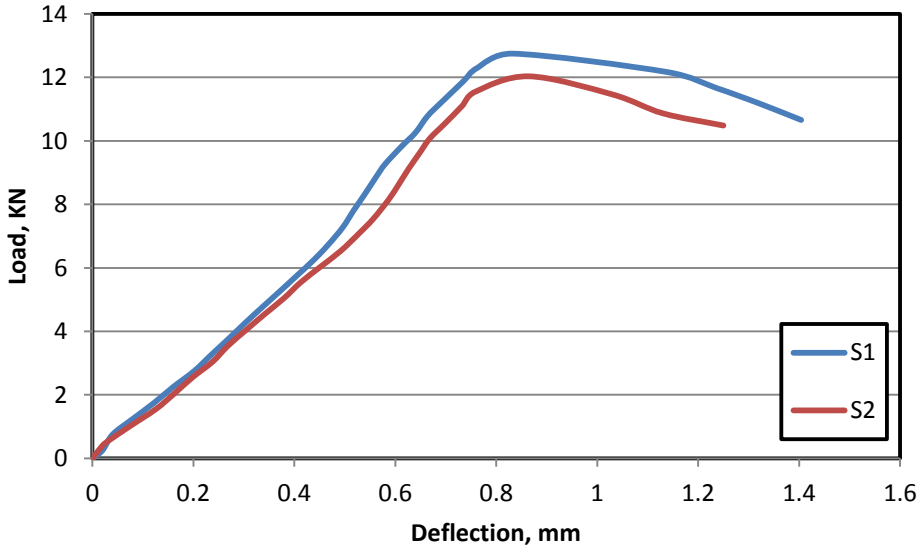

Figure B.27: Load-deflection response or RPC mixture M27.

APPENDIX C

LOAD-CRITICAL CRACK MOUTH OPENING DISPLACEMENT (CMOD) RESPONSE FOR RPC SPECIMENS PREPARED WITH VARIOUS MIX PROPORTIONS, TO CALCULATE K_{ic} AND G_f VALUES.

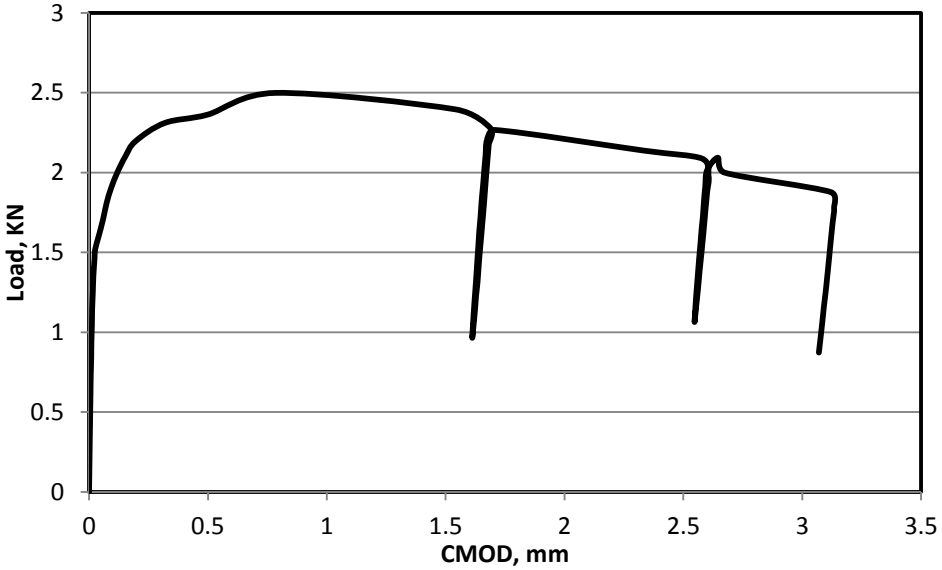

Figure 0C.1: Load-CMOD response of RPC mixture M1.

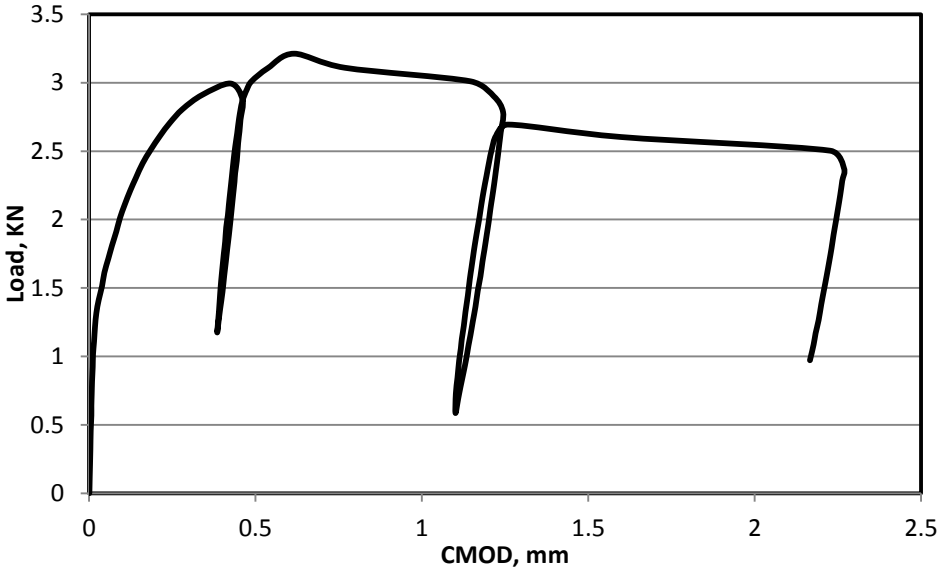

Figure 0C.2: Load-CMOD response of RPC mixture M3.

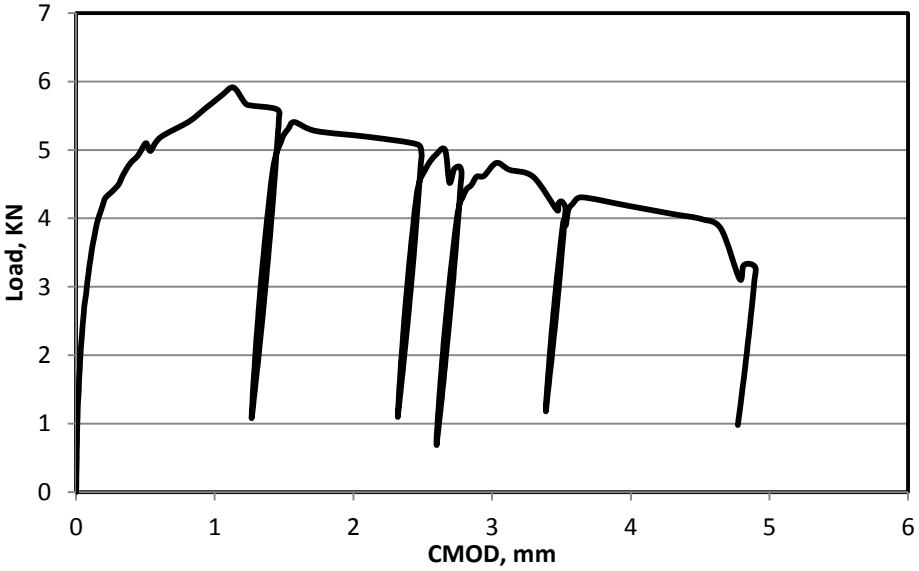

Figure 0C.3: Load-CMOD response of RPC mixture M7.

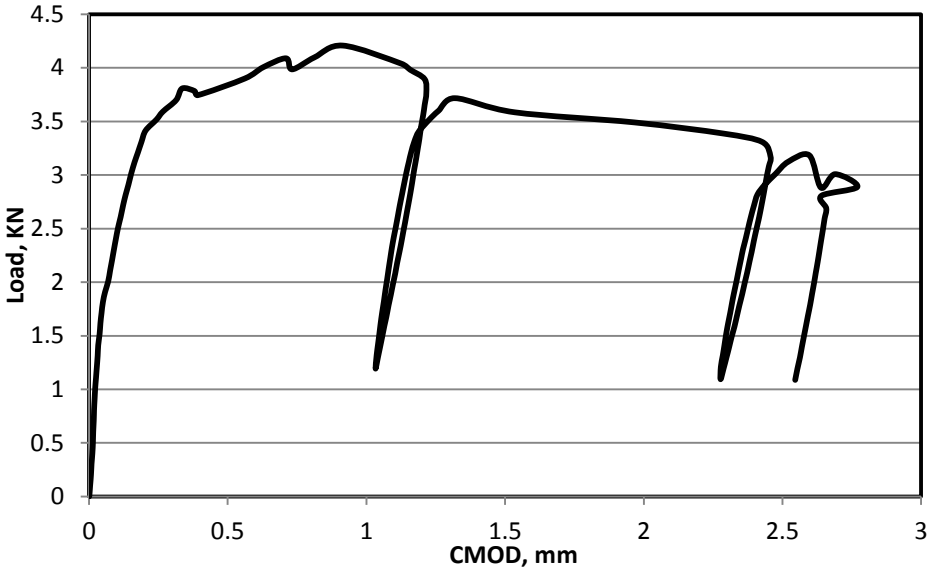

Figure 0C.4: Load-CMOD response of RPC mixture M9.

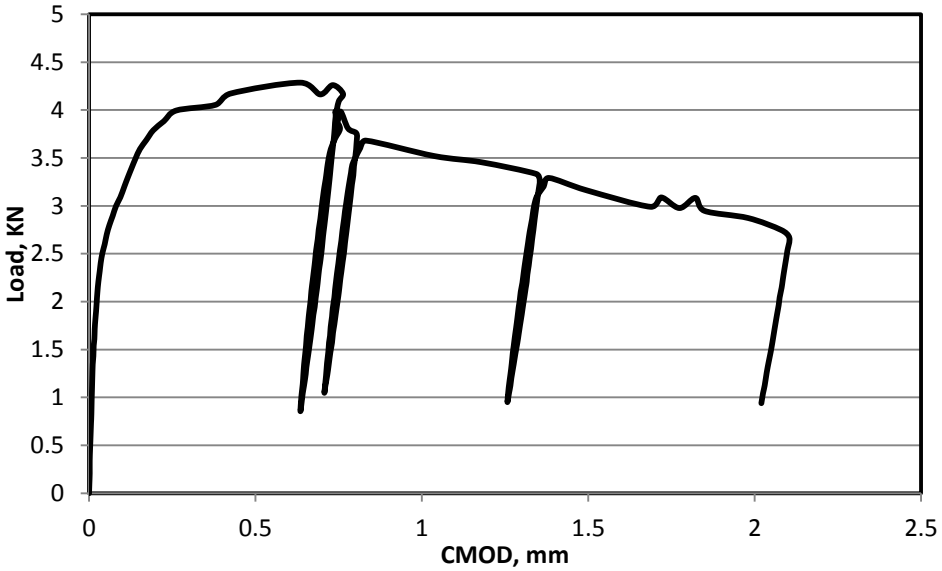

Figure 0C.5: Load-CMOD response of RPC mixture M10.

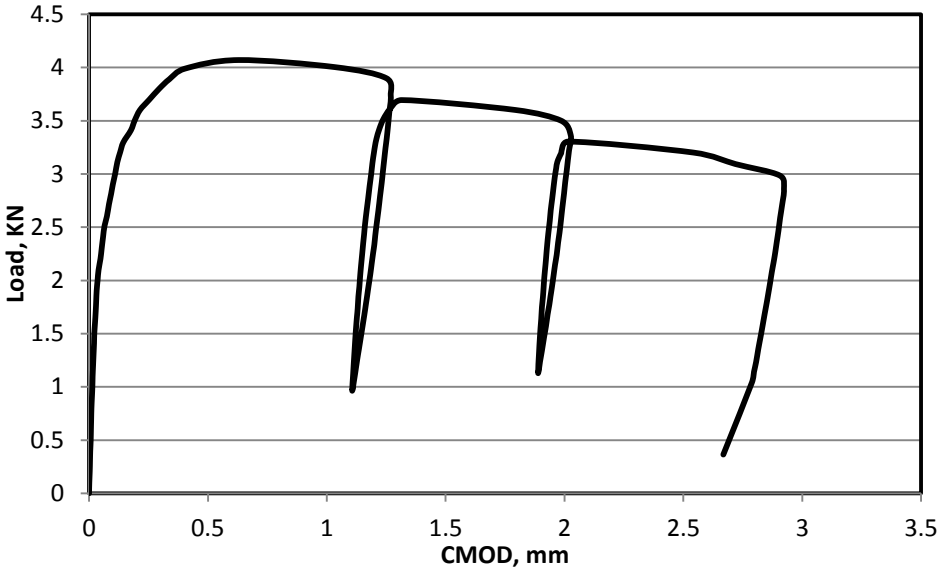

Figure 0C.6: Load-CMOD response of RPC mixture M12.

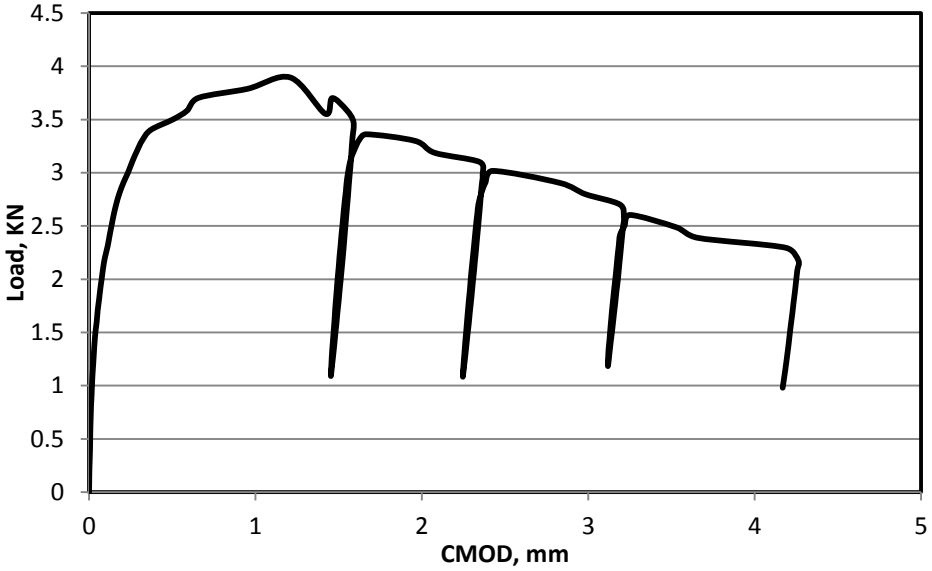

Figure 0C.7: Load-CMOD response of RPC mixture M16.

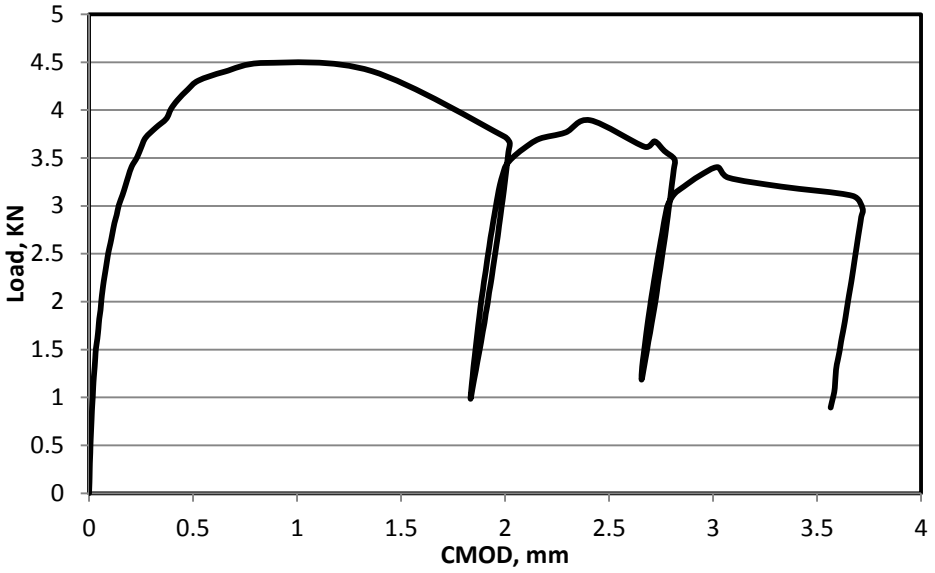

Figure 0C.8: Load-CMOD response of RPC mixture M18.

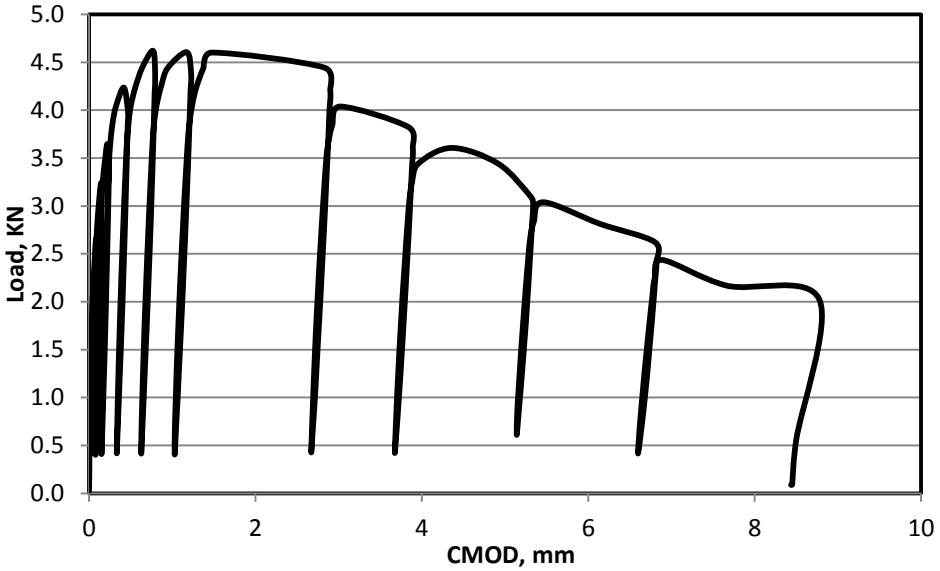

Figure 0C.9: Load-CMOD response of RPC mixture M19.

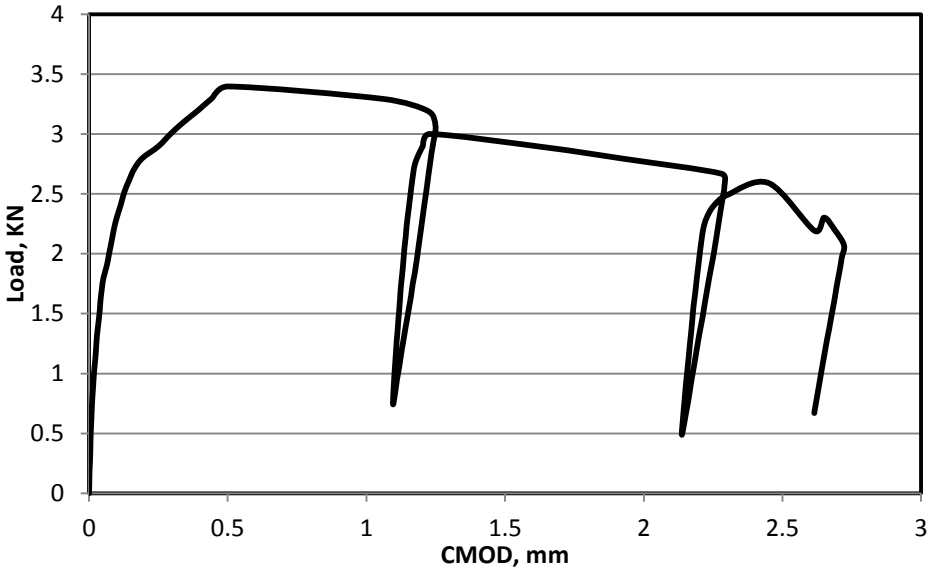

Figure 0C.10: Load-CMOD response of RPC mixture M21.

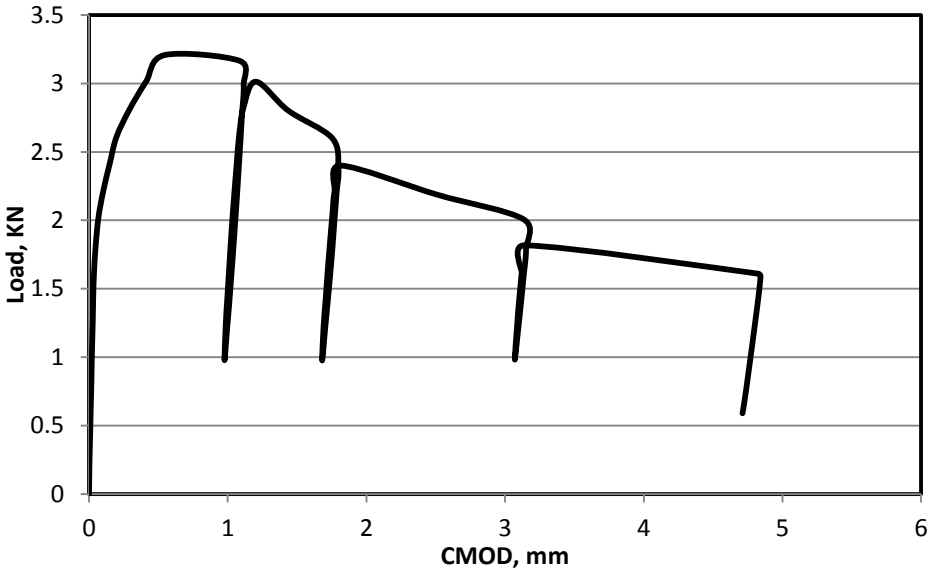

Figure 0C.11: Load-CMOD response of RPC mixture M26.

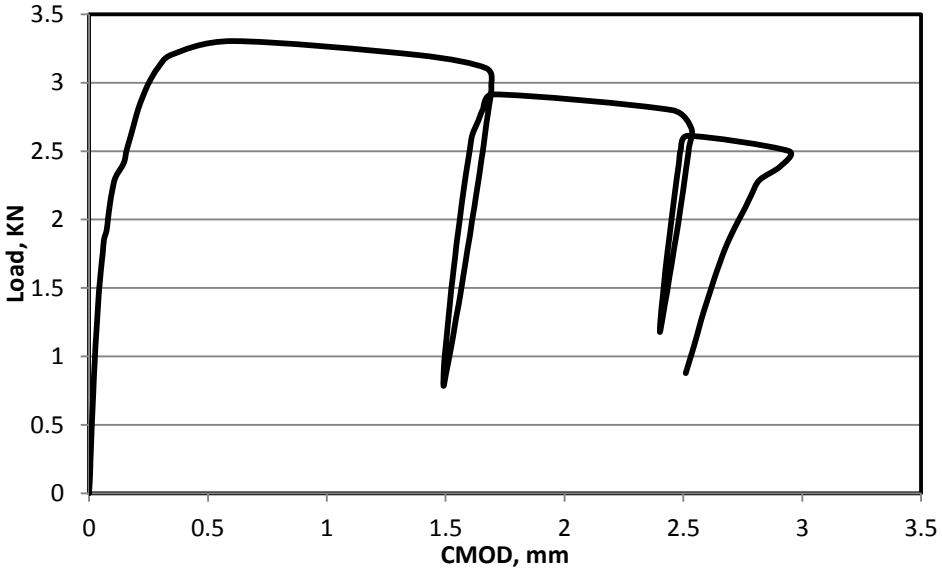

Figure 0C.12: Load-CMOD response of RPC mixture M27.

VITAE

Name : Ahmed Zubair

Nationality : Indian

Date of Birth : 12th July, 1987

Permanent Address : H. No.: 12-02-709/C/73,

Padmanabha Nagar, Mehdipatnam,

Hyderabad – 5000028, Andhra Pradesh, INDIA

Present Address : Room#802/218, Student Housing, KFUPM,

Dhahran, Saudi Arabia.

Email : azubair_53@yahoo.com

Phone : +91-9849691071

+91-40-23518241

+966-501109651

Degrees:

Bachelor of Engineer in Civil Engineering from Osmania University (Sept. 2005 – April 2009).

Experience:

Research Assistant in Civil Engineering Department of King Fahd University of Petroleum & Minerals (KFUPM) (Feb 2010 – Jul 2012).